MECHANOBIOLOGY OF THE BASEMENT MEMBRANE

Inauguraldissertation

zur

Erlangung der Würde eines Doktors der Philosophie
vorgelegt der
Philosophisch-Naturwissenschaftlichen Fakultät
der Universität Basel

von

PHILIPP OERTLE

aus Teufen (Appenzell-Ausserrhoden)

Basel, 2018

Genehmigt von der Philosophisch-Naturwissenschaftlichen Fakultät

auf Antrag von
Prof. Dr. Roderick Y. H. Lim
Prof. Dr. Ernst Meyer

Basel, den 21.6.2016

Prof. Dr. Jörg Schibler
Dekan

PREFACE

The microenvironment (ME) of epithelial cells lies at the heart of the function and architecture of most organs, especially those of the digestive, endocrine and the excretory systems of vertebrata. By creating tubes or cylindrical spaces in these organs, the ME divides the organs into an inside - the lumen - bearing epithelial cells performing their function, and the outside - stroma, connective tissue and fat - which gives rise to the macroscopic shape of the organ. Epithelial cells often define the function of the organ which can be as diverse as the production of milk in the alveoli of the mammary gland or the creation of glomerular filtrate, the first stage of urine, in the nephrons glomeruli. The stroma ensures that the highly specialized MEs within an organ are correctly assembled; in the human breast, the alveoli form groups, lobules, each of which drained by a lactiferous duct that transports the milk towards the mammilla. In the kidney, glomeruli, proximal, distal and collecting ducts are layed out such that the allow for concentrating the urine on its way to the renal medulla. A key organising element of the ME is the rather stiff basement membrane (BM), which is the structural part that passively, through its mechanical rigidity and actively through signalling via its components separates the luminal epithelia from the stromal fibroblasts, creating and maintaining tissue polarity to ensure proper function of the organ.

The primary goal of this work is to find universal features of the BM and epithelial cells across organs and to understand how the cells mechanobiology is influenced by the BM. The structure of BMs and behaviour of cells *in situ* in human tissue is elaborated and a strong focus is placed on the mechanobiology of epithelial cells grown on native human BMs *in vitro*. Two BMs are used for this purpose, one is the human inner limiting membrane (ILM), the BM separating the vitreous body in the eye from the retina, the other one is the mouse mesentery, a double BM which is a fold of the peritoneal wall that keeps the intestine and gut in place in the belly. The cells mechanobiology is defined by the interaction of the cells integrins with the BMs proteins, notably laminin, perlecan and collagen IV. Disturbing either of the interaction partners quickly leads to distinct new mechanobiological phenotypes of the epithelial cells, without the need for genetic modifications. By using artifical substrates with tunable stiffness and composition, it also became clear that

stiffness does not alone regulate cell stiffness, as important is the correct biochemical composition of the substrate. Further, I will show that changes to the BM by cancer cells are a key step in forming invasive carcinomas which goes together with recent research that shows that the mechanics of epithelial cells and extra-cellular matrix (ECM) are fundamentally altered.

The mechanics of cells reflects to a large extent the organization of the cytoskeleton, the presence and abundance of cytoskeletal fibres as well as their linkage to each other and various parts of the cell. In the case of BMs and the extracellular matrix in general, the mechanical properties are governed by the type of fibres and the state of cross-linking. The only tool available for characterizing this physical properties of cells and ECM components under physiological conditions is the atomic force microscope. It gives insight about stiffness and E-modulus on a sub-micrometer scale and is very sensitive to changes in the low Pascal-range. The combination with confocal light microscopy allows us to correlate changes in ridigity to cytoskeletion localisation, to understand what part of the cytoskeleton defines the mechanics and how this is changed by disturbing cell-BM interactions.

CONTENTS

LIST OF FIGURES

LIST OF TABLES

LIST OF SUPPLEMENTARY FIGURES

INTRODUCTION

1.1 EPITHELIA

Epithelia constitute most organs in our body and serve as the primary biological barriers against the outside environment, for instance lining the skin or gut. Epithelia are optimized for this task, owing to key organizational principles. They perform what is called the epithelial polarity program (EPP), summarized in figure 1.1. Epithelial cells form layers of homogeneously polarized cells that are kept together by calcium-dependent adhesive junction proteins (adherens junctions and desmosomes as discussed in detail in 'Intercellular junctions in mechanosensing') and cadherins that provide mechanical stability and density sensing. Epithelial cells contain an adhesive belt just below the apical surface that induces a small specialized micro domain in the plasma membrane (Knust et al. 2002) and separates the apical from the basolateral cell membrane domains (Mellman et al. 2008) for establishing polarity. The apical and basolateral membrane domains contain different transporters for nutrients, fluids and solutes. Moreover, the separated membranes are comprised of different lipids to carry out distinct secretory and absorptive functions, enabling vectorial transport in and across the cell via intercellular gap junctions (GJs) that open pores between two neighboring cells (planar cell polarity (PCP)). This directed transport is then further assisted by the endoplasmatic reticulum (ER) and the Golgi that ensure asymmetric distribution of proteins in the plasma membrane domains. The domains themselves also contain feedback loops to expel miss-located proteins for maintaining asymmetry. Malfunctions of the EPP lead to epithelial-mesenchymal transition (EMT) where cells lose their collective behavior, disrupt cell-cell junctions and become more motile. EMT is a hallmark of cancer (Hanahan et al. 2011).

A distinct hallmark of epithelia *in vitro* is contact inhibition (Abercrombie et al. 1954). The two forms are, inhibition of mitosis (Carter 1968; Stoker et al. 1967) and inhibition of locomotion (Abercrombie et al. 1976). Contact inhibition is most prominently disrupted in cancer where cells undergo hyperplasia (Hanahan et al. 2011). Under tissue homeostasis, epithelial layers strictly control the number of cells through the activation of cell-cell adhesion molecules through signaling pathways Wnt and Hippo (McClatchey
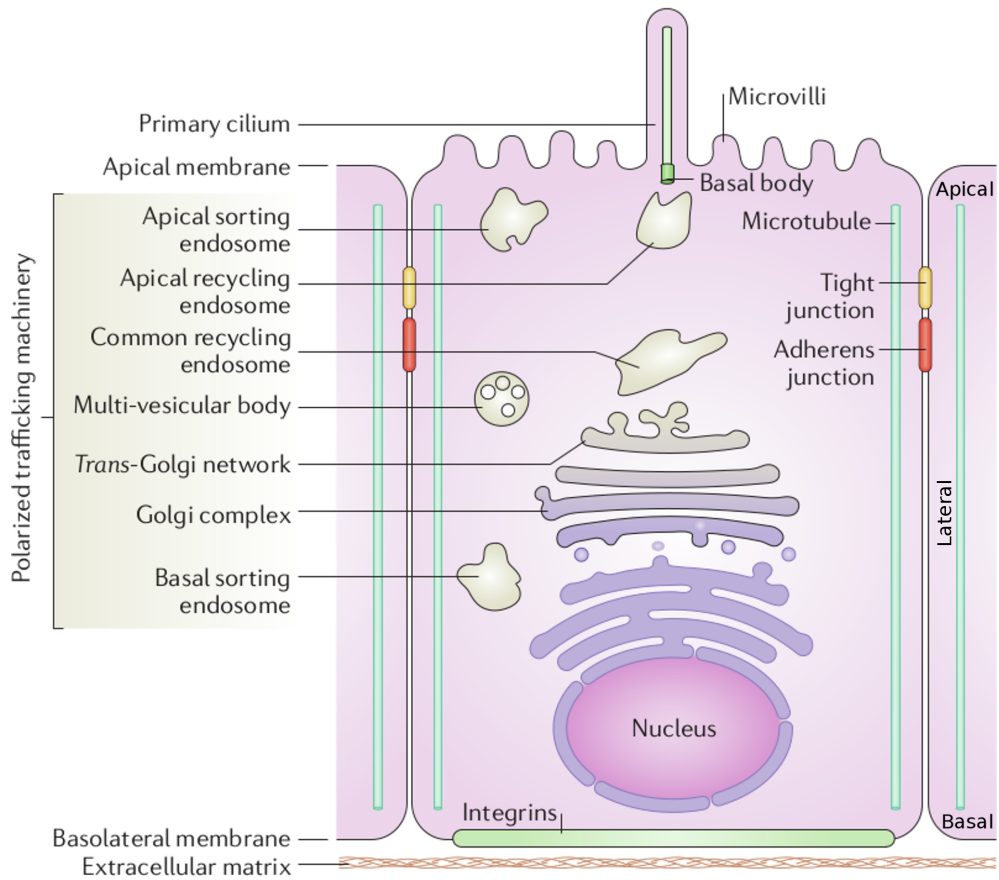
Figure 1.1 Features of the polarized epithelial phenotype.
Epithelial cells feature a clear separation into an apical and a basolateral cell membrane, separated by the tight junction; a polarized trafficking machinery maintains the proper protein and lipid composition of both compartments and enables transport of solutes along the apico-basal polarity axis. adherens junction (AJ) and desmosomes (not shown) anchor laterally to neighboring cells and enable planar cell polarity (PCP); integrins anchor the cell basally onto the basement membrane (BM), the top layer of the extra-cellular matrix (ECM). Adapted from Rodriguez-Boulan et al. 2014.

et al. 2012). Under physical deformation when the epithelium is compressed, overcrowding can lead to cell extrusion either apically or basally. On the other hand, if the epithelium is stretched, cells rapidly enter mitosis (Eisenhoffer et al. 2013).

1.2 TISSUE FORMATION

Epithelia start forming very early in embryogenesis. They first differentiate into epithelia of the primordial germ layers, endoderm, mesoderm and

ectoderm. Next they enter a process called organogenesis where highly specialized epithelia encompassed by a layer of extracellular matrix proteins form organs with unique functions. Basement membranes (BMs) form jointly with epithelia in these early stages of the embryogenesis (Li et al. 2003) and are critical for epithelial differentiation. In particular, they can be found shortly after differentiation of the morula, just prior to formation of the blastocyst where the cell mass is divided into the exterior trophoblast and the interior embryoblast. As such, BMs act as an adhesive substrate that prevent cells from mixing early on in the process of morphogenesis (Burgeson et al. 1997; Timpl et al. 1996).

The BM is a part of the cellular microenvironment, which is essential for epithelial maturation and maintenance, providing mechanical stability, signaling through ECM components and as a long-term reservoir for soluble growth factors. BM formation is initiated and then remodeled during embryogenesis, puberty and pregnancy, angiogenesis and in diseases such as cancer or diabetes. For further details, the distribution of BMs in various tissues can be found in the matrixome project[1]. Epithelial adult human BMs consist of a single to multiple micrometer thick bi-layer of collagen IV at the stromal side and the glycoprotein laminin at the epithelial side. Laminins always appear as heterotrimers of α, β, and γchains. Cells interact with laminins through the laminin α-chain; laminin α5β1γ1 (LN-511)/laminin α5β2γ1 (LN-521) and laminin α3β3γ2 (LN-332) which are the predominant laminins in adult epithelial tissues. BMs contain further glycoproteins (nidogen, agrin) and heparansulfate-proteoglycan (HSPG) such as perlecan. For in-depth discussion of the BM, the reader is referred to chapter 2.

1.3 BM IN MORPHOGENESIS

BM assembly is initiated when laminin heterotrimers bind to cell surfaces through integrins (McKee et al. 2007). This leads to an increase in local density of laminins by integrins, which in turn enables further laminin molecules to self-assemble into a polymeric network (Li et al. 2003). Our own data (see chapter 3) indicate that perlecan is co-assembled with laminin in the retina, however, in general perlecan location in the BM appears to be highly tissue dependent (Iozzo et al. 1994). This initial lattice serves as a scaffold for the addition of type IV collagen (Pöschl et al. 2004). This particular collagen, due to its ability to form dense networks instead of fibrillar arrangements

---

1 http://togodb.biosciencedbc.jp/togodb/view/matrixome_bodymap_protein_based

such as in collagen I, is usually considered to be the major contributor to the mechanical strength of BM (Khoshnoodi et al. 2008). Recent data show that laminin contributes much more to the mechanical rigidity than collagen IV (Halfter et al. 2013). In addition, it remains unclear which cell type is responsible for the secretion of specific ECM molecules since their deposition might be tissue dependent. Also the physical link between collagen IV and laminin remains unclear, but perlecan might prove a good linker candidate (Behrens et al. 2012). BM architecture and function changes throughout the lifespan of an individual, as they tend to thicken with age (Candiello et al. 2010). The thin BM sheets which are present during embryogenesis are arranged with the long axis of the ECM molecules and parallel to the cell surface (Abrams et al. 2003), while thicker BMs show globular arrangements of the laminin/perlecan side and arrangement of collagen IV that resembles a ball of wool (own observations).

The earliest expressed laminins in vertebrata are laminin α1β1γ1 (LN-111) and LN-511. LN-111 was shown to be essential already in the peri-implantation stage (Smyth 1999), while LN-511 provokes defects if absent in E14 to 17 (Miner et al. 1998). Other laminins that have likely evolved later, induce pre- or postnatal defects based on data from phenotypes in mice, flies and worm mutants (Li et al. 2003). In mammals, epithelia appear before gastrulation. Around the eight cell stage the blastomere compacts to form a morula, followed by a bifurcation that yields trophectodermal cells lining the blastomeric cavity and inner cell mass (ICM). Already at the eight cell stage, expression of α1 subunits is initiated followed by the expression of β1 and γ1 subunits (Cooper et al. 1983). At the blastocyst stage, two BMs are formed – one between the primitive endoderm and the rest of the ICM and the second one that covers trophectoderm. Upon blastocyst implantation at day E4.5 the ICM cells adjacent to this BM develop into the epiblast (primitive ectoderm) while the blastocyst development fails at this stage when laminin γ1 is absent. The fundamental requirement for the unmixing of different epithelia is also highlighted by the very early emergence of BM specific molecules like laminins and collagen IV in evolution. A genome analysis of the nematode C. elegans (Hutter et al. 2000) reveals the presence BM genes (or homologs) with four laminin subunits (αA and αB – precursors to the vertebrate α1, α2 and α3, α4, α5 respectively, for example, the same amount is found in D. melanogaster (Martin et al. 1999)), two collagen IV subunits, nidogen (entactin), perlecan (unc52), agrin and fibulin. In contrast, mammalian interstitial ECM components, such as fibrillary collagens, elastin and fibronectin are absent. Two α-integrin chains are found (*INA-1* is associated with laminin binding and

PAT-2 with tripeptide Arg-Gly-Asp (RGD)-binding) as well as one β-integrin chain (*PAT-3*) and dystroglycan and its cytoplasmic counterparts. In cnydaria it has been shown in Hydra that BM contain a laminin, type IV collagen, fibronectin, and heparan sulfate proteoglycan, whereas the stroma contains type I collagen (Sarras et al. 1991). From analysis of Hydra regeneration following removal of the head, or after body wall incisions, it appears that the laminin plays a critical role in epithelial morphogenesis (Shimizu et al. 2002).

In various organs of different epithelia and microenvironments, such as branching epithelia (Davies 2002), intestinal epithelium (Spenle et al. 2013) and the epithelia of the eye (Byström et al. 2006) it was shown that laminin functions are essential. In submandibular gland explants of embryonic mice, laminin blocking antibodies (Kadoya et al. 1995) and small peptides (Kadoya et al. 1998) that target α1 and α2 chains inhibit branching. Branching is also blocked by anti-laminin antibodies in a 3D mouse organotypic culture mimicking pancreas (Crisera et al. 2000), lung (Schuger et al. 1991), or mouse mammary gland remodeling in puberty (Klinowska et al. 2001). It was shown In salivary glands and kidneys of mouse embryos that inhibiting the laminin β2 nidogen-binding site with an antibody is sufficient to perturb epithelial development (Ekblom et al. 1994). In contrast to laminin, nidogen is secreted by the mesenchyme but its binding to laminin appears to be relevant for the formation of epithelia.

1.4 MECHANOSENSING AND -SIGNALING

By employing their cytoskeleton, cells have a set of tools at hand to interact with the microenvironment based on physical cues. Cells can actively pull on their environment, neighboring cells or ECM substrates and sense the rigidity of the probed structures with the cytoskeleton (Table 1.2). *in vitro*, these cellular tension forces are measured using laser ablation, traction force microscopy, adhesion strength or cytoskeletal polarization (Geiger et al. 2009). Cells employ pulling machines like the actin-myosin complex that pull through actin on cellular adaptor proteins or ECM proteins, to uncover binding sites of the stretched proteins that are hidden (cryptic) when not under load (Schoen et al. 2013). This mechanism is termed mechano-chemical signal transduction (Figure 1.2) and can be applied equally to basal and lateral junctions that contain adaptor proteins or link directly to the ECM. Generally, cells do not use specialized force sensing elements, rather many

proteins that are part of the cytoskeleton or the force-bearing junctions with intrinsic functions that are turned on or off by cycles of stretch and release.
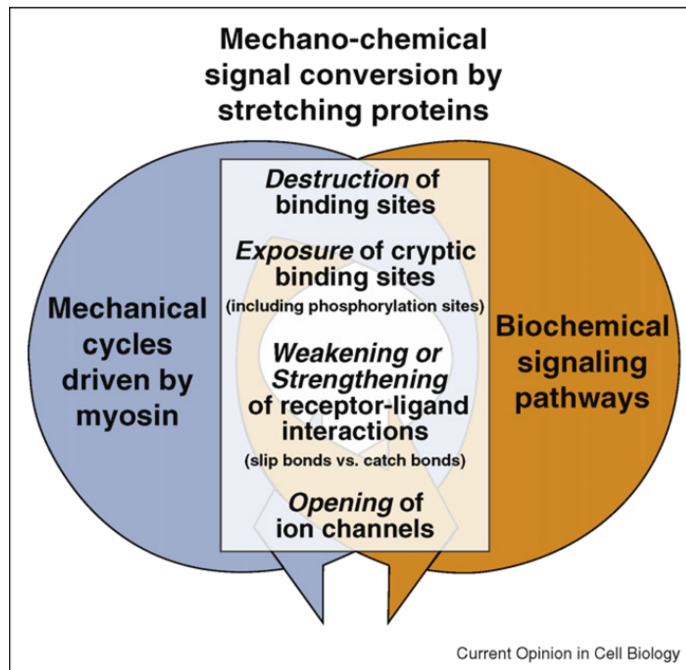
Figure 1.2 Mechano-chemical signal conversion.
Signaling networks are coupled to mechanics through adaptor and structural proteins that serve as mechano-chemical signal converters. Force-induced alterations of the equilibrium structure of proteins can destroy molecular binding motifs or expose cryptic binding sites (Ingham et al. 1997) that are buried in native protein folds. This includes exposing phosphorylation sites (Sawada et al. 2006), dissociation of non-covalent bonds or increase of binding strength of force-activated motifs (Evans et al. 2007). Finally, membrane stretching can open force-sensitive ion-channels (Coste et al. 2010). Adapted from Vogel et al. 2009.

Motor proteins complexes like the actin-myosin apparatus are used to generate contractile forces along the actin cables. The myosin II A and B form short filaments between two anti-parallel actin fibers and can thus move the actin fibers along each other in a sliding motion. The motion is driven by ATP hydrolysis and the movement can reach $100 - 1000$ nm/s (Schnitzer et al. 1997) up to a maximum load of approximately 1.7 pN per myosin molecule (Howard 2015). The built up tension is stored elastically when the ends of both actin fibers are anchored at distant sites in the cell, which can be observed by the recoil of laser cut actin fibers (Tanner et al. 2010). The force applied onto the actin cables spreads to the lateral cell-cell junctions and the basal cell-ECM junctions where actin is anchored in scaffold proteins via adaptor proteins

like α-actinin, filamin, tensin or plectin. The downstream signaling events are then orchestrated by the scaffolding proteins of the respective junctions that interact with the mentioned adaptor proteins, as well as kinases and proteases (reviewed extensively in (Pan et al. 2012; Zaidel-Bar et al. 2007)). In this way, scaffold proteins can trigger signaling cascades that lead to the reinforcement of the individual junction under load (Schoen et al. 2013) or also trigger signaling cascades like MAPK (Pan et al. 2012) or YAP/TAZ (McClatchey et al. 2012) which regulate wide range of cell programs, such as motility, proliferation and differentiation. Reported mechanical factors that modulate YAP/TAZ activity (Low et al. 2014) include stretching (Aragona et al. 2013; Legoff et al. 2013), cell density (Aragona et al. 2013; Kim et al. 2011; Varelas et al. 2010; Zhao et al. 2007), and substrate rigidity (Dupont et al. 2011; Swift et al. 2013; Thomasy et al. 2013). Furthermore, integrins and cadherins that anchor scaffold proteins in the cell membrane and the attached ECM proteins can also be stretched. Most importantly, all of them can alter their structure and hence the function under load (Ingber 1991; Little et al. 2009). Rigidity sensing follows directly from the concept of mechanosensing since cells on stiffer substrates can unveil a different set of cryptic sites. This is made possibley by the involved proteins that can be deformed to a further extent on stiff substrates than on soft substrates. Changing the composition of the substrate can in this way also alter rigidity sensing because the set of integrins and scaffolding proteins are substrate composition dependent (see chapter 3).

1.5 CELL-ECM INTERACTIONS IN VIVO

In this section I will focus on the interactions between epithelial cellular receptors with laminins and perlecan (Iozzo 2005) at the basal side. Laminins and perlecan act as main interaction parters of epithelial cells under physiological tissue conditions. The main cellular interaction partners of laminins are transmembrane integrin receptors expressed as αβ heterodimers (24 pairs) (Humphries et al. 2006). In addition, cells also interact with laminins through α-dystroglycan (Ido et al. 2004).

Integrins seem to co-evolve with their ECM partners. For example integrins that interact with fibrillary collagen or fibronectin or form cell-cell interactions are not present in nematodes or insects because their ECM partners are missing. All integrins except α6β4 have in common that the cytoplasmic domain of the protein is very short, only about 50 AA, which is in contrast to 1000 AA for α6β4 integrin. The α6β4 is also the only integrin heterodimer that
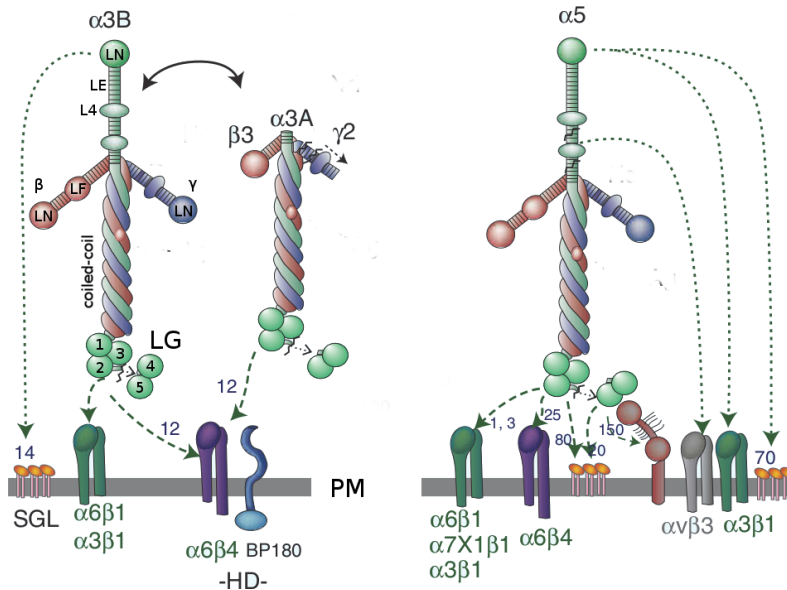
Figure 1.3 Basement membrane components, receptors, and intermolecular binding.
The schematic gives a comprehensive overview of the interactions of the most abundant laminins in human basement membranes (BMs), laminin α3β3γ2 (LN-332) (left) and laminin α5β1γ1 (LN-511) / laminin α5β2γ1 (LN-521) (right) with cellular receptors that are inserted into the plasma membrane (PM) of the cell. The laminins shown here are the only ones that are known to interact with hemidesmosomes (HDs) that are formed by α6β4 integrins. BP180 is also a protein associated with hemidesmosome (HD). HD in turn are the only cellular adhesion complexes that interact with intermediate filament (IF). All shown laminins also interact with α3β1 and α6β1, common integrins found in focal adhesion (FA) that connect to the microfilament (MF) cytoskeleton of the cell. There are two variations on LN-332, one with an α3A chain, the other a α3B chain, only the latter can bind sulfated glycolipids (SGL). SGL are important in the assembly of extracellular laminins. The domains of the laminin chains are indicated in the most-left laminin; amino-terminal laminin globule (LN), carboxy-terminal laminin globular domains (LG), unique globule of β-subunits (LF), laminin-type epidermal growth factor-like repeats (LE) and L4 (globule interrupting two half-LE domains). Heavy solid and thick dashed lines indicate strong interactions, thin dashed lines indicate weaker interactions. Where known, dissociation constants are shown (small numbers in nM values) (Talts et al. 1999; Hopf et al. 2001; Garbe et al. 2002; Nishiuchi et al. 2006; Harrison et al. 2007). Adapted from Yurchenco 2012.

interacts with intermediate filaments (through HD) on the cytoplasmic side while all other integrin heterodimers interact exclusively with the actin-based FA cytoskeleton (Flier et al. 2001).

Integrins can signal inside-out and outside-in, which means that activators can push apart the short cytoplasmic domains, thereby opening the large extra-cellular domains for interactions with ECM molecules and vice versa. For example, interaction with ECM molecules can push apart the cytoplasmic domains to initiate intracellular signaling. Importantly, there is no redundant integrins since any knockout provokes a distinct phenotype (Hynes 2002;

Table 1.1 Dissociation constants of recombinant integrins toward laminin isoforms (low Kd favors bound state). Adapted from (Nishiuchi et al., 2006)
[a] Means $\pm$ SD of three independent experiments.
[b] ND: the dissociation constant could not be determined due to the absence of significant binding.
[c] ND(+): the dissociation constant could not be determined due to only partial saturation at the highest integrin concentration.

| | K_d [nM][a] | | | | |
	LN-111	LN-211/LN-221	LN-332	LN-411	LN-511/LN-521
α3 β1	ND	ND(+)	14 $\pm$ 3	ND	3.4 $\pm$ 0.8
α6 β1	9.5 $\pm$ 3.3	ND(+)	7.5 $\pm$ 2.7	ND(+)	0.73 $\pm$ 0.22
α6 β4	ND	ND	12 $\pm$ 3	ND	25 $\pm$ 1
α7X1 β1	ND(+)	0.64 $\pm$ 0.35	ND	ND(+)	1.2 $\pm$ 0.5
α7X2 β1	0.97 $\pm$ 0.26	2.6 $\pm$ 0.7	ND	ND	ND(+)

Yurchenco et al. 2004). For example, knockouts of laminin binding integrins α3 and 6 lead to perinatal death; through kidney failure, skin blistering reduced branching in the lung and lamination defects in cortex and retina (Anton et al. 1999; DiPersio et al. 1997; Georges-Labouesse et al. 1996; Georges-Labouesse et al. 1998). The α7 integrin is associated with muscular BMs and in case of absence or knockout leads to muscular dystrophy (Mayer et al. 1997).

By using function blocking antibodies in cell-adhesion studies, the main interaction partners for laminins; integrins α3β1, α6β1, α7β1 and α6β4 have been revealed (Belkin et al. 2000; Wondimu et al. 2013). Studies with laminin mutants and laminin-blocking antibodies demonstrated that the main interaction partner for integrins is the LG laminin domain in general, hence laminin α-chains will dominate this interaction (Colognato et al. 2000; Ido et al. 2004). Nishiuchi and colleagues fully characterized binding kinetics of α3β1, α6β1 purified from placenta (Nishiuchi et al. 2003) and recombinant fusion proteins (Nishiuchi et al. 2006) of α3β1, α6β1, α7X1β1, α7X2β1 (two splicing variants X1 and X2) and α6β4 against a panel of laminins containing different α-chains (Table 1.1). Among the five heterodimers investigated, α3β1 and α6β4 show a clear preference for LN-332, LN-511 and LN-521 while they seemed not to interact with LN-111 at all, which is the only laminin component of artificial and *in vitro* reconstituted BMs. This finding highlights the importance of HDs for cell adhesion on BMs containing either LN-511 and LN-521 or LN-332 or both. The integrin α6β1 can interact with the laminin α-chains 1, 3 and 5 but shows a markedly higher binding affinity towards the α5 containing LN-511 and LN-521. The two α7β1 variations could bind all laminins except LN-332. However, the strongest binding affinity of α7β1 was shown to be

towards laminin α2β1γ1 (LN-211) and laminin α2β2γ1 (LN-221), which is supported additionally by the importance of α7β1 in muscle differentiation and maintenance. Interestingly, laminin α4β1γ1 (LN-411) proved to be a very poor ligand for all tested integrin heterodimers. Given the fact that LN-511 and LN-521 are the most widely expressed laminins in adult human tissues, the strong interaction with most integrin heterodimers supports their relevance for the mechanical and functional stability of epithelia in maintaining tissue homeostasis.

1.6 THE EPITHELIAL CYTOSKELETON

The main components of the epithelial cytoskeleton are actin MFs, microtubules (MTs) and IFs (Figure 1.4). MFs and MTs are evolutionary much more conserved while IFs are only found in the metazoans. Three subunits, α, β and γ actin and tubulin are available to form the MF (actin) and MT (tubulin). MFs are 8 nm in diameter, while MTs are 25 nm and IFs have a diameter of 10 nm (Table 1.1).

Table 1.2 Physical properties of cytoskeleton components.
Yield strain is defined as the strain at which the filament breaks when pulled along the long axis. Persistence length lb is the characteristic length-scale at which the tangent-tangent correlation along the filament decays and is proportional (for a simple cylinder) to the bending stiffness k_b, $l_b = k_b/kT$. The contour length l_c is the length of the fully stretched filament and is on the order of few micrometers for all cytoskeleton filaments.

Physical property	MT	IF	MF	Reference
Diameter [nm]	25	10	8	(Herrmann et al. 2009)
Yield strain [%]	10	200	10	(Wen et al. 2011)
Persistence length l_b [m]	$>10^{-3}$	10^{-7} to 10^{-6}	10^{-5}	(Wen et al. 2011)
Stiffness regime	stiff	soft	semi-flexible	

While MTs and MFs display their polarity in the form of a plus and a minus end, which enables directed transport, IFs are apolar. The IFs are assembled from a pool of about 70 genes in humans, which can have very different amino acid sequences but share a common domain organization. IFs can be further divided into cytoplasmic such as keratins, vimentin and desmin and the nuclear lamins that are located beneath the inner nuclear membrane (INM) of the nucleus. Lamins are found in almost all cell types, whereas the cytoplasmic IF are cell-type specific; keratins (8 basic or neutral cytokeratins and 10 acidic cytokeratins) are a hallmark of epithelial cells, vimentin is found in mesenchymal, endothelial and hematopoietic cells and myoblasts contain desmin synemin and syncoilin (Herrmann et al. 2009).

In this text I focus on MF, MT and cytokeratin (CK) and their connections to cell-cell and cell-BM interactions and their role in cell mechanics.

IFs are anchored into the inner plate of HDs and through desmoplakin onto desmosomes(Wiche 1998). They can anchor to AJ and tight junction (TJ) by means of α-catenin, ZO-1, Vinculin and VASP (Vasioukhin et al. 2001) or to FA via vinculin, paxilin and talin (Mitra et al. 2005). In particular, they will form a cage around the nucleus that is tightly associated with the cell membrane and anchored into the basolateral membrane and to the nucleus itself. MFs appear similar but in addition are able to build a very tight actin cortex beneath the apical surface where IFs only show some fibers above the nucleus. In this regard, MTs are quite different, since they do not anchor into the membrane but instead originate from the MTOC that is usually located above the nucleus and can push the MTs throughout the cell (Herrmann et al. 2007). It has been suggested that MT also interact with desmosomes through desmoplakin (Lechler et al. 2007). While MT can exert pushing forces inside the cell, MF are able to pull by the opposing actin fibers that can be pulled towards each other via myosin. In this manner, neighboring cells can exert tension on each other. On the other hand, IFs due to their apolar nature cannot exert force on their own.

The crosslinking of MFs, MTs and IFs is established by members of the plakin family (Bouameur et al. 2014). Mammalians comprise seven members of the plakin family with varying degree of specialization. Plectin, desmoplakin and BPAG1 are found in most epithelia. Plectin is the only member of the family that connects all three cytoskeleton filaments and is involved in MF dynamics through activation of Rho, Rac and Cdc42. Desmoplakin is essential for desmosomes and BPAG1 is a part of the HD that interacts with α6β4 integrins as well as with BP180 (also called BPAG2 or collagen XVII), another HD protein and through its C-terminus with CK5/14. Further, periplakin and envoplakin are epidermis specific proteins associated with desmosomes and the spectraplakin MACF1 is an epidermis specific protein that connects MFs and MTs.

1.7 MECHANOBIOLOGY OF INTERCELLULAR JUNCTIONS

To establish and maintain polarization in development and tissue homeostasis, epithelia employ a series of intercellular and extracellular junctions, later connecting to the underlying ECM (Figure 1.4). AJ are particularly involved in mechanosensing (Harris et al. 2010), since they are directly connected to the actin network (Figure 1.5) and contain mechanosensory actinins and
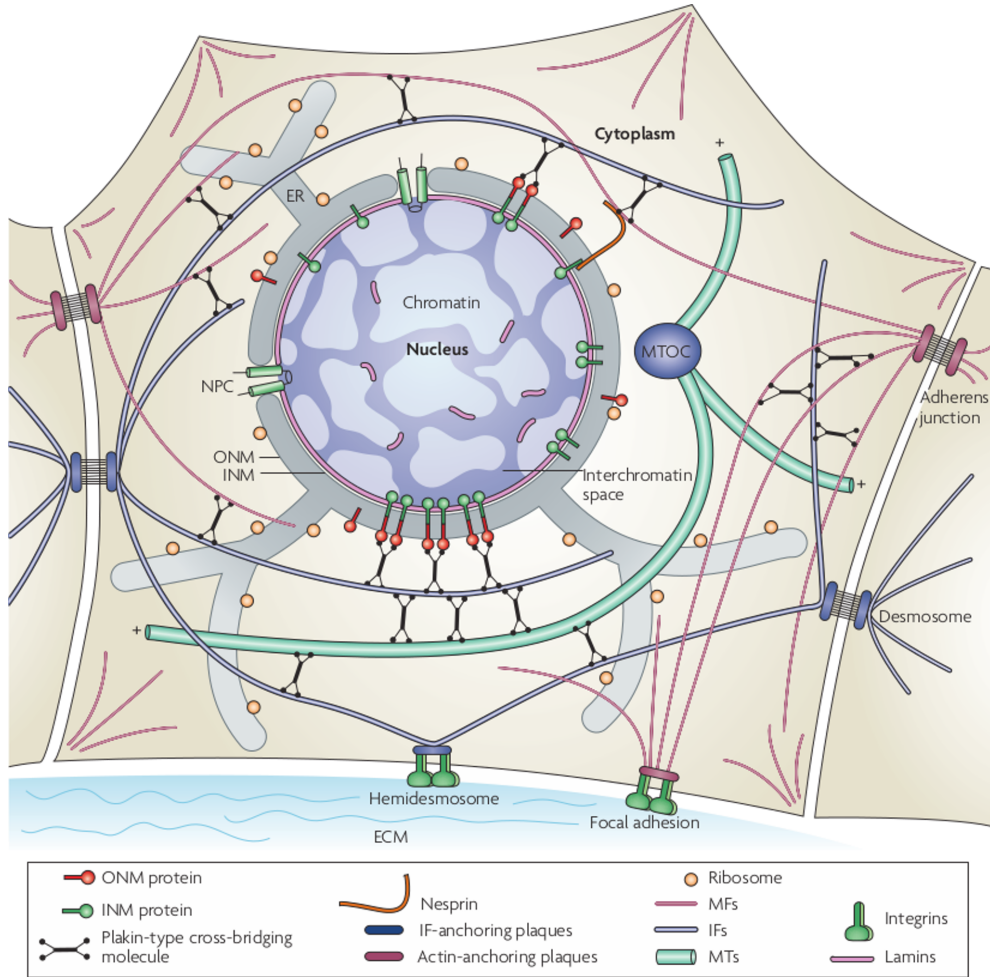
Figure 1.4 Cytoskeleton filament organization in metazoan cells.
Microfilaments (MFs), microtubules (MTs) and intermediate filaments (IFs) are the three major components of the cytoskeleton. They are interconnected to each other through junctions established by members of the plakin familiy, such as plectins and bullous pemphigoid antigen 1 (BPAG1). All junctions rely on so called plaques, dense structures of scaffolding proteins like plakins and catenins that show up in electron microscopy (EM) as plaques and connect cytoskeleton proteins with transmembrane proteins. adherens junctions (AJs) connect to the MF network and neighboring cells while desmosomes link the IFs of neighboring cells. Both junction types rely on cadherins as transmembrane linkers. focal adhesions (FAs) and hemidesmosomes (HDs) are the basal pendants to AJs and desomsomes. FAs link the actin network to the substrate, HDs the IFs. In both cases, integrins are the transmembrane proteins that contact extra-cellular matrix (ECM) proteins outside the cell. The MT network is organized by the microtubule organizing center (MTOC) and crosslinks to IFs through plakins. MF (through Nesprin) and IF can link to outer nuclear membrane (ONM) proteins that connect to inner nuclear membrane (INM) proteins which link to the nuclear lamina, hence connecting cytoplasmic and nucleoplasmic cytoskeletons. Adapted from Herrmann et al. 2007.

catenins. Desmosomes, which link to the intermediate filaments (Garrod et al. 2008) are derived from the evolutionary older AJs and are predominantly present in tissues that are under strong physical stress, such as skin or in the heart musculature (Garrod et al. 2008). In both cases the extracellular link is established through members of the cadherin superfamily. However, they differ in interaction strength and the cytoplasmic binding partners in AJ and desmosomes. There are also notable differences in the density packing between cadherins and desmosomes. Desmosomes are able to reach maximum packing with a spacing of about 7.5 nm between two cadherins, while in AJs cadherins never reach this maximum although it might be possible based on their size and spacing between two cadherins. For example, the human skin has a predicted number of 17'500 cadherins per μm^2 (Al-Amoudi et al. 2007) whereas the packing in AJ is in the order of 700 (Miyaguchi 2000) or 1'200 per μm^2 (McGill et al. 2009) (Figure 1.6). Desmosomes seem to pack into homogeneously dense cadherin structures localizing the applied adhesion forces on distinct spots whereas AJ are more heterogeneous with areas of low and high cadherin densities, eventually required for their quick reorganization during morphogenesis.

The major cadherin in vertebrate AJ are E-cadherin in epithelia and VE-cadherin (vascular endothelial) in endothelia. They contain five extracellular cadherin domains. The first extracellular cadherin domain 1 (EC1) is necessary for homophilic interaction of two cadherins. In contact two EC1 expand β-sheet arms that interact with hydrophobic grooves in the opposing EC1 thereby forming a 'strand exchange dimer'. The binding strength between two EC1 is quite weak and it is assumed that EC2-5 contribute to adhesive strength (Pokutta et al. 2007). The cytoplasmic domain of classical cadherins is highly conserved and directly links to the actin and MT networks via catenins. The interaction between cytoskeleton and cadherins can be described as a positive feedback loop where, actin and MT support AJ formation and AJs can attract more actin and MT. Classical cadherins are sequestered from the ER in conjunction with β-catenin which in turn stabilizes the cytoplasmic domain of the cadherin and prevents exocytosis. Once in the plasma membrane, α-catenin is recruited immediately, forming the cadherin-catenin complex. P120 catenin further stabilizes the complex, preventing endocytosis and degradation and provides the linkage to MT. Finally, α-catenin is essential for AJ function by providing the interface to the actin cytoskeleton. The nature of this link is not yet understood, most probably because the mode of action might be tissue and cell specific since α-catenin can interact with a variety of proteins, such as formin, ZO-1, Vinculin and α-actinin. Moreover, there is a
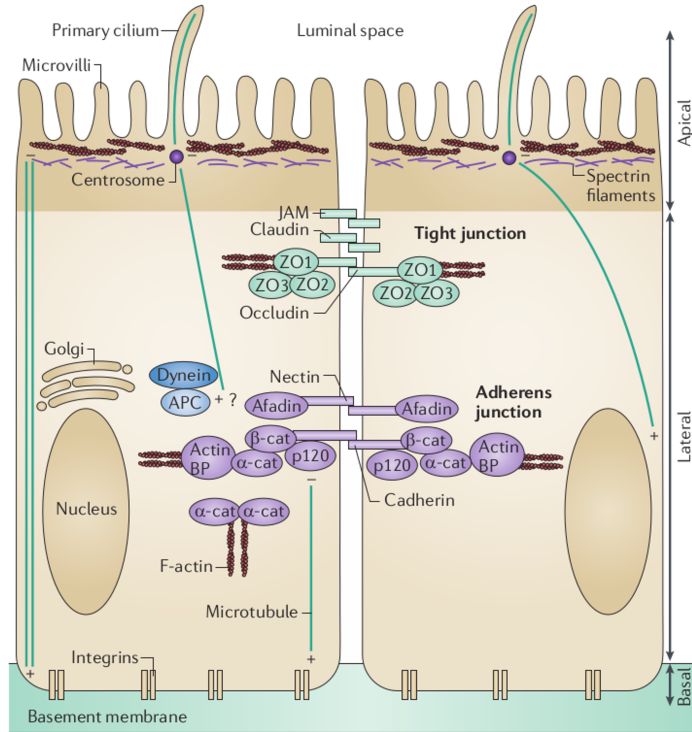
Figure 1.5

positive feedback-loop where cadherin-catenin complex clusters will connect with the actin network and remodel it to further promote AJ growth, enabling highly dynamic AJs (Vasioukhin et al. 2001).

Desmosomes (Figure 1.8) are adhesive junctions in epithelia that provide very strong mechanical anchoring. These junctions consist of members of the desmosomal cadherin families, desmocollin and desmoglein which are derived from E-cadherin (Hulpiau et al. 2009) and the cytoplasmic linker proteins desmoplakin, plakoglobin (γ-catenin) and plakophilin. The latter two are armadillo proteins like β-catenin. In the cytoplasm, this complex links to the CKs. Mutations in any of these structures are related to severe to lethal diseases of the skin, like epidermolysis bullosa (Jonkman et al. 2005) and skin fragility syndrome (McGrath et al. 1997). Desmosomes owe their adhesive strength to high density of cadherins, that enable them to become hyper-adhesive. Classical cadherins in AJ release the EC1 binding if extracellular Ca^{2+} is removed. On the other hand, desmosomal cadherins can be packed densely, such that the Ca^{2+} cannot be removed simply by

Figure 1.5 *(previous page)* TJ and AJ in epithelial cells.

Adherens junctions (AJ) and tight junctions (TJs) participate in the establishment and maintenance of apical-basal polarity in simple epithelia. Two protein complexes define the adhesiveness of adherens junctions: cadherin-catenin and nectin-afadin complexes. Classical cadherins mediate homophilic calcium-dependent cell–cell adhesions through their extracellular domains. Cadherins bind via their cytoplasmic tail to β-catenin and to p120-catenin (p120). Through interactions with actin-binding proteins (actin BP), β-catenin binds to monomeric α-catenin that indirectly anchors the cadherin-catenin complexes to the actin cytoskeleton. The α-catenin dimer preferentially binds actin filaments. Additionally, β-catenin binds to the microtubule motor dynein, and p120-catenin connects cadherin–catenin complexes to microtubules. Nectin through its cytoplasmic domain interactis with afadin and ZO-1, both of them actin-binding proteins. TJ are distributed along the border of the apical and the basolateral domain, located just apically of AJ. The restrict the mobility of proteins and lipids to either of the two domains, in addition they seal the space between neighboring cells to restrict flow in the intercellular space. Occludin, claudin, tricellulin (not shown) and junctional adhesion molecule (JAM) are TJ proteins that bind to several intracellular scaffolding proteins through their cytoplasmic domain. The proteins include ZO1-3, multi-PDZ domain protein 1 (MUPP1) and cingulin (not shown). Adapted from Martin-Belmonte et al. 2012.
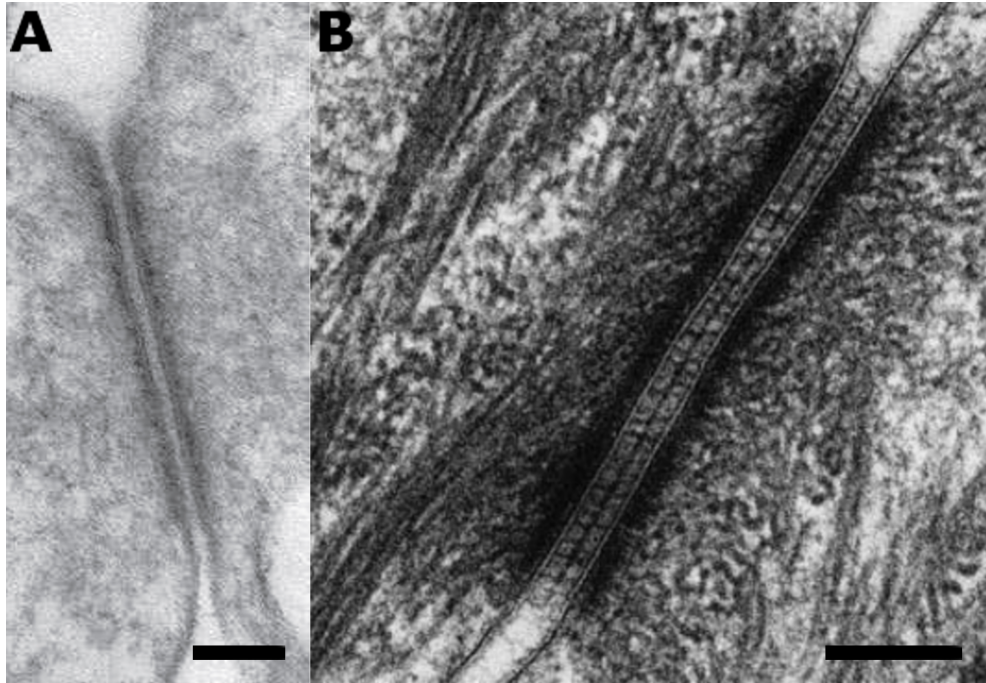
Figure 1.6 TEM micrographs of adherens junction (AJ) and desmosomes.

(A) Adherens junctions (AJ) and (B) desmosomes form junctions with a very electron dense plaque at the plasmamembrane of the cell. However, the plaque itself and the inter-cellular space appear in comparison to their surrounding much electron-denser, indicating the higher packing density in desmosomes than AJ. Scale bars are 100 nm. Adapted from Harris et al. 2010 and He et al. 2003.

depleting extracellular ions and the junction stays adhesive. This very dense packing seems to be controlled from inside the cell via protein kinase C (PKC).

Hyper-adhesiveness is a hallmark of confluent epithelia and is not observed in sub-confluent state (Garrod et al. 2005). Plakoglobin is found both in AJ and desmosomes, but interacts much stronger with desmosomal cadherins. The expression of plakophilin is highly tissue-specific. Plakoglobin through its arm repeats links to desmosomal cadherins and to the plakin domain in desmoplakin, which in turn binds to intermediate filaments. Plakophilin can interact with all these proteins and is thought to support lateral growth of desmosomes.

The catenins and plakins found in AJ and desmosomes are important adaptor proteins used in mechanosensing. Catenins are for instance involved in local re-organization of the actin network when expanding cell-cell junctions where they actively push the actin cortex away to expand the junction through Rac1 and Rho (Yamada et al. 2007). Further, cells put each other into pre-stress in a kind of tug-of-war. This in turn allows for exposing mechanosignaling sites of the adaptor proteins. In this manner, cells are able to maintain a constant ratio of cell-cell forces to cell-ECM forces. This implies that cells on stiffer substrates experience higher cell-cell tension, however, the cell-cell force does not depend on cadherin intensity and the cause of this direct relation between cell-cell and cell-ECM forces remain unclear (Maruthamuthu et al. 2011). The total force at the cell-cell junction is observed to be independent of the junction length and is usually in the order of 10^{-8} to 10^{-7} N (Liu et al. 2010), which is comparable to the order of magnitude of force used in AFM experiments. An example of mechanosignaling to the nucleus is contact inhibition of proliferation (CIP), known to restrict proliferation by activating Hippo through cadherins (McClatchey et al. 2012). However, it was not clear if there is a mechanical link or is this purely due to β-catenin signaling. Recently it has been shown that cells in CIP enter proliferation again when being stretched (Dupont et al. 2011), indicating that stress can break the CIP induced, cadherin mediated Hippo trigger. As described above, stiffer substrates also increase the level of pre-stress in a cell, making it more similar to the physiological state found *in vivo*. This allows for more densely packed epithelia than on soft substrates (see chapter 3).

1.8 CELL-ECM INTERACTIONS FOR RIGIDITY SENSING

Since numerous artificial substrates of varying stiffness, geometry and biological activity are available, cell-ECM interactions have been studied much more extensively than cell-cell interactions. In addition, with traction force microscopy and micro post-substrates there are two technologies available

to easily measure the force applied by the cell onto the substrate. Cells that establish new contacts with a surface usually build up such contacts within 10 to 15 minutes (Fu et al. 2010), with the force increase typically of few nN per minute. The maximum applied force per adhesion site is still a matter of debate (Trichet et al. 2012) but has been shown to increase with substrate stiffness (Saez et al. 2005). Adhesion can be obstructed by using integrin blocking antibodies against the extracellular domain, stressing the importance of extracellular action to reinforce integrin clusters. These interactions are mediated by integrin interactions with cytoskeleton via HD ($\alpha 6 \beta 4$) or FA (all the other heterodimers). While FA have been studied extensively, the mechanosignaling of HD was much less examined. Nevertheless, from table 1.2 it is evident that the two structures must couple to cytoskeleton in very different ways since it is much more difficult to build up force by pulling on IF than on MF because IF can be strained up to 20 times more than MF.
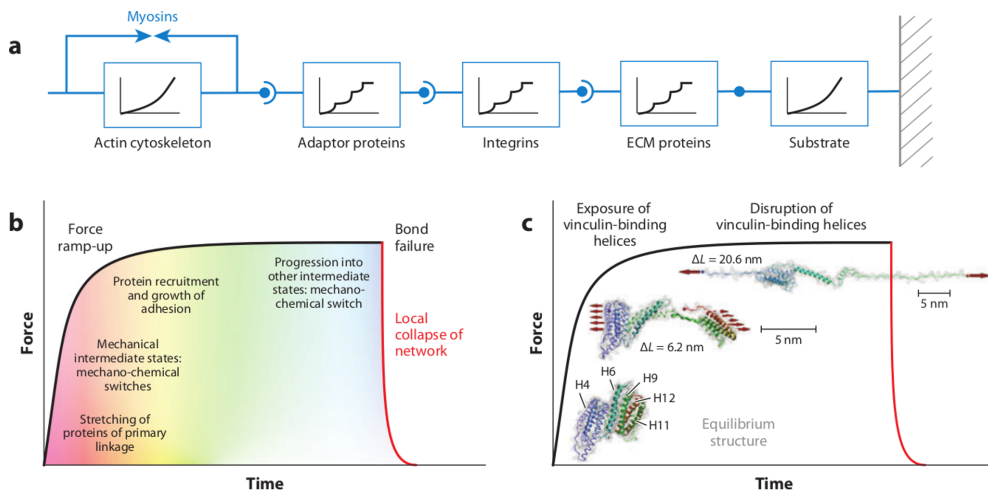
Figure 1.7 Motor-generated forces stretch all proteins of the force-bearing network on which they act. (a) The schematic shows a series of mechanically coupled elements from the cytoskeleton until the substrate of the extra-cellular matrix (ECM). Myosins can pull on anti parallel actin fibers and act as continuous force generators. Adaptor proteins, integrins and ECM proteins all show incremental elongation with force increase, indicating different unfolding states. Also, the joints (except for ECM-substrate) are disconnected, since they can rupture under to much load. (b) Behavior of a hypothetical adaptor protein, integrin or ECM molecule. While the force is ramping up, the molecule quickly undergoes conformational changes exposing cryptic binding sites to recruit more proteins to grow the adhesion site and go into the next conformational state or relapse to the initial state if the bond to actin or other adaptors breaks. (c) In the case of talin, cryptic binding sites for vinculin are exposed under load. The vinculin binding helices become exposed during a certain time before they are straightened further and cannot bind vinculin anymore. The relapse happens probably by breakage of the talin-actin connection. Adapted from Hytönen et al. 2008.

FA are very well studied, together with so called actin stress fibers (Rio et al. 2009). Actin stress fibers may be a pure cell culture artifact but they are a very handy tool to observe basic mode of operation of FA mechanosensing. In FA, the adaptor protein talin connects integrins and actin (Kanchanawong et al. 2010). Under load, multiple cryptic binding sites for vinculin are uncovered and vinculin is then recruited to promote lateral growth of the FA. However this is only possible in a specific force regime since stretching talin too much prevents vinculin from binding again. Additional adapters like paxilin and the scaffold protein p130Cas are recruited to the same site and under load can recruit further β-integrins that can in turn bind more talin (Figure 1.7). In this manner, force on an adhesion site can be steadily increased until no more binding partners can be recruited and the force starts to break the FA (Hytönen et al. 2008). For HD, the mechanistic picture is not clear and only observations are available (Litjens et al. 2006; Underwood et al. 2006) with no models assessing mechanosignaling, even though HD are very much present in mechanically loaded epithelia like skin. One study suggests that stiff substrates in the absence of laminin obstruct clustering of β4 integrins into hemidesmosomes and subsequently PI3K/Rac1 activation by free integrins induces malignancy and cancer cell invasion (Chaudhuri et al. 2014). In terms of signaling pathways, rigidity sensing seems to play a very important role in YAP/TAZ signaling, where simply by switching from soft matrix (<1 kPa) to a stiffer matrix (>40 kPa) enables relocation of YAP/TAZ from the cytoplasm to the nucleus. This indicates that stiff substrates promote proliferation (Dupont et al. 2011). In 3D models this also leads to bigger acini with tubules, instead of small growth-arrested acini. In the light of my work this is consistent with our data, which show that cells are significantly more proliferative on stiff native BM as compared to soft reconstituted BM In addition; this might provide a switch from proliferation to migration once cells encounter softer ECM beyond BM.

1.9 THE RELEVANCE OF BMS IN CANCER CELL INVASION

In cancer, two major cell types are involved: 1) cancer cells that originate from epithelial cells which lost key features such as polarity and 2) CAFs, fibroblasts of in cancerous stromal microenvironment (Bissell et al. 2011). Cancer cells experience atypical mechanical and chemical signaling during invasion (Figure 1.8) due to microenvironmental changes from cell-BM junctions (epithelium) to mostly cell-cell contacts (neoplastic environment) from the early stages to the onset of metastasis. During this progression they experience

environments softer than 1 kPa - neighboring cancer cells (Plodinec et al. 2012) - intermediate environments between 1 and 10 kPa (stroma) and very stiff environments >10 kPa (BM). This implies that their mechanosensation is altered dynamically. Since cells migrate away from the laminin/collagen IV rich BM into collagen I, fibronectin and vitronectin rich stroma, a likely shift might occur from laminin binding integrins (α6β4, α3,6,7β1) to collagen (α2β1, α1β1) and fibronectin/vitronectin (αVβ1,3,6 and αIIβ3, α5,8β1 integrins). In this case, clustering of integrin α6β4 is lost and HD cannot be formed which leads to loss of mechanosensation (Chaudhuri et al. 2014) and increased malignancy through activation of PI3K/Rac both promoting a malignant phenotype (Chaudhuri et al. 2014). Local stiffness sensing is very difficult to study *in situ* since cells are able to pull on fibers very locally (Smith et al. 2007) and ECM fibers usually exhibit strain stiffening (Helvert et al. 2016). Nevertheless, these cells are probably surrounded by a myriad of stiffness regimes. However, a common scheme is that focal adhesion kinase (FAK) and Src are activated (Geiger et al. 2009) and downstream integrin effectors like Rac and Rho reinforce cell protrusion and rear contraction (Riento et al. 2003). A prominent non-integrin linker is CD44, a membrane protein which binds extracellular glycosaminoglycans, heparan sulfates, collagen and fibronectin and intracellular connects to actin via the adaptors ezrin, radixin and moesin (ERM). In this manner, various growth factors are recruited in combination with ECM signalling at this point. It is not clear if CD44 relies on mechanosignaling or if it simply provides co-signaling (Friedl et al. 2011).

In addition, cells form non-classical E-N cadherin junctions with CAFs to migrate collectively (Theveneau et al. 2013) and plakoglobin-based junctions with other cancer cells to metastasize as small clusters (Aceto et al. 2015). The E-N cadherin junctions are supported(Eswaramoorthy et al. 2010; Shintani et al. 2008) by interaction of discoidin domain receptor 1 (DDR1) and discoidin domain receptor 2 (DDR2), two membrane proteins that interact with fibrillar collagen and signal to cytoskeleton regulators although they do not physically crosslink to actin. At the same time, cancer cells in order to invade their surrounding need to break junctions at the rear and form new junctions at the front to move forward. In this context, they can make space either by proteolytically degrading the basement membrane or stroma with MMPs, physically pushing the predominantly fibrillar ECM proteins away or break them. In addition, as a third option they can follow a path that has been previously made by CAFs. DDR1 and DDR2 serve as activators for MMP-1, MMP-2, MMP-9 and MMP-10 (Ruiz et al. 2011) which is triggered by fibrillar collagens. Since BM lacks fibrillar collagen, MMP-independent modes of ECM
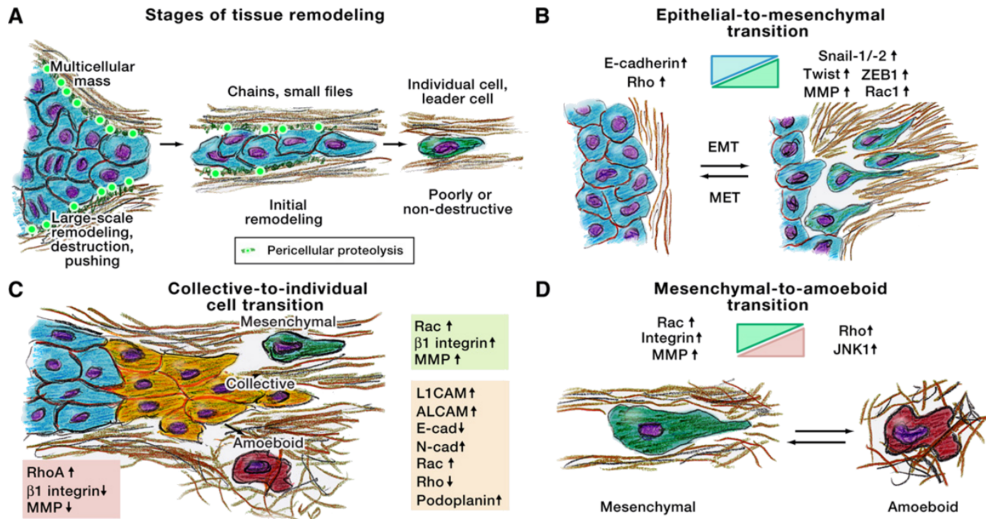
Figure 1.8 Plasticity of Cell-Matrix Interaction, Invasion, and Tissue Remodeling.
(A) Crowded cancer cells break through the basement membrane (BM) and get into contact with the stroma and leave the cell mass either as small clusters connected by strong cell-cell junctions or as individual cells. (B) epithelial-mesenchymal transition (EMT) occurs by downregulating cell-cell junctions, upregulation of motility and breakdown of extra-cellular matrix (ECM). (C and D) Various modes of invasion display irreversible changes of cell phenotype (plasticity) for instance transition from collective cell migration to individual cell migration by down or up regulation of proteins that regulate the cytoskeleton (Rac, Rho) and adhesion molecules (integrins, cadherins) and proteases to degrade ECM - matrix metalloproteinases (MMPs). (D) Transition between mesenchymal (interacting with stroma) and amoeboid movement types (disconnected, rather fluid). Adapted from Friedl et al. 2011.

transmigration are required as suggested in (see chapter 2). Experiments examining the cancer cell invasion on native basement membranes substrates *in vitro* were so far only performed in the labs of Stephen Weiss (Hotary et al. 2006; Rowe et al. 2008) and Danijela Vignjevic (Schoumacher et al. 2013). In both cases, groups utilized mouse mesentery. The Weiss group has observed that soluble MMP are not sufficient to drive invasion and that membrane-type matrix metalloproteinase (MT-MMP) are required, in particular MT-MMP 1, 2 and 3. They could also observe that cells, which are not able to use MT-MMP 1-3, are also not able to develop other means to proteolytically change the mesentery BM. Proteolytic activity is supported by actin-initiated invadopodia that perforate the BM and upon prolongation recruit also microtubules and vimentin intermediate filaments. Fascinatingly, this system can then be used to physically disrupt the BM (Schoumacher et al. 2010).

1.10 TISSUE CULTURE MODELS IN VITRO

The above sections substantiate the importance of ECM in a proper functioning of epithelial cells as well as the relevance to study cell behavior in the physiological ECM context. For this purpose, rBM gels, especially Matrigel (Benton et al. 2011), have been established and extensively used to mimic natural ECM for culturing mammary acini and tumor spheroids in 3D tissue cultures (Lee, Kenny, Lee, & Bissell, 2007) (Lee et al. 2007). These *in vitro* reconstituted environments offer great potential to study early embryogenesis (Li et al. 2003), acinar formation (Debnath et al. 2003) or angiogenesis (Bignon et al. 2011). However, all gel-based 3D models used so far lack the correct protein composition. They are based on LN-111 only (Kleinman et al. 2005) which is mostly absent in adult human BMs. In this case, the ultrastructural assembly of the usually highly polymerized laminin and collagen IV could not be recapitulated and as a consequence density and orientation of the signals provided to epithelia are not defined. Furthermore, these gels are generally softer than epithelial cells. In contrast, native BMs are several orders of magnitude stiffer than the inlying epithelial cells.

Beyond native BM and gels, also protein solutions (laminin, collagen I and fibronectin or poly-L-lysine) are used, either coated directly onto glass or plastic, or in a more physiological setting by tuning stiffness and composition of polymers (Discher et al. 2005; Tse et al. 2010). Another option is to employ culture cells to secret ECM proteins onto a given substrate and then replace the ECM secreting cells by the cells of interest (Vuoristo et al. 2013). The most commonly used artificial polymers are poly-acrylamide (PA) and polydimethylsiloxane (PDMS), which can be easily coated with the BM proteins. They can be produced as thin layers and the stiffness is tunable over a wide range of values and heterogeneity within the same sample (Sunyer et al. 2012). A key technical advantage is that beads can be embedded in these transparent substrates and the forces exerted by cells can be visualized directly using traction force microscopy (Munevar et al. 2001). Currently these systems are predominantly used for migration assays (Roca-Cusachs et al. 2013) but they might also provide means to fabricate invasion assays.

The extravasation process through basement membrane *in vivo* is poorly understood and most of the knowledge is based on studies using spheroids or acini grown in rBMs (Debnath et al. 2003). In this context, matrigel is a very useful tool to study acinar formation *in vitro* and to validate pathways that are activated or shut down during formation of acini, multi-lumen acini or acini that form tubular structures (Debnath et al. 2005). However, very

often this system is used for performing invasion studies where failure to form acini or extrusion of single cells through the basal side is interpreted as invasion (Benton et al. 2011). However, in most of these cases it can be argued that Matrigel is simply not strong enough to prevent extrusion and the term invasion is inappropriate. It has been shown that acini (commonly used for MCF10) and spheroids (commonly used for MDCK, other non-breast epithelia) secrete their own BM LN-332 which is reported as non-polymerizing due to lack of the short arms of the α-subunit (Miner et al. 2004). Hence, LN-332 cannot contribute any mechanical strength that could restrain invasion. Taken together, these data substantiate the need to use native BMs as substrates to study behavior of epithelia *in vitro*.

Rowe and Weiss provided a history of BM 'transmigration' assays (Rowe et al. 2008). In short, in the 70's and 80's the amniotic membrane (Mignatti et al. 1986) and the peritoneum (Buck 1973) attracted a lot of attention. However, the amnion being a very specialized structure exhibited a very complex composition containing collagens I, III, IV, V and VII as well laminins 1, 5, 6 and 7 (Dua et al. 2004). Amnion is a multilayered BM and not simply one bilayered BM which can be up to 1 mm thick in humans. The peritoneum on the other hand is a single BM with a monolayered epithelium (Witz et al. 2001). More recently, mesentery BM has been employed for invasion studies (Schoumacher et al. 2013). The mesentery is a fold of peritoneum and hence a double BM. Further potential basement membranes that are extractable and contain laminin and collagen IV for invasion studies are the bladder (Abrams et al. 2003) and dermis (Garbe et al. 2002). However, it remains to be clarified if they form bilayers of laminin and collagen IV and if their physiological stiffness can be preserved in the extraction process. Finally, ocular BM, the LC, Descemet's membrane (DM), the ILM and Bruch's membrane (BrM) offer a range of variably thick BM that constitute the laminins 1, 10 and 11, similar to kidney and gut for instance, on one side and collagen IV on the other side. With the exception of BrM, these BMs can be extracted as cell-free BM sheets and used directly for *in vitro* culture, preserving their *in vivo* composition and mechanical rigidity (Halfter et al. 2013; Halfter et al. 2015; Uechi et al. 2014).

1.11 PHYSICS OF LIVING CELLS

Living cells are a complex mixture of fibers and solutes, cross-linkers and anchoring points to the ECM, neighboring cells and the nucleus. This entire biological toolbox can be used to mechanically trigger signaling pathways. Unfortunately, the transduction of external stresses into intracellular me-

chanical changes is still poorly understood. The technical limitations in microscopy tools and analysis make it difficult to deduce which part of the cytoskeleton is responsible for triggering specific signaling pathways at a given time. Moreover, a living cell is not a passive element but can pull itself on substrates and neighbors. Thus far, four universal behaviors of the cytoskeleton have been identified (Trepat et al. 2008). (1) Cell rheology is scale free (Figure 1.9). This means that the frequency dependence of neither the storage nor the loss modulus exhibit plateaus or peaks in the frequency space that could be associated with certain structures cytoskeleton. Or in other words, the cytoskeleton does not have a distinct resonance frequency, since it is a complex mix of many different structures, highly crosslinked and embedded in a viscous cytoplasm. Instead, the time-dependence follows a weak power-law, indicating a multitude of time constants in the mechanical system. This has been observed by Fabry and co-workers (Fabry et al. 2003) using optical magnetic twisting cytometry (OMTC). The same has been found for isolated nuclei (Dahl et al. 2005) and neutrophils (Roca-Cusachs et al. 2006) using AFM. However, it remains unclear if specific components such as cell junctions display scale-dependent behavior. (2) Cells are suspected to pre-stress which makes them very different from other soft materials. Prestress serves to fulfil basic biological functions of the cell like rigidity sensing of substrates and neighboring cells. Stress also reveals cryptic sites of filamentous proteins (motifs that are hidden when not under stress) and stressed areas in a cell coincide with higher biological activity. Pre-stress was first observed in fibroblasts that wrinkle the substrate they move on (Harris et al. 1980). Subsequent research identified the location and mechanisms of how pre-stress is built up in cells (Roure et al. 2005; Sabass et al. 2008). (3) Diffusion in cells is anomalous. The dynamics of the cytoskeleton has been studied using microbeads embedded in cells or directly attached to the cytoskeleton. If diffusion in cells was governed by thermal fluctuations, the mean square displacement (MSD) of the observed beads would be a linear function of the time steps $\Delta t\beta$($\beta= 1$). However, the cytoskeleton seems to be sub-diffusive at small Δt (<1 second, $\beta\approx 0.2$) (An et al. 2011) and super-diffusive at bigger time scales ($\beta\approx 1.6$) (Bursac et al. 2005). An interpretation of this is that the cytoskeleton stalls at timescales below 1 second since diffusion preferably occurs away from the direction of the last step (sub-diffusive) but that it progresses quickly into a given direction (super-diffusive) at timescales bigger than seconds. (4) Stiffness and dissipation are altered by substantial stretch, since all cells experience prestress; this adds another dimension of complexity to cellular stiffness. A very important finding is that cellular stiffness does

not only depend on the magnitude of applied stretch but especially on the timescale. While cells under sustained load stiffen (Pourati et al. 1998) which likely arises from the activation of biochemical pathways, over the course of minutes (Matthews et al. 2006). Living cells under short load, i.e. high loading rates, tend to soften and behave more like a fluid (Yap et al. 2005), which goes hand in hand with an increase of cytoskeleton remodeling speed (Trepat et al. 2007).
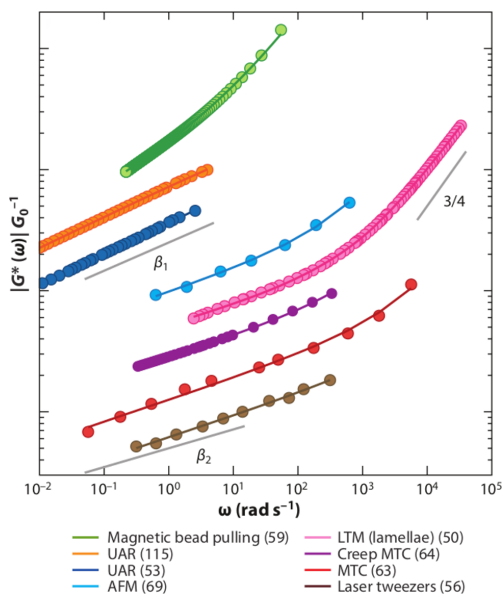
Figure 1.9 Cellular rheology is scale free.
Frequency dependence of the normalized modulus for several different measurement techniques show a power law dependence with a very low power ($\beta_1 = 0.24$ - 0.29, $\beta_2 = 0.13$ - 0.17) in the in the low frequency regime and a transition to higher powers ($3/4$) above frequencies of 1000 Hz. atomic force microscope (AFM); laser tracking microscopy (LTM); magnetic twisting cytometry (MTC); uniaxial rheometry (UAR). Adapted from Hoffman et al. 2009

Rheology (from greek, to flow) studies the reaction of a body to applied force and several models exist in the field that can faithfully describe physical behavior of living cells (Hoffman et al. 2009). Among these models are: the sol-gel hypothesis, the tensegrity model or the glassy rheology model, (Hoffman et al. 2009). Unfortunately, cell mechanics models still lack the ability to link bulk properties of a cell with properties of its single constituents. The sol-gel hypothesis assumes that cells can switch between a liquid state (sol) with shorter cytoskeleton filaments or little crosslinking and a gel phase with longer and more cross-linked filaments that exhibit

elasticity. In this model, the rheology of cells should correspond to the one of *in vitro* assemblies of purified cytoskeleton components. However, the behavior of *in vitro* cytoskeletons matches with cells only at high frequency regimes, showing the limitations of this approach (Hoffman & Crocker, 2009) (Hoffman et al. 2009). The tensegrity model (R. Buckminster Fuller) suggests that mechanically stable structures can be assembled from structures that form a continuous tension, rather than compressive and shear forces. For a cell or any other structure this means that a constant pre-stress is necessary to prevent the structure from collapsing. Actin (myosin) and intermediate filaments (through cell-cell, cell-ECM) connections are assumed to provide this tension, whereas microtubules provide compressive forces (Wang et al. 2000; Wang et al. 2002). The tensegrity model performs well in the quantitative prediction between a linear relation of cell prestress and cell stiffness but since it is a macroscopic model it cannot explain strain stiffening phenomena observed in experiments (Storm et al. 2005). In addition, tensegrity cannot predict the distinct power-law rheology found in cells. soft glass rheology (SGR), first described in 1998 for soft materials (Sollich 1998) and in 2001 applied to cells (Fabry et al. 2001) could faithfully predict the power-law rheology exhibited by cells. The common denominator between cells and soft glass material (SGM) like foams, slurries, pastes or emulsions is that all of them are in disorder and are metastable. A major difference however between cells and SGM is that cytoskeleton rearrangements in cells are driven by ATP consumption whereas SGM are thermally driven. The presence of power-law rheology in cells and SGM could be explained by the fact that cytoskeletal components in cells are trapped in much deeper energy wells, which are similarly shaped as the wells in SGMs.

To summarize, so far there is no model that can predict all observed mechanical properties of cells nor merge macroscopic rheological findings with a mechanistic understanding of the cytoskeleton. New technologies that allow observation of cytoskeleton component rearrangements simultaneously with cell rheology are necessary. One of the few technologies that allows for measurements of subcellular components and whole-cell rheology at the same time is AFM. AFM is used for mechanical characterization of cells and tissues is presented in this thesis and its mode of operation is described in detail in the next section. An important aspect of reliable cell physicss models is to predict how a cell changes when it enters a chemically and mechanically different microenvironment for example during agein, in diabetes or cancer. Relations between cellular properties and microenvironment changes like age or diabetes induced stiffening could be predicted and altered cellular function

be based on changes in mechanical properties of cells or microenvironment. Knowing the pre-stress that cells can build up in a given environment would also allow to predict how mechanosensitive the cell is and hence at what time and under what conditions certain signaling events take place.

1.12 CELL AND TISSUE MECHANICS MEASURED BY AFM AT THE NANOMETER SCALE

The last decade has seen the advent of many technologies, that enable us to study to reaction of a cell to a certain changes in its environment, physical and chemical and to quantify the feedback that the cell is generating. Enabling techniques, among others are, laser-ablation, traction force microscopy (TFM) and atomic force microscope (AFM), high-speed and high-resolution light microscopies and on the cellular level *in vitro* labelling of various structural proteins and sensors to directly measure displacements in a cell such as microbeads or FRET. Recent developments in atomic force microscopy enable researchers to combine high-resolution nanometer scale imaging with quantitative mapping of physical, chemical and biological properties of living matter (Pfreundschuh et al. 2014). Indentation techniques such as atomic force microscopy can measure stiffness by indenting a probe into the sample surface and by alterations of the probe size and shape, mechanical properties of the sample can be assessed both at the micrometer and nanometer scale. The AFM raster-scan technology allows for sequential indentation across large areas and the gain of contextual information from the biological material.

The heart of an AFM consists of four components. A probe (1), referred to as cantilever, made from silicon or silicon-nitride with an indenter of spherical or pyramidal shape attached to its end. The actuator (2) is made from piezo elements owing to their extremely high spatial resolution in the picometer range (Cai et al. 2014) and is used to press the indenter into the sample, or vice versa to pull the cantilever away from a sample. The detection scheme (3) consists of laser and photodiode. The laser is directed onto the backside of the cantilever and reflected to the photodiode, thus reporting the exact position of the cantilever while it is approaching towards, indenting into and retracting from the sample (Figure 1.10 A). Plotting the cantilever deflection against the actuator displacement yields the so-called force curve from which quantities such as stiffness, topography or adhesive forces are extracted (indentation mode) (Cappella et al. 1999; Oliver et al. 1992) (Figure 1.10 B). Additional actuators in x-, y- and z-direction can be added to cover sample sizes from nanometers to millimeters and enable scanning of large cells or complete

tissue resection specimens. The x-y scanner (4) moves either the sample or the probe in order to record 2D maps of force curves (= force-maps) or to hover the probe across the sample surface at a constant cantilever deflection, recording the sample topography (imaging contact mode).
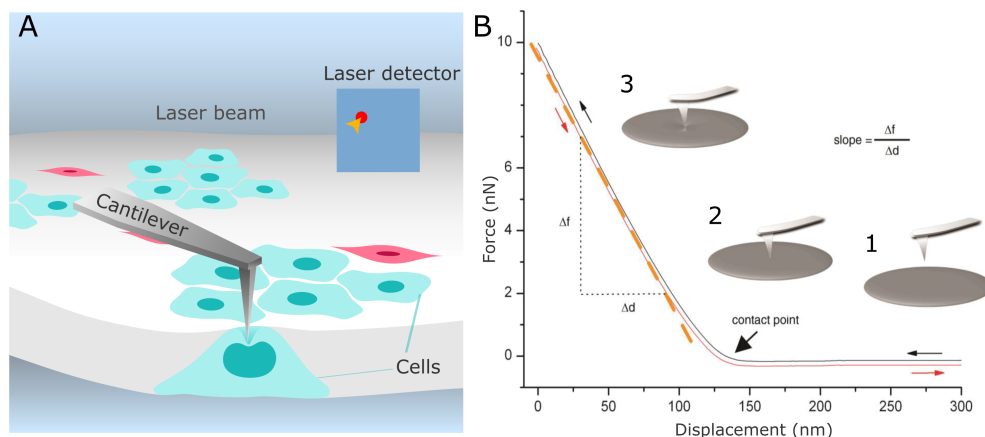
Figure 1.10 Atomic force microscope (AFM) for cell measurements.
(A) atomic force microscope (AFM) cantilever probing cells in a confluent layer. (B) Generation of an indentation force curve while indenting the sample. From Asgeirsson et al. 2015.

The many combinations of lever stiffness, indenter shape (sphere, cone, pyramid, needle, etc.) and the high precision piezo positioning allow for application of loading forces and mechanical measurements at a wide range of spatial and force resolutions. Importantly, this broadens the scope of biological specimens that can be examined. AFM cantilevers are typically a few hundred micrometers in length and some dozen micrometers in width and have a rectangular or triangular shape. Geometry and the type of material will define the lever stiffness k (Sader et al. 1999) which can range from 0.002 (SiN) to 80 N/m (Si). Very soft levers (k <0.01 N/m) are commonly used to characterize (bio-) polymer brushes, single proteins, or soft cells such as red blood cells. Soft levers (0.01 N/m <k <0.2 N/m) are used to measure epithelial cells or fibroblasts and very soft tissues (Dufrêne et al. 2013). Stiffer cantilevers (0.2 N/m <k) are useful for measuring cartilage, bone or teeth. The size of the indenter is the critical defining feature of the spatial resolution that can be achieved using AFM. The tip is either a micrometer-sized bead or an up-side-down pyramidal tip with a diameter between 10 and 25 nanometers. Generally, spherical indenters are used to apply higher forces, in the micro- to millinewton range and at a lower

spatial and force resolution. This is due to the fact that spheres have larger areas that come in direct contact with the sample than pyramids that are measuring forces in the pico- to micronewton range. Spherical indenters measure averaged bulk stiffness of the components within the contact area and can therefore not resolve fine details such as cell compartments or individual ECM fibers. However, the advantage is that measurements can be performed much faster, as long as no high spatial resolution is necessary. In contrast, the nanometer-scale pyramidal tips are able to resolve individual ECM fibers, for example 67-nm axial repeat distance in the collagen fibers (Stolz et al. 2004), or the local stiffness heterogeneities resulting from the complex cytoarchitecture. In summary, these considerations suggest that the spherical AFM tip is large enough to measure the bulk elastic modulus of entire tissues on the micrometer scale, similarly to other rheology methods. On the other hand, the sharp pyramidal AFM tip depicts the elastic properties of living cell and tissue fine structure (Figure 1.11).
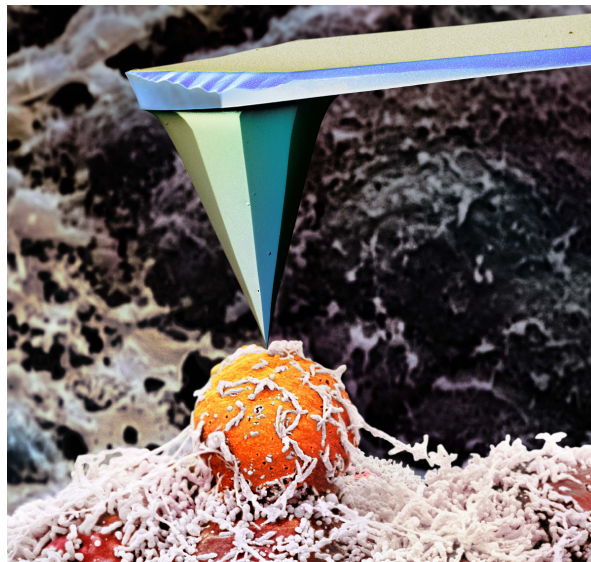
Figure 1.11 Cantilever tip probes escaping cancer cell.
Colored scanning electron microscopy (SEM) image of a cantilever slightly touching a breast cancer cell that is espacing its microenvironment. Adapted from (Plodinec et al. 2012).

The most important point to consider when performing AFM measurements on biological specimens is the choice of an appropriate loading force. Very precise force control is required because biomolecules and tissues probed with AFM are typically heterogeneous, respond nonlinearly and due to high

water content, are highly viscoelastic. Consequently, the stiffness will depend in a non-linear fashion on the amplitude and rate of the applied load. Hence, applied loads and displacements have to be reproducible for comparing the mechanical responses across specimens. A high inter-experimental force control can be achieved by proper calibration of the AFM setup prior to each measurement which includes the spring constant *k* of the cantilever, the deflection sensitivity (DS) relating to the cantilever bending and laser deflection on the photodiode, as well as the actuator expansion for the applied voltage.

Originally invented for research in physics with focus on condensed matter in 1986 (Binnig et al. 1986), AFM was soon applied in life sciences, first to study macro-molecules under non-physiological conditions (Engel 1991) and subsequently for studying cell cultures and primary cells (Cross et al. 2008; Cross et al. 2007; Hoh et al. 1994; Lekka et al. 1999; Lu et al. 2013; Park et al. 2013; Radmacher et al. 1996). In addition to cell stiffness measurements, AFM was readily used to directly measure individual ligand-receptor forces under near-physiological conditions to map antigenic sites on a cell surface by molecular recognition of an antigen by an antibody tethered to an AFM tip (Fritz et al. 1998; Hinterdorfer et al. 1996; Ludwig et al. 1997). Interestingly, first AFM measurements on tissues started much later and were initially performed on stiff specimens such as bone (Diez-Perez et al. 2010; Hansma et al. 2009). Only in recent years, AFM is being used for measuring a variety of soft tissues (Gautier et al. 2015; Mow et al. 1992; Müller et al. 2008; Müller et al. 2011) and tissue biopsies to provide functional information about soft tissue properties from micrometer to nanometer scale which is illustrated in detail in Table 1.3.

Living cells or tissues exhibit rough surfaces that are in the range of micrometers or even millimeters. This is a challenge for AFM measurements, since the indenter is typically 5 to 15 μm long. Ideally, a sample surface should be planar with topology corrugations in a height range of the probe tip and not obstructing the process of indentation. This problem can be easily bypassed by using longer indenters or mounting the whole sample in a way such that the region of interest is elevated (Plodinec et al. 2015). Another key parameter that has to be considered as potential obstacle for the AFM setup is a macroscopic "waviness" of the tissue surface. Tissues exhibiting excessive surface waviness, can for instance cause uneven levelling that will result in cantilever breakage and measurement failure. Native breast tissue biopsies, for instance, exhibit a waviness between 250 - 500 μm, a microscopic tissue "roughness" of approximately 1 to 5 μm, as well as a local ECM porosity of approximately 200 nm. Such problems can be solved by

Table 1.3 Atomic force microscopy for tissue measurements
* spherical indenter
† pyramidal indenter
Contact model: (S)neddon, (O)liver-(P)harr, (H)ertz, (C)alibrator, (D)ynamic measurement Species: (B)ovine, (P)orcine, (M)ouse, (H)uman, (E)we, (G)uinea Pig, (C)hick, (R)at

Tissue type	Organ	Context	Species, Stiffness [kPa]	Reference
Connective tissue	Cartilage	Mechanobiology	(B), 160-600(S)†	(Weisenhorn et al. 1999)
			(P), 2600(OP)*, 20-30(C)†	(Stolz et al. 2004)
			(P), 1300(OP)*, 20-400(OP)†	(Loparic et al. 2010)
			(M), 800-5000(OP)*, 20-60(C)†	(Stolz et al. 2009)
			(B), 200-900(D)*, 200-1100(D)†	(Han et al. 2011)
			(B), 50-600(H+D)*	(Nia et al. 2011)
			(P), 20-400(H)*	(Sanchez-Adams et al. 2013)
		Osteoarthritis	(H), 1300(OP)*, 5-90(C)†	(Stolz et al. 2009)
			(M), 10-10000(D)*	(Nia et al. 2015)
	Bone	Mechanobiology	(E), 16-24(H)†	(Cueru et al. 2011)
	Tendon	Collagen	(B), 1200(H)†	(Grant et al. 2008)
	Basement	Mechanobiology	(H) Ocular BMs, 40-200(OP)†	(Halfter et al. 2013)
	membrane		(H) ILM, 1200-4200(S)†	(Candiello et al. 2010)
			(H) ILM, 50-200(OP)†	(Henrich et al. 2012)
			(C) ILM, 800-4400(S)†	(Candiello et al. 2007)
		Diabetes	(H) LC, 50-800(OP)†	(To et al. 2013)
Muscle tissue	EDL	Muscular dystrophy	(M), 8-24(H)†	(Engler et al. 2004)
	Paravertebral		(H), 1.2-14.8(H)†	(Van Zwieten et al. 2014)
	Tibialis ant.		(M), 1.2-3.9(S)†	(Puttini et al. 2009)
Nervous tissue	Retina	Mechanobiology	(G), 0.9-1.8(H)†	(Franze 2011)
	Hippocampus	Traumatic brain injury	(R), 0.1-0.3(H)*	(Elkin et al. 2007)
	Cerebellum	Mechanobiology	(R), 0.3-0.45(H)*	(Christ et al. 2010)
	Cerebral Cortex	Development	(M), 0.1-0.7(H)*, 0.5-3(S)†	(Iwashita et al. 2014)
Epithelial tissue ((H))	Breast	Cancer	0.5-10(OP)†	(Plodinec et al. 2012)
			0.3-2(H)†	(Lekka et al. 2012)
			0.5-10(H)†	(Mouw et al. 2014)
			0.1-6(H)*	(Acerbi et al. 2015)
			0.1-8(H)†	(Lopez et al. 2011)
	Uterus		0.5-6(H)†	(Lekka et al. 2012)
	Vulva		0.3-2(H)†	(Lekka et al. 2012)
	Liver		0.3-15(H)†	(Tian et al. 2015)
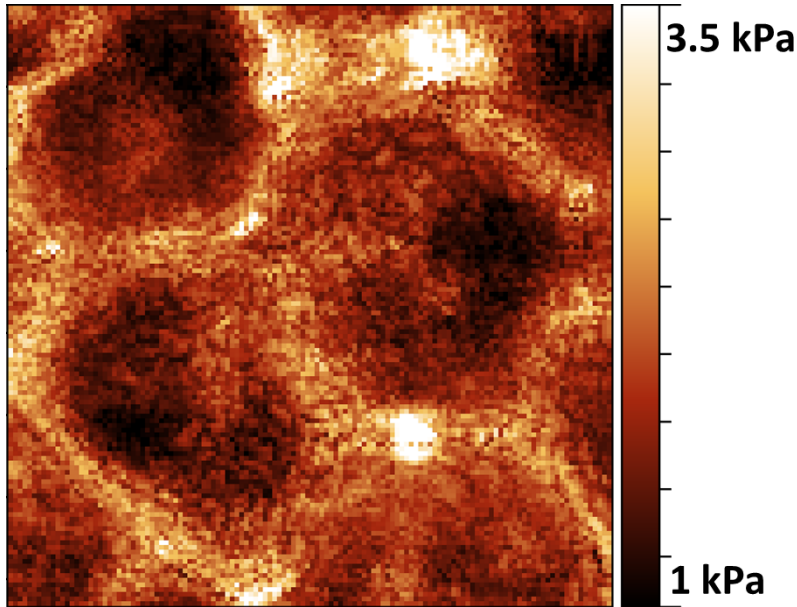
Figure 1.12 High-resolution stiffness map of MDCK cells.
High-resolution stiffness map of MDCK cells with 128 x 128 force curves on 30 x 30 μm.

implementing levelling algorithms and additional actuators that are able to circumvent waviness / roughness by controlled stepwise height changes in the z-direction. To obtain physiologically relevant measurements of living biological specimens, control of the culture medium pH, CO_2 concentration and temperature control should be implemented in the AFM setup. Animal organs and human tissue samples are generally much more resilient than cultured cells, since they are embedded into a fully functional ECM scaffold. However, these samples should also be stored and measured in physiological buffers, such as Ringer solution supplemented with protease inhibitors or Custodiol, in order to prevent tissue alterations and RNA degradation.

1.13 EVALUATION OF AFM STIFFNESS MEASUREMENTS

Stiffness measurements using AFM are performed by slowly, usually μm/s, expanding the piezo carrying either the sample or cantilever, to indent the tip of the cantilever into the sample until a certain piezo extension (height controlled) or a given cantilever deflection (force controlled). In this work, only force control was used, because of two important reasons; (1) cells and

tissues are active materials that can respond to indentation with changing actomyosin contractility and the response is a function of the applied force and (2) cells are very heterogeneous materials and the measured stiffness is a complex function of the applied force. When applying constant force, the response of the cell is always the stiffness can be compared between samples of the same type (cells, BMs, and so forth). This does not hold true for controlled height measurements because the applied force differs for each single force curve due to the high local heterogeneity of stiffness in biological specimen (Figure 1.12).

In order to control the force F applied on the sample, only two parameters of the indentation system need to be known. The spring constant k (in [N/m]) of the cantilever and the so called deflection sensitivity DS (in [nm/V]) of the optical readout of the AFM. Hooke's law (Equation 1.1) states that for small deflections of the cantilever, the applied force is a linear function of the deflection of cantilever.

$$F = k \times d \tag{1.1}$$

The spring constant k is determined an intrinsic property of the cantilever and depends on the lever geometry and the material and is slightly different for each lever. To arrive at comparable results it is very important to calibrate each cantilever. This is commonly done by recording the frequency spectrum of the cantilever. Here, k can subsequently be calculated from the cantilever width and length, the quality factor Q and the resonance frequency f_c (Sader et al. 1999). Because the cantilever deflection d [m] is measured with a photodiode [V], the deflection on the photodiode d needs to be correlated with the physical deflection of the lever c_d using the calibration DS (Equation 1.2) which converts deflection in [V] to deflection in [m].

$$F = k \times c_d \times DS \tag{1.2}$$

The deflection sensitivity DS is determined on a stiff substrate in the same medium in which the experiment is performed. By recording a force curve on an infinitely stiff substrate, DS ca be extracted from the inverse of the slope of the curve (Figure 1.13 A). At this point, the force exerted by the cantilever is known, and constant force measurements can be performed. However, the stiffness of the sample cannot be determined from the collected force curves directly. For stiffness measurements, the stiffness of the indenter and the sample should be around the same order of magnitude and as a result, the sample and the lever both bend when the in contact. The bending of

the cantilever must be subtracted (Equation 1.3) from the total force curve ("Deflection vs. Piezo distance") with the piezo-distance p_d to obtain the sample force curve ("Force vs. Indentation"). The new x-axis, the tip-sample distance, *tsd* experiences a compression in the contact region of the force curve, the curve bends to the left (Figure 1.13 B), i.e. has a steeper slope and gets stiffer because the softness of the lever is removed.

$$tsd = p_d - c_d \times DS \tag{1.3}$$

Finally, there is a couple of contact models that allow us to extract the E-modulus E from the force curve (Equation 1.4). Here, only the Oliver-Pharr model (Oliver et al. 1992) is shown that is used throughout this thesis since its assumptions come closest to the reality of biological samples. Other widespread models are the Hertz and Sneddon models (Sneddon 1965).

$$E = \frac{\sqrt{\Pi}}{2} \left(1 - v^2\right) \frac{S}{\sqrt{A_c\left(h\right)}} \tag{1.4}$$

In the Oliver-Pharr model, E increases linearly with the slope or stiffness S of the force curve of the sample and with power -0.5 dependence on the contact area A_c between the sample and the indenter. Calculation of the contact area for a four-sided pyramidal indenter, the most common shape in nano-indentation, is given in equation 1.5. Here, the indentation depth h is the distance between first contact of sample and tip and maximum indentation (Figure 1.13). The angle Θ is half the opening angle of the pyramid and the Poisson ratio v is assumed to be 0.5, which is the value for incompressible bodies and is good approximation for biological material which is 80 - 90 % water.

$$A_c\left(h\right) = \left(2h \tan\left(\Theta\right)\right)^2 \tag{1.5}$$

The difficulty in most cases lies in accurately determining the contact point c_p in order to extract the indentation depth for calculating the contact area. To improve the contact point search, custom made algorithms were written to automatically determine the contact point. Based on the c_p estimate, a power-law curve is fitted onto the raw data. The slope S is then extract from the fitted curve. All above mentioned contact models assume power-law behavior with an exponent between 1.5 and 2, typically found on very hard material, however values up to three 3 are found on biological materials. This is probably due to a the high viscoelasticity of biological samples. In addition, the calculation of the contact area is derived from imaging the indent on hard

substrates like metals or minerals (Oliver et al. 1992). The contact area will likely be very different on a complex soft material such as livings cells. Both questions could so far not be addressed on biological materials and await the combination of nano-indentation and fast high-resolution optical microscopy (see chapter 4).

1.14 OPEN QUESTIONS & AIM OF THE THESIS

The mechanobiology of epithelial cells is important in developing and maintaining proper cell function based on interactions with their microenvironment. A lot of effort is being made towards designing microenvironments in which stiffness and protein composition can be tuned to the experimental needs. Generally, it has been acknowledged that stiffness and geometries matter and that it is important to study cells in two and three dimensions and not simply on a dish. Uncoupling stiffness and composition of the various microenvironments to dissect the contributing mechano-chemical signals is a tedious task and is a major part of chapter 3.

However, the possibilities to study adult epithelial cells in conditions that are as physiological as possible is emerging rather slowly with only a handful of groups (see section 1.10) working with native basement membranes (BMs) that enable us to study the interactions encoutered by cells *in vivo*, in health and disease. The goal of the presented work is to

1. understand in more detail what the epithelial microenvironment looks like *in vivo* (chapter 3)

2. develop an *in vitro* assay that recapitulates as close as possible the *in vivo* microenvironment and lets us study the mechanobiology at the same time (chapter 3)

3. elucidate what are the key regulators of cellular mechanobiology in this cell-BM *in vitro* assay and what is the impact of silencing them (chapter 3) and finally

4. since we know that the cellular mechanophenotype is related to cancer malignancy, to understand how invasive cancer cells interact with native BM (chapter 2).
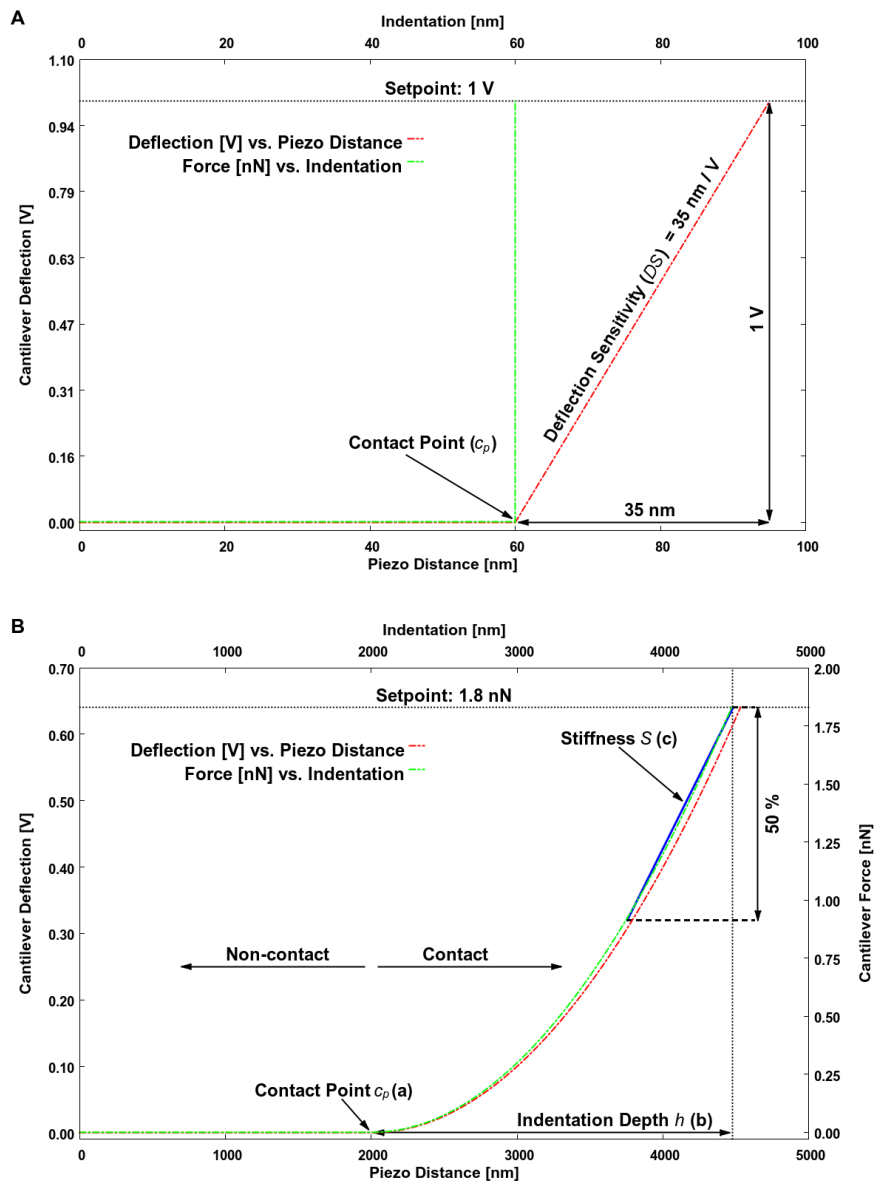
Figure 1.13 Atomic force microscope (AFM) force curve analysis.
Models of AFM force curve recorded on an infinitely stiff substrate (A) and a hypothetical soft material (B) with typical deflections, loads and indentations of biological samples. From Plodinec et al. 2015.

REFERENCES

Abercrombie, M and J E Heaysman (1954). „Observations on the social behaviour of cells in tissue culture. II. Monolayering of fibroblasts." In: *Experimental cell research* 6.2, pp. 293–306. DOI: 10.1016/0014-4827(54)90176-7.

Abercrombie, M and J E Heaysman (1976). „Invasive behavior between sarcoma and fibroblast populations in cell culture.“ In: *Journal of the National Cancer Institute* 56.3, pp. 561–70.

Abrams, George A. et al. (2003). „Ultrastructural basement membrane topography of the bladder epithelium.“ In: *Urological Research* 31.5, pp. 341–346. DOI: 10.1007/s00240-003-0347-9.

Acerbi, I et al. (2015). „Human breast cancer invasion and aggression correlates with ECM stiffening and immune cell infiltration.“ In: *Integr. Biol.* 7.10, pp. 1120–1134.

Aceto, Nicola et al. (2015). „En Route to Metastasis: Circulating Tumor Cell Clusters and Epithelial-to-Mesenchymal Transition.“ In: *Trends in Cancer* 1.1, pp. 44–52. DOI: 10.1016/j.trecan.2015.07.006.

Al-Amoudi, Ashraf et al. (2007). „The molecular architecture of cadherins in native epidermal desmosomes.“ In: *Nature* 450.7171, pp. 832–7. DOI: 10.1038/nature05994.

An, Steven S et al. (2011). „Role of heat shock protein 27 in cytoskeletal remodeling of the airway smooth muscle cell Role of heat shock protein 27 in cytoskeletal remodeling of the airway smooth muscle cell.“ In: 02115.January 2004, pp. 1701–1713. DOI: 10.1152/japplphysiol.01129.2003.

Anton, E S, J a Kreidberg, and P Rakic (1999). „Distinct functions of alpha3 and alpha(v) integrin receptors in neuronal migration and laminar organization of the cerebral cortex.“ In: *Neuron* 22.2, pp. 277–289. DOI: 10.1016/S0896-6273(00)81089-2.

Aragona, Mariaceleste et al. (2013). „A mechanical checkpoint controls multicellular growth through YAP/TAZ regulation by actin-processing factors.“ In: *Cell* 154.5, pp. 1047–1059. DOI: 10.1016/j.cell.2013.07.042.

Asgeirsson, Daphne et al. (2015). „Nanotechnology for Human Health.“ In: ed. by Bert Mueller and Marcel Van de Voorde. 1st edition. Chap. The Nanomechanical Signature of Tissues in Health and Disease.

Behrens, D. T. et al. (Apr. 2012). „The Epidermal Basement Membrane Is a Composite of Separate Laminin- or Collagen IV-containing Networks Connected by Aggregated Perlecan, but Not by Nidogens.“ In: *Journal of Biological Chemistry* 287.22, pp. 18700–18709. DOI: 10.1074/jbc.m111.336073.

Belkin, Alexey M. and Mary Ann Stepp (2000). „Integrins as receptors for laminins.“ In: *Microscopy Research and Technique* 51.3, pp. 280–301. DOI: 10.1002/1097-0029(20001101)51:3<280::AID-JEMT7>3.0.CO;2-O.

Benton, Gabriel et al. (2011). „Multiple uses of basement membrane-like matrix (BME/Matrigel) in vitro and in vivo with cancer cells." In: *International Journal of Cancer* 128.8, pp. 1751–1757. DOI: 10.1002/ijc.25781.

Bignon, Marine et al. (2011). „Lysyl oxidase-like protein-2 regulates sprouting angiogenesis and type IV collagen assembly in the endothelial basement membrane." In: *Blood* 118.14, pp. 3979–3989. DOI: 10.1182/blood-2010-10-313296.

Binnig, G., C. F. Quate, and Ch. Gerber (Mar. 1986). „Atomic Force Microscope." In: *Phys. Rev. Lett.* 56.9, pp. 930–933. DOI: 10.1103/physrevlett.56.930.

Bissell, Mina J and William C Hines (2011). „Why don't we get more cancer? A proposed role of the microenvironment in restraining cancer progression." In: *Nature medicine* 17.3, pp. 320–329.

Bouameur, Jamal-Eddine, Bertrand Favre, and Luca Borradori (2014). „Plakins, a versatile family of cytolinkers: roles in skin integrity and in human diseases." In: *The Journal of investigative dermatology* 134.4, pp. 885–94. DOI: 10.1038/jid.2013.498.

Buck, Robert C (1973). „Walker 256 Tumor Implantation in Normal and Injured Peritoneum Studied by Electron Microscopy , Scanning Electron Microscopy , and Autoradiography Walker 256 Tumor Implantation in Normal and Injured Peritoneum Studied by Electron Microscopy , Scanning Ele." In: DECEMBER, pp. 3181–3188.

Burgeson, Robert E. and Angela M. Christiano (1997). „The dermal-epidermal junction." In: *Current Opinion in Cell Biology* 9.5, pp. 651–658. DOI: 10.1016/S0955-0674(97)80118-4.

Bursac, Predrag et al. (2005). „Cytoskeletal remodelling and slow dynamics in the living cell." In: *Nature materials* 4.7, pp. 557–561. DOI: 10.1038/nmat1404.

Byström, Berit et al. (2006). „Distribution of laminins in the developing human eye." In: *Investigative Ophthalmology and Visual Science* 47.3, pp. 777–785. DOI: 10.1167/iovs.05-0367.

Cai, Jianming, Fedor Jelezko, and Martin B Plenio (2014). „Signal transduction and conversion with color centers in diamond and piezo-elements." In: *arXiv preprint arXiv:1404.6393*.

Candiello, Joseph, Gregory J. Cole, and Willi Halfter (June 2010). „Age-dependent changes in the structure, composition and biophysical properties of a human basement membrane." In: *Matrix Biology* 29.5, pp. 402–410. DOI: 10.1016/j.matbio.2010.03.004.

Candiello, Joseph et al. (2007). „Biomechanical properties of native basement membranes." In: *FEBS Journal* 274.11, pp. 2897–2908. DOI: 10.1111/j.1742-4658.2007.05823.x.

Cappella, Brunero and Giovanni Dietler (1999). „Force-distance curves by atomic force microscopy." In: *Surface science reports* 34.1, pp. 1–104.

Carter, S.B (1968). „Tissue Homeostasis and the biological basis of cancer." In: *Nature* 220, pp. 970–974. DOI: 10.1038/220970a0.

Chaudhuri, Ovijit et al. (2014). „Extracellular matrix stiffness and composition jointly regulate the induction of malignant phenotypes in mammary epithelium." In: *Nature Materials* 13.June, pp. 1–35. DOI: 10.1038/nmat4009.

Christ, Andreas F et al. (2010). „Mechanical difference between white and gray matter in the rat cerebellum measured by scanning force microscopy." In: *Journal of biomechanics* 43.15, pp. 2986–2992.

Colognato, Holly and Peter D Yurchenco (2000). „Form and Function : The Laminin Family of Heterotrimers." In: 234.January, pp. 213–234.

Cooper, Ashley R. and Hilary A. MacQueen (1983). „Subunits of laminin are differentially synthesized in mouse eggs and early embryos." In: *Developmental Biology* 96.2, pp. 467–471. DOI: 10.1016/0012-1606(83)90183-5.

Coste, Bertrand et al. (2010). „Piezo1 and Piezo2 are essential components of distinct mechanically activated cation channels." In: *Science (New York, N.Y.)* 330.6000, pp. 55–60. DOI: 10.1126/science.1193270.

Crisera, Christopher a et al. (2000). „Pancreatic Organogenesis." In: *Diabetes* 49.June, pp. 25–30.

Cross, Sarah E et al. (2007). „Nanomechanical analysis of cells from cancer patients." In: *Nature nanotechnology* 2.12, pp. 780–783.

Cross, Sarah E et al. (2008). „AFM-based analysis of human metastatic cancer cells." In: *Nanotechnology* 19.38, p. 384003.

Cueru, L et al. (2011). „Mechanical and physicochemical multiscale analysis of cortical bone." In: *Computer Methods in Biomechanics and Biomedical Engineering* 14.sup1, pp. 223–225.

Dahl, Kris Noel et al. (2005). „Power-law rheology of isolated nuclei with deformation mapping of nuclear substructures." In: *Biophysical journal* 89.4, pp. 2855–2864. DOI: 10.1529/biophysj.105.062554.

Davies, Jamie A. (2002). „Do different branching epithelia use a conserved developmental mechanism?" In: *BioEssays* 24.10, pp. 937–948. DOI: 10.1002/bies.10161.

Debnath, Jayanta and Joan S Brugge (Sept. 2005). „Modelling glandular epithelial cancers in three-dimensional cultures." In: *Nature reviews. Cancer* 5.9, pp. 675–88. DOI: 10.1038/nrc1695.

Debnath, Jayanta, Senthil K. Muthuswamy, and Joan S. Brugge (July 2003). „Morphogenesis and oncogenesis of MCF-10A mammary epithelial acini grown in three-dimensional basement membrane cultures." In: *Methods* 30.3, pp. 256–268. DOI: 10.1016/S1046-2023(03)00032-X.

Diez-Perez, Adolfo et al. (2010). „Microindentation for in vivo measurement of bone tissue mechanical properties in humans." In: *Journal of Bone and Mineral Research* 25.8, pp. 1877–1885.

DiPersio, C M et al. (1997). „alpha3beta1 Integrin is required for normal development of the epidermal basement membrane." In: *The Journal of cell biology* 137.3, pp. 729–742.

Discher, Dennis E, Paul Janmey, and Yu-Li Wang (Nov. 2005). „Tissue cells feel and respond to the stiffness of their substrate." In: *Science (New York, N.Y.)* 310.5751, pp. 1139–43. DOI: 10.1126/science.1116995.

Dua, Harminder S. et al. (2004). „The amniotic membrane in ophthalmology." In: *Survey of Ophthalmology* 49.1, pp. 51–77. DOI: 10.1016/j.survophthal.2003.10.004.

Dufrêne, Yves F et al. (2013). „Multiparametric imaging of biological systems by force-distance curve-based AFM." In: *Nature methods* 10.9, pp. 847–854.

Dupont, Sirio et al. (2011). „Role of YAP/TAZ in mechanotransduction." In: *Nature* 474.7350, pp. 179–183. DOI: 10.1038/nature10137.

Eisenhoffer, George T. and Jody Rosenblatt (2013). „Bringing balance by force: Live cell extrusion controls epithelial cell numbers." In: *Trends in Cell Biology* 23.4, pp. 185–192. DOI: 10.1016/j.tcb.2012.11.006. arXiv: NIHMS150003.

Ekblom, P et al. (1994). „Role of mesenchymal nidogen for epithelial morphogenesis in vitro." In: *Development (Cambridge, England)* 120.7, pp. 2003–2014.

Elkin, Benjamin S et al. (2007). „Mechanical heterogeneity of the rat hippocampus measured by atomic force microscope indentation." In: *Journal of neurotrauma* 24.5, pp. 812–822.

Engel, Andreas (1991). „Biological applications of scanning probe microscopes." In: *Annual review of biophysics and biophysical chemistry* 20.1, pp. 79–108.

Engler, Adam J et al. (2004). „Myotubes differentiate optimally on substrates with tissue-like stiffness pathological implications for soft or stiff microenvironments." In: *The Journal of cell biology* 166.6, pp. 877–887.

Eswaramoorthy, Rajalakshmanan et al. (2010). „DDR1 regulates the stabilization of cell surface E-cadherin and E-cadherin-mediated cell aggregation." In: *Journal of Cellular Physiology* 224.2, pp. 387–397. DOI: 10.1002/jcp.22134.

Evans, Evan A and David A Calderwood (2007). „Forces and Bond Dynamics in Cell Adhesion." In: 316.5, pp. 1148–1154.

Fabry, Ben et al. (2001). „Scaling the microrheology of living cells." In: *Physical Review Letters* 87.14, pp. 1–4. DOI: 10.1103/PhysRevLett.87.148102.

Fabry, Ben et al. (2003). „Time scale and other invariants of integrative mechanical behavior in living cells." In: *Physical review. E, Statistical, nonlinear, and soft matter physics* 68.4 Pt 1, p. 041914. DOI: 10.1103/PhysRevE.68.041914.

Flier, Arjan van der and Arnoud Sonnenberg (Sept. 2001). „Function and interactions of integrins." In: *Cell and Tissue Research* 305.3, pp. 285–298. DOI: 10.1007/s004410100417.

Franze, Kristian (2011). „Atomic force microscopy and its contribution to understanding the development of the nervous system." In: *Current opinion in genetics & development* 21.5, pp. 530–537.

Friedl, Peter and Stephanie Alexander (2011). „Cancer invasion and the microenvironment: Plasticity and reciprocity." In: *Cell* 147.5, pp. 992–1009. DOI: 10.1016/j.cell.2011.11.016.

Fritz, Jürgen et al. (1998). „Force-mediated kinetics of single P-selectin/ligand complexes observed by atomic force microscopy." In: *Proceedings of the National Academy of Sciences* 95.21, pp. 12283–12288.

Fu, J et al. (2010). „Mechanical regulation of cell function with geometrically modulated elastomeric substrates." In: *Nat Methods* 7.9, pp. 733–736. DOI: 10.1038/nmeth.1487.

Garbe, Jörg H O et al. (2002). „Complete sequence, recombinant analysis and binding to laminins and sulphated ligands of the N-terminal domains of laminin alpha3B and alpha5 chains." In: *The Biochemical journal* 362.Pt 1, pp. 213–21. DOI: 10.1042/0264-6021:3620213.

Garrod, D and M Chidgey (2008). „Desmosome structure, composition and function." In: *Biochimica et Biophysica Acta - Biomembranes* 1778.3, pp. 572–587. DOI: 10.1016/j.bbamem.2007.07.014.

Garrod, David R et al. (2005). „Hyper-adhesion in desmosomes: its regulation in wound healing and possible relationship to cadherin crystal structure." In: *Journal of cell science* 118.Pt 24, pp. 5743–5754. DOI: 10.1242/jcs.02700.

Gautier, Hélène OB et al. (2015). „Atomic force microscopy-based force measurements on animal cells and tissues." In: *Methods in cell biology* 125, pp. 211–235.

Geiger, Benjamin, Joachim P Spatz, and Alexander D Bershadsky (2009). „Environmental sensing through focal adhesions." In: *Nature reviews. Molecular cell biology* 10.1, pp. 21–33. DOI: 10.1038/nrm2593.

Georges-Labouesse, Elisabeth et al. (Aug. 1998). „Essential role of α6 integrins in cortical and retinal lamination." In: *Current Biology* 8.17, 983–S1. DOI: 10.1016/s0960-9822(98)70402-6.

Georges-Labouesse, E et al. (1996). „Absence of integrin alpha 6 leads to epidermolysis bullosa and neonatal death in mice." In: *Nature genetics* 13.3, pp. 370–373. DOI: 10.1038/ng0796-370.

Grant, Colin A et al. (2008). „Effects of hydration on the mechanical response of individual collagen fibrils." In: *Applied Physics Letters* 92.23, p. 233902.

Halfter, Willi et al. (2015). „New concepts in basement membrane biology." In: *FEBS Journal* 282.23, pp. 4466–4479.

Halfter, Willi et al. (Jan. 2013). „The bi-functional organization of human basement membranes." In: *PloS one* 8.7, e67660. DOI: 10.1371/journal.pone.0067660.

Han, Lin et al. (2011). „Time-dependent nanomechanics of cartilage." In: *Biophysical journal* 100.7, pp. 1846–1854.

Hanahan, Douglas and Robert A Weinberg (2011). „Hallmarks of cancer: the next generation." In: *cell* 144.5, pp. 646–674.

Hansma, Paul et al. (2009). „The tissue diagnostic instrument." In: *Review of Scientific Instruments* 80.5, p. 054303.

Harris, a K, P Wild, and D Stopak (1980). „Silicone rubber substrata: a new wrinkle in the study of cell locomotion." In: *Science (New York, N.Y.)* 208.4440, pp. 177–179. DOI: 10.1126/science.6987736.

Harris, T J and U Tepass (2010). „Adherens junctions: from molecules to morphogenesis." In: *Nat Rev Mol Cell Biol* 11.7, pp. 502–514. DOI: nrm2927[pii]$\backslash$r10.1038/nrm2927. arXiv: 77953878405.

Harrison, David et al. (2007). „Crystal structure and cell surface anchorage sites of laminin α1LG4-5." In: *Journal of Biological Chemistry* 282.15, pp. 11573–11581.

He, Wanzhong, Pamela Cowin, and David L Stokes (2003). „Untangling desmosomal knots with electron tomography." In: *Science (New York, N.Y.)* 302.5642, pp. 109–113. DOI: 10.1126/science.1086957.

Helvert, S van and P Friedl (2016). „Strain stiffening of fibrillar collagen during individual and collective cell migration identified by AFM nanoindentation." In: *ACS Appl Mater Interfaces* (in press). DOI: 10.1021/acsami.6b01755.

Henrich, Paul B. et al. (June 2012). „Nanoscale Topographic and Biomechanical Studies of the Human Internal Limiting Membrane." In: *Investigative Opthalmology & Visual Science* 53.6, p. 2561. DOI: 10.1167/iovs.11-8502.

Herrmann, Harald et al. (2007). „Intermediate filaments: from cell architecture to nanomechanics." In: *Nature Reviews Molecular Cell Biology* 8.7, pp. 562–573. DOI: 10.1038/nrm2197.

Herrmann, Harald et al. (2009). *Intermediate filaments: Primary determinants of cell architecture and plasticity.* DOI: 10.1172/JCI38214.

Hinterdorfer, Peter et al. (1996). „Detection and localization of individual antibody-antigen recognition events by atomic force microscopy." In: *Proceedings of the National Academy of Sciences* 93.8, pp. 3477–3481.

Hoffman, Brenton D. and John C. Crocker (2009). „Cell Mechanics: Dissecting the Physical Responses of Cells to Force." In: *Annual Review of Biomedical Engineering* 11.1, pp. 259–288. DOI: 10.1146/annurev.bioeng.10.061807.160511.

Hoh, Jan H and Cora-Ann Schoenenberger (1994). „Surface morphology and mechanical properties of MDCK monolayers by atomic force microscopy." In: *Journal of cell science* 107.5, pp. 1105–1114.

Hopf, Michael et al. (2001). „Mapping of binding sites for nidogens, fibulin-2, fibronectin and heparin to different IG modules of perlecan." In: *Journal of molecular biology* 311.3, pp. 529–541.

Hotary, Kevin et al. (2006). „A cancer cell metalloprotease triad regulates the basement membrane transmigration program." In: *Genes & development* 20.19, pp. 2673–2686.

Howard, Jonathon (2015). „Mechanics of Motor Proteins and the Cytoskeleton." In: *Aging* 7.11, pp. 956–963. DOI: 10.1017/CBO9781107415324.004. arXiv: arXiv:1011.1669v3.

Hulpiau, Paco and Frans van Roy (2009). „Molecular evolution of the cadherin superfamily." In: *International Journal of Biochemistry and Cell Biology* 41.2, pp. 349–369. DOI: 10.1016/j.biocel.2008.09.027.

Humphries, Jonathan D, Adam Byron, and Martin J Humphries (Oct. 2006). „Integrin ligands at a glance." In: *Journal of cell science* 119.Pt 19, pp. 3901–3. DOI: 10.1242/jcs.03098.

Hutter, Harald et al. (2000). „Cell Adhesion and Extracellular Matrix Genes." In: 287.February, pp. 989–995. DOI: 10.1126/science.287.5455.989.

Hynes, RO (2002). „Integrins: bidirectional, allosteric signaling machines." In: *Cell* 110.Table 1, pp. 673–687.

Hytönen, Vesa P and Viola Vogel (2008). „How Force Might Activate Talin's Vinculin Binding Sites: SMD Reveals a Structural Mechanism." In: *Current*

Science 4.2, pp. 1435–1439. DOI: 10.1371/journal.pcbi.0040024.eor. arXiv: 1203.2655.

Ido, Hiroyuki et al. (2004). „Molecular Dissection of the alpha-Dystroglycan- and Integrin-binding Sites within the Globular Domain of Human Laminin-10." In: *Journal of Biological Chemistry* 279.12, pp. 10946–10954. DOI: 10.1074/jbc.M313626200.

Ingber, Donald E (1991). „Integrins as mechanochemical transducers." In: *Current Opinion in Cell Biology* 3.5, pp. 841–848. DOI: 10.1016/0955-0674(91)90058-7.

Ingham, Kenneth C. et al. (1997). „Cryptic self-association sites in type III modules of fibronectin." In: *Journal of Biological Chemistry* 272.3, pp. 1718–1724. DOI: 10.1074/jbc.272.3.1718.

Iozzo, R V et al. (1994). „The biology of perlecan: the multifaceted heparan sulphate proteoglycan of basement membranes and pericellular matrices." In: *Biochemical Journal* 302.3, pp. 625–639.

Iozzo, Renato V. (Aug. 2005). „Basement membrane proteoglycans: from cellar to ceiling." In: *Nature Reviews Molecular Cell Biology* 6.8, pp. 646–656. DOI: 10.1038/nrm1702.

Iwashita, Misato et al. (2014). „Systematic profiling of spatiotemporal tissue and cellular stiffness in the developing brain." In: *Development* 141.19, pp. 3793–3798.

Jonkman, Marcel F et al. (2005). „Loss of desmoplakin tail causes lethal acantholytic epidermolysis bullosa." In: *American journal of human genetics* 77.4, pp. 653–60. DOI: 10.1086/496901.

Kadoya, Y. et al. (1995). „Antibodies against domain E3 of laminin-1 and integrin a6 subunit perturb branching epithelial morphogenesis of submandibular gland, but by different modes." In: *Journal of Cell Biology* 129.2, pp. 521–534. DOI: 10.1083/jcb.129.2.521.

Kadoya, Yuichi et al. (1998). „Laminin a1 chain G domain peptide, RKR-LQVQLSIRT, inhibits epithelial branching morphogenesis of cultured embryonic mouse submandibular gland." In: *Developmental Dynamics* 212.3, pp. 394–402. DOI: 10.1002/(SICI)1097-0177(199807)212:3<394::AID-AJA7>3.0.CO;2-C.

Kanchanawong, Pakorn et al. (2010). „Nanoscale architecture of integrin-based cell adhesions." In: *Nature* 468.7323, pp. 580–4. DOI: 10.1038/nature09621.

Khoshnoodi, Jamshid, Vadim Pedchenko, and Billy G. Hudson (2008). „Mammalian collagen IV." In: *Microscopy Research and Technique* 71.5, pp. 357–370. DOI: 10.1002/jemt.20564.

Kim, Nam-Gyun et al. (2011). „E-cadherin mediates contact inhibition of proliferation through Hippo signaling-pathway components." In: *Proceedings of the National Academy of Sciences of the United States of America* 108.29, pp. 11930–11935. DOI: 10.1073/pnas.1103345108.

Kleinman, Hynda K and George R Martin (2005). „Matrigel: basement membrane matrix with biological activity." In: *Seminars in cancer biology*. Vol. 15. 5. Elsevier, pp. 378–386.

Klinowska, T C et al. (2001). „Epithelial development and differentiation in the mammary gland is not dependent on alpha 3 or alpha 6 integrin subunits." In: *Developmental biology* 233.2, pp. 449–467. DOI: 10.1006/dbio.2001.0204.

Knust, E and O Bossinger (2002). „Composition and formation of intercelular junctions in epithelial cells." In: *Science* 298.2002, pp. 1955–1959. DOI: 10.1126/science.1072161.

Lechler, Terry and Elaine Fuchs (2007). „Desmoplakin: An unexpected regulator of microtubule organization in the epidermis." In: *Journal of Cell Biology* 176.2, pp. 147–154. DOI: 10.1083/jcb.200609109.

Lee, Jiwoon and Jeffrey M. Gross (June 2007). „Laminin β1 and γ1 Containing Laminins Are Essential for Basement Membrane Integrity in the Zebrafish Eye." In: *Investigative Opthalmology & Visual Science* 48.6, p. 2483. DOI: 10.1167/iovs.06-1211.

Legoff, Loïc, Hervé Rouault, and Thomas Lecuit (2013). „A global pattern of mechanical stress polarizes cell divisions and cell shape in the growing Drosophila wing disc." In: *Development (Cambridge, England)* 140.19, pp. 4051–9. DOI: 10.1242/dev.090878.

Lekka, Małgorzata et al. (2012). „Cancer cell detection in tissue sections using AFM." In: *Archives of Biochemistry and Biophysics* 518.2, pp. 151–156. DOI: 10.1016/j.abb.2011.12.013.

Lekka, M et al. (1999). „Elasticity of normal and cancerous human bladder cells studied by scanning force microscopy." In: *European Biophysics Journal* 28.4, pp. 312–316.

Li, Shaohua et al. (2003). „The role of laminin in embryonic cell polarization and tissue organization." In: *Developmental Cell* 4.5, pp. 613–624. DOI: 10.1016/S1534-5807(03)00128-X.

Litjens, Sandy H M, José M de Pereda, and Arnoud Sonnenberg (July 2006). „Current insights into the formation and breakdown of hemidesmosomes." In: *Trends in cell biology* 16.7, pp. 376–83. DOI: 10.1016/j.tcb.2006.05.004.

Little, William C. et al. (2009). „Stretched extracellular matrix proteins turn fouling and are functionally rescued by the chaperones albumin and casein." In: *Nano Letters* 9.12, pp. 4158–4167. DOI: 10.1021/nl902365z.

Liu, Z. et al. (2010). „Mechanical tugging force regulates the size of cell-cell junctions." In: *Proceedings of the National Academy of Sciences* 107.22, pp. 9944–9949. DOI: 10.1073/pnas.0914547107.

Loparic, Marko et al. (June 2010). „Micro- and Nanomechanical Analysis of Articular Cartilage by Indentation-Type Atomic Force Microscopy: Validation with a Gel-Microfiber Composite." In: *Biophysical Journal* 98.11, pp. 2731–2740. DOI: 10.1016/j.bpj.2010.02.013.

Lopez, Jose I et al. (2011). „In situ force mapping of mammary gland transformation." In: *Integrative Biology* 3.9, pp. 910–921.

Low, Boon Chuan et al. (2014). „YAP/TAZ as mechanosensors and mechanotransducers in regulating organ size and tumor growth." In: *FEBS Letters* 588.16, pp. 2663–2670. DOI: 10.1016/j.febslet.2014.04.012.

Lu, Yun-Bi et al. (2013). „Biomechanical properties of retinal glial cells: Comparative and developmental data." In: *Experimental eye research* 113, pp. 60–65.

Ludwig, M, W Dettmann, and HE Gaub (1997). „Atomic force microscope imaging contrast based on molecular recognition." In: *Biophysical journal* 72.1, p. 445.

Martin-Belmonte, Fernando and Mirna Perez-Moreno (2012). „Epithelial cell polarity, stem cells and cancer." In: *Nature reviews. Cancer* 12.1, pp. 23–38. DOI: 10.1038/nrc3169.

Martin, Doris et al. (1999). „wing blister, A new Drosophila laminin chain required for cell adhesion and migration during embryonic and imaginal development." In: *Journal of Cell Biology* 145.1, pp. 191–201. DOI: 10.1083/jcb.145.1.191.

Maruthamuthu, Venkat et al. (2011). „Cell-ECM traction force modulates endogenous tension at cell-cell contacts." In: *Proceedings of the National Academy of Sciences* 108.10, pp. 4057–4062. DOI: 10.1073/pnas.101.

Matthews, Benjamin D et al. (2006). „Cellular adaptation to mechanical stress: role of integrins, Rho, cytoskeletal tension and mechanosensitive ion channels." In: *Journal of cell science* 119.Pt 3, pp. 508–518. DOI: 10.1242/jcs.02760.

Mayer, Ulrike et al. (1997). „Absence of integrin alpha7 causes a novel form of muscular dystrophy." In: *Nature Genetics* 17, pp. 318–323. DOI: 10.1038/ng0595-111.

McClatchey, Andrea I. and Alpha S. Yap (2012). „Contact inhibition (of prolif-eration) redux.“ In: *Current Opinion in Cell Biology* 24.5, pp. 685–694. DOI: 10.1016/j.ceb.2012.06.009. arXiv: 84867874350.

McGill, Melanie A., R. F Andrew McKinley, and Tony J C Harris (2009). „Independent cadherin-catenin and Bazooka clusters interact to assemble adherens junctions.“ In: *Journal of Cell Biology* 185.5, pp. 787–796. DOI: 10.1083/jcb.200812146.

McGrath, J a et al. (1997). „Mutations in the plakophilin 1 gene result in ectodermal dysplasia/skin fragility syndrome.“ In: *Nature genetics* 17, pp. 240–244. DOI: 10.1038/ng1097-240.

McKee, Karen K. et al. (2007). „Role of laminin terminal globular domains in basement membrane assembly.“ In: *Journal of Biological Chemistry* 282.29, pp. 21437–21447. DOI: 10.1074/jbc.M702963200.

Mellman, Ira and W James Nelson (2008). „Coordinated protein sorting, targeting and distribution in polarized cells.“ In: *Nature reviews. Molecular cell biology* 9.11, pp. 833–845. DOI: 10.1038/nrm2525. arXiv: NIHMS150003.

Mignatti, Paolo and Edith Robbins (1986). „Tumor Invasion through the Human Amniotic Membrane : Requirement for a Proteinase Cascade.“ In: 47, pp. 487–498. DOI: 10.1016/0092-8674(86)90613-6.

Miner, Jeffrey H., Jeanette Cunningham, and Joshua R. Sanes (Dec. 1998). „Roles for Laminin in Embryogenesis: Exencephaly, Syndactyly, and Pla-centopathy in Mice Lacking the Laminin $\alpha 5$ Chain.“ In: *J Cell Biol* 143.6, pp. 1713–1723. DOI: 10.1083/jcb.143.6.1713.

Miner, Jeffrey H. and Peter D. Yurchenco (Jan. 2004). „Laminin functions in tissue morphogenesis.“ In: *Annual review of cell and developmental biology* 20.M, pp. 255–84. DOI: 10.1146/annurev.cellbio.20.010403.094555.

Mitra, S K, D A Hanson, and D D Schlaepfer (2005). „Focal adhesion kinase: in command and control of cell motility.“ In: *Nature review of Molecular Cell Biology* 6.1, pp. 56–68. DOI: 10.1038/nrm1549.

Miyaguchi, Katsuyuki (2000). „Ultrastructure of the Zonula Adherens Re-vealed by Rapid-Freeze Deep-Etching.“ In: *Journal of Structural Biology* 132.3, pp. 169–178. DOI: 10.1006/jsbi.2000.4244.

Mouw, Janna K et al. (2014). „Tissue mechanics modulate microRNA-dependent PTEN expression to regulate malignant progression.“ In: *Nature medicine* 20.4, p. 360.

Mow, Van C, Anthony Ratcliffe, and A Robin Poole (1992). „Cartilage and diarthrodial joints as paradigms for hierarchical materials and structures.“ In: *Biomaterials* 13.2, pp. 67–97.

Müller, Daniel J and Yves F Dufrene (2008). „Atomic force microscopy as a multifunctional molecular toolbox in nanobiotechnology." In: *Nature nanotechnology* 3.5, pp. 261–269.

Müller, Daniel J and Yves F Dufrêne (2011). „Atomic force microscopy: a nanoscopic window on the cell surface." In: *Trends in cell biology* 21.8, pp. 461–469.

Munevar, Steven, Yu-Li Wang, and Micah Dembo (2001). „Traction Force Microscopy of Migrating Normal and H-ras Transformed 3T3 Fibroblasts." In: *Biophysical Journal* 80.4, pp. 1744–1757. DOI: 10.1016/S0006-3495(01)76145-0.

Nia, Hadi Tavakoli et al. (2011). „Poroelasticity of cartilage at the nanoscale." In: *Biophysical journal* 101.9, pp. 2304–2313.

Nia, Hadi T et al. (2015). „High-bandwidth AFM-based rheology is a sensitive indicator of early cartilage aggrecan degradation relevant to mouse models of osteoarthritis." In: *Journal of biomechanics* 48.1, pp. 162–165.

Nishiuchi, Ryoko et al. (2003). „Characterization of the Ligand-Binding Specificities of Integrin $\alpha 3\beta 1$ and $\alpha 6\beta 1$ Using a Panel of Purified Laminin Isoforms Containing Distinct α Chains." In: *Journal of Biochemistry* 134.4, pp. 497–504. DOI: 10.1093/jb/mvg185.

Nishiuchi, Ryoko et al. (2006). „Ligand-binding specificities of laminin-binding integrins: A comprehensive survey of laminin-integrin interactions using recombinant a3b1, a6b1, a7b1 and a6b4 integrins." In: *Matrix Biology* 25.3, pp. 189–197. DOI: 10.1016/j.matbio.2005.12.001.

Oliver, W.C. and G.M. Pharr (June 1992). „An improved technique for determining hardness and elastic modulus using load and displacement sensing indentation experiments." In: *Journal of Materials Research* 7.06, pp. 1564–1583. DOI: 10.1557/jmr.1992.1564.

Pan, Catherine Qiurong et al. (2012). „Modularity and functional plasticity of scaffold proteins as p(l)acemakers in cell signaling." In: *Cellular Signalling* 24.11, pp. 2143–2165. DOI: 10.1016/j.cellsig.2012.06.002.

Park, Soyeun and Yong J Lee (2013). „Nano-mechanical compliance of Müller cells investigated by atomic force microscopy." In: *International journal of biological sciences* 9.7, p. 702.

Pfreundschuh, Moritz et al. (2014). „Multiparametric high-resolution imaging of native proteins by force-distance curve–based AFM." In: *nature protocols* 9.5, pp. 1113–1130.

Plodinec, Marija and Roderick YH Lim (2015). „Nanomechanical Characterization of Living Mammary Tissues by Atomic Force Microscopy." In: *Mammary Stem Cells: Methods and Protocols*, pp. 231–246.

Plodinec, Marija et al. (Nov. 2012). „The nanomechanical signature of breast cancer.“ In: *Nature nanotechnology* 7.11, pp. 757–65. DOI: 10.1038/nnano.2012.167.

Pokutta, Sabine and William I Weis (2007). „Structure and mechanism of cadherins and catenins in cell-cell contacts.“ In: *Annual review of cell and developmental biology* 23, pp. 237–261. DOI: 10.1146/annurev.cellbio.22.010305.104241.

Pöschl, Ernst et al. (2004). „Collagen IV is essential for basement membrane stability but dispensable for initiation of its assembly during early development.“ In: *Development (Cambridge, England)* 131.7, pp. 1619–1628. DOI: 10.1242/dev.01037.

Pourati, J et al. (1998). „Is cytoskeletal tension a major determinant of cell deformability in adherent endothelial cells?“ In: *The American journal of physiology* 274.5 Pt 1, pp. C1283–C1289.

Puttini, Stefania et al. (2009). „Gene-mediated restoration of normal myofiber elasticity in dystrophic muscles.“ In: *Molecular Therapy* 17.1, pp. 19–25.

Radmacher, Manfred et al. (1996). „Measuring the viscoelastic properties of human platelets with the atomic force microscope.“ In: *Biophysical journal* 70.1, pp. 556–567.

Riento, Kirsi and Anne J Ridley (2003). „Rocks: multifunctional kinases in cell behaviour.“ In: *Nature reviews. Molecular cell biology* 4.6, pp. 446–56. DOI: 10.1038/nrm1128.

Rio, Armando et al. (2009). „Stretching Single Talin Rod.“ In: 323.January, pp. 638–641. DOI: 10.1126/science.1162912.

Roca-Cusachs, Pere, Raimon Sunyer, and Xavier Trepat (2013). „Mechanical guidance of cell migration: Lessons from chemotaxis.“ In: *Current Opinion in Cell Biology* 25.5, pp. 543–549. DOI: 10.1016/j.ceb.2013.04.010.

Roca-Cusachs, Pere et al. (2006). „Rheology of passive and adhesion-activated neutrophils probed by atomic force microscopy.“ In: *Biophysical journal* 91.9, pp. 3508–3518. DOI: 10.1529/biophysj.106.088831.

Rodriguez-Boulan, Enrique and Ian G. Macara (2014). „Organization and execution of the epithelial polarity programme.“ In: *Nature Reviews Molecular Cell Biology* 15.4, pp. 225–242. DOI: 10.1038/nrm3775.

Roure, Olivia du et al. (2005). „Force mapping in epithelial cell migration.“ In: *Proceedings of the National Academy of Sciences of the United States of America* 102.7, pp. 2390–2395. DOI: 10.1073/pnas.0408482102.

Rowe, R. Grant and Stephen J. Weiss (Nov. 2008). „Breaching the basement membrane: who, when and how?“ In: *Trends in Cell Biology* 18.11, pp. 560–574. DOI: 10.1016/j.tcb.2008.08.007.

Ruiz, Pedro A. and Gabor Jarai (2011). „Collagen I induces discoidin domain receptor (DDR) 1 expression through DDR2 and a JAK2-ERK1/2-mediated mechanism in primary human lung fibroblasts." In: *Journal of Biological Chemistry* 286.15, pp. 12912–12923. DOI: 10.1074/jbc.M110.143693.

Sabass, Benedikt et al. (2008). „High resolution traction force microscopy based on experimental and computational advances." In: *Biophysical journal* 94.1, pp. 207–220. DOI: 10.1529/biophysj.107.113670.

Sader, John E, James WM Chon, and Paul Mulvaney (1999). „Calibration of rectangular atomic force microscope cantilevers." In: *Review of Scientific Instruments* 70.10, pp. 3967–3969.

Saez, Alexandre et al. (2005). „Is the Mechanical Activity of Epithelial Cells Controlled by Deformations or Forces?" In: *Biophysical Journal* 89.6, pp. L52–L54. DOI: 10.1529/biophysj.105.071217.

Sanchez-Adams, Johannah, Rebecca E Wilusz, and Farshid Guilak (2013). „Atomic force microscopy reveals regional variations in the micromechanical properties of the pericellular and extracellular matrices of the meniscus." In: *Journal of Orthopaedic Research* 31.8, pp. 1218–1225.

Sarras, Michael P, Darrel Meador, and Xiaoming Zhang (1991). „Extracellular matrix (mesoglea) of Hydra vulgaris. II. Influence of collagen and proteoglycan components on head regeneration." In: *Developmental Biology* 148.2, pp. 495–500. DOI: 10.1016/0012-1606(91)90267-7.

Sawada, Yasuhiro et al. (2006). „Force Sensing by Mechanical Extension of the Src Family Kinase Substrate p130Cas." In: *Cell* 127.5, pp. 1015–1026. DOI: 10.1016/j.cell.2006.09.044.

Schnitzer, M J and S M Block (1997). „Kinesin hydrolyses one ATP per 8-nm step." In: *Nature* 388.6640, pp. 386–90. DOI: 10.1038/41111.

Schoen, Ingmar, Beth L. Pruitt, and Viola Vogel (2013). „The Yin-Yang of Rigidity Sensing: How Forces and Mechanical Properties Regulate the Cellular Response to Materials." In: *Annual Review of Materials Research* 43.1, pp. 589–618. DOI: 10.1146/annurev-matsci-062910-100407.

Schoumacher, Marie et al. (2010). „Actin, microtubules, and vimentin intermediate filaments cooperate for elongation of invadopodia." In: *The Journal of cell biology* 189.3, pp. 541–556.

Schoumacher, Marie et al. (2013). „Basement membrane invasion assays: native basement membrane and chemoinvasion assay." In: *Adhesion Protein Protocols*, pp. 133–144.

Schuger, Lucia et al. (1991). „Identification of laminin domains involved in branching morphogenesis: Effects of anti-laminin monoclonal antibodies

on mouse embryonic lung development." In: *Developmental Biology* 146.2, pp. 531–541. DOI: 10.1016/0012-1606(91)90254-Z.

Shimizu, Hiroshi et al. (2002). „Epithelial morphogenesis in hydra requires de novo expression of extracellular matrix components and matrix metalloproteinases." In: *Development (Cambridge, England)* 129.6, pp. 1521–1532.

Shintani, Yasushi et al. (2008). „Collagen I-mediated up-regulation of N-cadherin requires cooperative signals from integrins and discoidin domain receptor." In: *Journal of Cell Biology* 180.6, pp. 1277–1289. DOI: 10.1083/jcb.200708137.

Smith, Michael L. et al. (2007). „Force-induced unfolding of fibronectin in the extracellular matrix of living cells." In: *PLoS Biology* 5.10, pp. 2243–2254. DOI: 10.1371/journal.pbio.0050268.

Smyth, N. (Jan. 1999). „Absence of Basement Membranes after Targeting the LAMC1 Gene Results in Embryonic Lethality Due to Failure of Endoderm Differentiation." In: *The Journal of Cell Biology* 144.1, pp. 151–160. DOI: 10.1083/jcb.144.1.151.

Sneddon, Ian N. (May 1965). „The relation between load and penetration in the axisymmetric boussinesq problem for a punch of arbitrary profile." In: *International Journal of Engineering Science* 3.1, pp. 47–57. DOI: 10.1016/0020-7225(65)90019-4.

Sollich, Peter (1998). „Rheological constitutive equation for model of soft glassy materials." In: *Physical Review E* 58.1, p. 738. DOI: 10.1103/PhysRevE.58.738. arXiv: 9712001 [cond-mat].

Spenle, Caroline et al. (2013). „Laminin a5 guides tissue patterning and organogenesis." In: *Cell Adhesion and Migration* 7.1, pp. 90–100. DOI: 10.4161/cam.22236.

Stoker, M and H Rubin (1967). „Density dependent inhibition of cell growth in culture." In: *Nature* 215, pp. 171–172. DOI: 10.1038/215171a0.

Stolz, Martin et al. (2009). „Early detection of aging cartilage and osteoarthritis in mice and patient samples using atomic force microscopy." In: *Nature Nanotechnology* 4.3, pp. 186–192.

Stolz, Martin et al. (2004). „Dynamic elastic modulus of porcine articular cartilage determined at two different levels of tissue organization by indentation-type atomic force microscopy." In: *Biophysical journal* 86.5, pp. 3269–3283.

Storm, Cornelis et al. (2005). „Nonlinear elasticity in biological gels." In: *Nature* 435.5, pp. 191–194. DOI: 10.1038/nature03497.1.. arXiv: 0406016 [cond-mat].

Sunyer, Raimon et al. (2012). „Fabrication of Hydrogels with Steep Stiffness Gradients for Studying Cell Mechanical Response." In: *PLoS ONE* 7.10, pp. 1–9. DOI: 10.1371/journal.pone.0046107.

Swift, Joe et al. (2013). „Nuclear Lamin-A Scales with Tissue Stiffness and Enhances Matrix-Directed Differentiation." In: DOI: 10.1126/science.1240104.

Talts, Jan F. et al. (1999). „Binding of the G domains of laminin $\alpha 1$ and $\alpha 2$ chains and perlecan to heparin, sulfatides, α-dystroglycan and several extracellular matrix proteins." In: *EMBO Journal* 18.4, pp. 863–870. DOI: 10.1093/emboj/18.4.863.

Tanner, Kandice et al. (2010). „Dissecting regional variations in stress fiber mechanics in living cells with laser nanosurgery." In: *Biophysical Journal* 99.9, pp. 2775–2783. DOI: 10.1016/j.bpj.2010.08.071.

Theveneau, Eric et al. (2013). „Chase-and-run between adjacent cell populations promotes directional collective migration." In: *Nature Cell Biology* 15.7, pp. 763–772. DOI: 10.1038/ncb2772.

Thomasy, Sara M. et al. (2013). „Substratum stiffness and latrunculin B modulate the gene expression of the mechanotransducers YAP and TAZ in human trabecular meshwork cells." In: *Experimental eye research* 113, pp. 66–73. DOI: 10.1016/j.exer.2013.05.014.

Tian, Mengxin et al. (2015). „The nanomechanical signature of liver cancer tissues and its molecular origin." In: *Nanoscale* 7.30, pp. 12998–13010.

Timpl, Rupert and Judith C. Brown (Feb. 1996). „Supramolecular assembly of basement membranes." In: *Bioessays* 18.2, pp. 123–132. DOI: 10.1002/bies.950180208.

To, Margaret et al. (Nov. 2013). „Diabetes-induced morphological, biomechanical, and compositional changes in ocular basement membranes." In: *Experimental Eye Research* 116, pp. 298–307. DOI: 10.1016/j.exer.2013.09.011.

Trepat, Xavier, Guillaume Lenormand, and Jeffrey J. Fredberg (2008). „Universality in cell mechanics." In: *Soft Matter* 4.9, p. 1750. DOI: 10.1039/b804866e.

Trepat, Xavier et al. (May 2007). „Universal physical responses to stretch in the living cell." In: *Nature* 447.7144, pp. 592–5. DOI: 10.1038/nature05824.

Trichet, Léa et al. (2012). „Evidence of a large-scale mechanosensing mechanism for cellular adaptation to substrate stiffness." In: *Proceedings of the National Academy of Sciences of the United States of America* 109.18, pp. 6933–8. DOI: 10.1073/pnas.1117810109.

Tse, Justin R and Adam J Engler (June 2010). „Preparation of hydrogel substrates with tunable mechanical properties." In: *Current protocols in cell*

biology / editorial board, Juan S. Bonifacino ... [et al.] Chapter 10.June, Unit 10.16. DOI: 10.1002/0471143030.cb1016s47.

Uechi, Guy et al. (July 2014). „Proteomic View of Basement Membranes from Human Retinal Blood Vessels, Inner Limiting Membranes, and Lens Capsules." In: *Journal of proteome research*. DOI: 10.1021/pr5002065.

Underwood, Jean M et al. (2006). „The Ultrastructure of MCF-10A Acini." In: *Journal of cellular physiology* 207.1, pp. 12–22. DOI: 10.1002/JCP.

Van Zwieten, Ruthger W et al. (2014). „Assessing dystrophies and other muscle diseases at the nanometer scale by atomic force microscopy." In: *Nanomedicine* 9.4, pp. 393–406.

Varelas, Xaralabos et al. (2010). „The Crumbs Complex Couples Cell Density Sensing to Hippo-Dependent Control of the TGF-β-SMAD Pathway." In: *Developmental Cell* 19.6, pp. 831–844. DOI: 10.1016/j.devcel.2010.11.012.

Vasioukhin, V. and E. Fuchs (2001). „Actin dynamics and cell-cell adhesion in epithelia." In: *Current Opinion in Cell Biology* 13.1, pp. 76–84. DOI: 10.1016/S0955-0674(00)00177-0.

Vogel, Viola and Michael P. Sheetz (2009). „Cell fate regulation by coupling mechanical cycles to biochemical signaling pathways." In: *Current Opinion in Cell Biology* 21.1, pp. 38–46. DOI: 10.1016/j.ceb.2009.01.002.

Vuoristo, Sanna et al. (2013). „A Novel Feeder-Free Culture System for Human Pluripotent Stem Cell Culture and Induced Pluripotent Stem Cell Derivation." In: *PLoS ONE* 8.10, pp. 1–14. DOI: 10.1371/journal.pone.0076205.

Wang, N and D Stamenović (2000). „Contribution of intermediate filaments to cell stiffness, stiffening, and growth." In: *American journal of physiology. Cell physiology* 279.1, pp. C188–C194. DOI: 10.1109/IEMBS.1999.802102.

Wang, Ning et al. (2002). „Cell prestress. I. Stiffness and prestress are closely associated in adherent contractile cells." In: *American journal of physiology. Cell physiology* 282.3, pp. C606–C616. DOI: 10.1152/ajpcell.00269.2001.

Weisenhorn, a L et al. (1999). „Deformation and height anomaly of soft surfaces studied with an AFM." In: *Nanotechnology* 4.2, pp. 106–113. DOI: 10.1088/0957-4484/4/2/006.

Wen, Qi and Paul A. Janmey (2011). „Polymer physics of the cytoskeleton." In: *Current Opinion in Solid State and Materials Science* 15.5, pp. 177–182. DOI: 10.1016/j.cossms.2011.05.002.

Wiche, G (1998). „Role of plectin in cytoskeleton organization and dynamics." In: *Journal of cell science* 111 (Pt 1, pp. 2477–2486. DOI: 10.1096/fj.08-124453.

Witz, Craig A et al. (2001). „Composition of the Extracellular Matrix of the Peritoneum.“ In: *Obstetrics & Gynecology* 8, pp. 299–304.

Wondimu, Zenebech et al. (2013). „A Novel Monoclonal Antibody to Human Laminin $\alpha5$ Chain Strongly Inhibits Integrin-Mediated Cell Adhesion and Migration on Laminins 511 and 521.“ In: *PLoS ONE* 8.1, pp. 14–24. DOI: 10.1371/journal.pone.0053648.

Yamada, Soichiro and W. James Nelson (2007). „Localized zones of Rho and Rac activities drive initiation and expansion of epithelial cell-cell adhesion.“ In: *Journal of Cell Biology* 178.3, pp. 517–527. DOI: 10.1083/jcb.200701058.

Yap, Belinda and Roger D. Kamm (2005). „Cytoskeletal remodeling and cellular activation during deformation of neutrophils into narrow channels.“ In: *Journal of applied physiology* 99.6, pp. 2323–2330. DOI: 10.1152/japplphysiol.00503.2005.

Yurchenco, Peter D (2012). „Basement Membranes : Cell Scaffoldings and Signaling Platforms.“ In: pp. 1–28.

Yurchenco, Peter D. and William G. Wadsworth (2004). „Assembly and tissue functions of early embryonic laminins and netrins.“ In: *Current Opinion in Cell Biology* 16.5, pp. 572–579. DOI: 10.1016/j.ceb.2004.07.013.

Zaidel-Bar, Ronen et al. (2007). „Functional atlas of the integrin adhesome.“ In: *Nature Cell Biology* 9.8, pp. 858–867. DOI: 10.1038/ncb0807-858.

Zhao, Bin et al. (2007). „Inactivation of YAP oncoprotein by the Hippo pathway is involved in cell contact inhibition and tissue growth control.“ In: *Genes & Development*, pp. 2747–2761. DOI: 10.1101/gad.1602907.Hpo/Sav.

2

REVISITING BASEMENT MEMBRANE BIOLOGY

Based on

New concepts in Basement Membrane Biology

Willi Halfter, Philipp Oertle, Christophe A. Monnier, Leon Camenzind, Magaly Reyes-Lua, Huaiyu Hu, Joseph Candiello, Anatalia Labilloy, Manimalha Balasubramani, Paul Bernhard Henrich and Marija Plodinec

and

The Bi-Functional Organization of Human Basement Membranes

Willi Halfter, Christophe Monnier, David Müller, Philipp Oertle, Guy Uechi, Manimalha Balasubramani, Farhad Safi, Roderick Lim, Marko Loparic, Paul Bernhard Henrich

Basement membranes BMs are highly specialized extra-cellular matrizes (ECMs). They ensheath epithelia, muscle fibers, blood vessels and peripheral nerves. BM have been recognized as crucial structures providing signalling to cells that adhere to them. Compiled data presented in this chapter demonstrates architectural aspects of BM organization and compoisition that were not described previously. The current description of structure and function of BMs in literature is mainly based on data obtained with transmission electron microscopy (TEM) imaging and *in vitro* protein-binding assays. Therefore, recently, we have examined human BMs by immunofluorescence, mechanical testing by atomic force microscope (AFM) and mass spectrometry (MS). It has become evident that most BMs in the human body are not intermixed networks of laminin and collagen IV of few hundred nanometers thickness only, instead they comprise micrometer-thick sheets of a laminin and collagen IV bilayer with a distinct distribution of nidogen and perlecan. The unmixing of laminin and collagen IV is thought to have major implications on cell behaviour in development, tissue homeostasis and disease. We showed that epithelial cells adhere stronger to the laminin side while for example fibroblasts showed no preference. Furthermore various human BMs were found to be much stiffer than the surrounding ECM or the attached epithelia. Interestingly, data have revealed that laminin is roughly two to three times stiffer than collagen IV. Hence, in contrast to the existing hypothesis in the field, it is laminin rather than collagen IV that governs mechanical stability of the BM.

2.1 INTRODUCTION

Basement membrane (BM) proteins are evolutionary very old components of tissue. They arose together with cell adhesion molecules during separation between the yeast-metazoan and nematode-chordate lines, while interstitial matrices appeared in the vertebrate lineage (Hutter et al. 2000). Importantly, with the emergence of BM proteins, separation of cell layers was introduced (Shimizu et al. 2002). BMs are omnipresent in all tissues (Yurchenco et al. 2009), yet they are very difficult to isolate due to firm anchorage to the connective tissue that surrounds them. First studies BM proteins emerged when large quantities of these proteins were extracted from yolk sac tumors since those produce large quantities of BM like extra-cellular matrix (ECM) (Timpl et al. 1996; Erickson et al. 2000). electron microscopy (EM) studies (Yurchenco et al. 1992) and protein-binding assays of yolk sack proteins and recombinant proteins (Nishiuchi et al. 2006) significantly contributed to our understanding of BMs. These data showed that proteins comprising BM are mostly multi-domain proteins with various cell-ECM and ECM-ECM interaction sites. These data together with architectural studies of BMs in mouse embryos and embryoid bodies gave rise to a model of BMs as a very thin and fragile sheet where major components such as laminin and collagen IV form intertwined networks (Figure 2.3) connected through perlecan and nidogen (Fox et al. 1991).

Several recent papers provide emerging evidence that BMs are indeed not thin mesh works of laminin and collagen IV but instead show that BM are asymmetric structures with distinct laminin and collagen IV sides. The BM of the human skin separates the dermis from the epidermis and is made of a collagen IV and a laminin side that are connected by perlecan with nidogen found in both layers (Behrens et al. 2012). Furthermore, there have been recent indications that kidney glomeruli have bi-layered BMs (Suleiman et al. 2013; Lennon et al. 2014). The data presented in this chapter demonstrates that ocular and vascular BMs consist of distinct laminin and collagen IV layers, both in terms of architecture and mechanical response. Furthermore, cell adhesion assays show that fibroblasts show no preference and epithelial cells prefer the laminin side. Further generalization of this concept to other tissues as well as precise mechanisms of cell adhesion to BM are shown in detail in chapter 3.

The relevance of BMs for tissue and organ organization is clearly demonstrated by the dramatic phenotypes provoked by lack or mutations in major BM proteins. In this context, are prominent kidney malfunctions (Willem

et al. 2002; Kashtan 1998), eye deficiencies (Fukai 2002; Lee et al. 2007), neuro-muscular deficiencies (Gautam et al. 1996; Michele et al. 2002), malformations (Miner et al. 1998), cartilage maintenance issues (Costell 1999) or embryonic lethality in the case of knockouts (Smyth 1999; Bader et al. 2005; Gould 2005). In addition to hereditary disease, pathological changes in BMs have been described predominantly in cancer where, depending on the tissue, loss or increase of secretion of BM proteins is associated with disease progression and also cross-linking and protease dependent degradation. Furthermore, changes of the BM are reported in diabetes (Hainsworth et al. 2002), ageing (Candiello et al. 2010; Vázquez et al. 1996; Xi et al. 1982) and Alzheimer (Zipser et al. 2007). BMs are becoming thicker or brittle through advanced glycation endproducts (AGE) with disease progression in diabetes, or thinner, leading to leaky blood vessels in Alzheimer's disease. In age-related macular degeneropathy, Bruch's membrane (BrM) of the retinal epithelium is involved where the integrity of BrM is lost with disease progression, enabling choroid blood vessels to breach the membrane and disrupt the retina (Chong et al. 2005).

2.2 BM COMPOSITION

Crucial identification of BM proteins occurred with the discovery that mouse yolk sac tumors produce a BM-typical ECM in gram quantities (Orkin et al. 1977; Chung et al. 1977; Kleinman et al. 2005). Analysis of these tumor matrices showed that its major components laminin (Timpl et al. 1979; Chung et al. 1979), nidogen/entactin (Carlin et al. 1981; Timpl et al. 1983), perlecan (Hassell et al. 1980) and collagen IV (Kleinman et al. 1982) are large multidomain glycoproteins with molecular weights between 150 kD and 1000 kD.

Laminins are large extracellular matrix proteins that are solely found in BM and are important for the organization of the BM during development(Morrissey et al. 2015; Spenle et al. 2013), adhesion, migration and cell mechanics (Timpl et al. 1996). All laminins known at present are glycoprotein heterotrimers, each made up of α-, β- and γ-subunits. The individual polypeptide chains are held together by coiled-coils which form one long arm and up to three short arms (Beck et al. 1993). The short arms contain rods and globular structures while the long arm consists of a long coiled-coil, with the G-domain of five β-sheet carboxy-terminal laminin globular domains (LG) modules. In mammals, five α, four βand three γencoding genes are known, with two splicing variants for α3; namely α3A and α3B, these form the 15

Table 2.1 Laminin nomenclature

Classical	Short	Long
Laminin-1:	LN-111	α1β1γ1
Laminin-2:	LN-211	α2β1γ1
Laminin-3:	LN-121	α1β2γ1
Laminin-4:	LN-221	α2β2γ1
Laminin-5:	LN-332	α3Aβ3γ2
Laminin-5B:	LN-332B	α3Bβ3γ2
Laminin-6:	LN-311	α3β1γ1
Laminin-7:	LN-321	α3β2γ1
Laminin-8:	LN-411	α4β1γ1
Laminin-9:	LN-421	α4β2γ1
Laminin-10:	LN-511	α5β1γ1
Laminin-11:	LN-521	α5β2γ1
Laminin-12:	LN-213	α2β1γ3
Laminin-14:	LN-423	α4β2γ3
Laminin-15:	LN-523	α5β2γ3

currently recognized trimers, summarized in Table 2.1 (Burgeson et al. 1994; Ferrigno et al. 1997; Koch et al. 1999; Miner et al. 1995).

Laminins 1-4 possess three short arms with LN domains, LE repeats and internal globular (LV4) domains with identical arrangements. The only known laminin that contains β3 and γ2 chains is LN-332 with rod-like structures enriched in epithelia where the short arms are truncated. The N-terminal end of the γ2 short arm, as well as the 2 terminal LG domains of the long arm can be cleaved by bone-morphogenetic protein-1 (BMP1), matrix metalloproteinase (MMP)-2, membrane-type matrix metalloproteinase (MT-MMP)-1 and plasmin (Sugawara et al. 2008). These proteases affect nidogen, fibulin and heparin-binding activities, affect cell migration and hemidesmosome promotion (Gagnoux-Palacios et al. 2001). The only laminins that contain an α5 subunit with short arms comprising amino-terminal laminin globule (LN) domains and multiple laminin-type epidermal growth factor-like repeats (LE) repeats between the globular domains are LN-511 and LN-521. The laminins 1, 4, 5, 10 and 11 constitute the major laminins of most tissues. For example, LN-332 is a major component in skin and other ectodermal BMs, while muscle BM is known to contain mostly α2 bearing laminins. The remaining laminins are found in smaller amounts or in specific BMs.
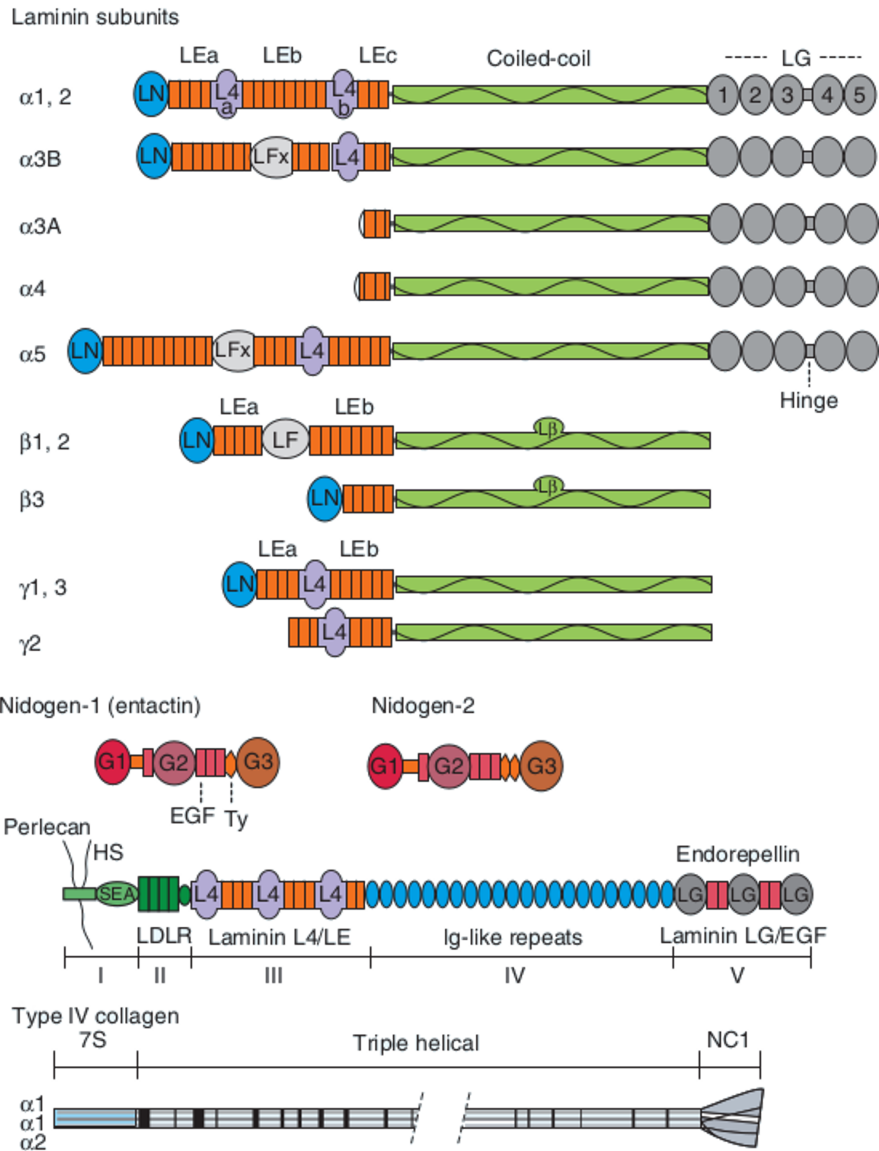
Beyond laminin, BM the second major constituent is collagen IV (Miner et al. 1994) and several glycoproteins such as nidogen, perlecan (contains LG domains similar to the ones in laminin α1 (McCarthy 2015)) and agrin (Figure 2.1). Nidogen, also termed entactin, is a small glycoprotein commonly though of as stabilizer during BM development (Ho et al. 2008). It is commonly accepted BMs are thin structures with a thickness of approximately 100 nm

Figure 2.1 (*previous page*) Basement membrane proteins and domains
Proteins of basement membranes (BMs) consist of tandem repeats of various protein motifs. The laminin subunits contain amino-terminal laminin globule (LN) and laminin-type epidermal growth factor-like repeats (LE) that form rod-like regions, L4 domains, globules which interrupt two half-LE domains, LFs, unique globules of β-subunits, and modified LF domains (LFx) unique to αchains. A long coiled-coil domain follows with L$_\beta$, a knob-like subdomain in βsubunits and then only in α-subunits, carboxy-terminal laminin globular domains (LG) domains, each a β-sandwich. Each laminin consists of an α, β, and γsubunit bundled together at the coiled-coil domain and between the βand γsubunits near the C-terminus. Nidogens are laminin-binding proteins that with globular domains (G1-G3) separated by epidermal growth factor (EGF)-like domains, Ty, and a unique rodlike segment next to G1. Perlecan is split into five regions; an N-terminal domain followed by heparansulfate (HS) and sea urchin enterokinase and agrin domain (SEA) domains, low density lipoprotein (LDL)-receptor repeats, a laminin short-arm region consisting of duplicated L4 and LE domains, immunoglobulin (Ig) repeats, and laminin-type LG domains separated by EGF-type repeats. Type IV collagen is explained here on the example of the most abundant type IV collagen heterotrimer (α1$_2$ α2[IV]). The N-terminal 7S domain forms quartets with other 7S domains, forming the junctions of a collagen IV network, the C-terminal non-collagenous (NC) domain forms dimers and joins the free ends of two collagen IV trimers. Adapted from Yurchenco 2012.

with a chicken-wire configuration of collagen IV, accomodoating the other BM proteins (Figure 2.3). However, recent reports show that mature BMs form bilayered sheets where collagen IV and laminins are spatially separated (Halfter et al. 2013; Suleiman et al. 2013). Both proteins can connect to each other and the connection is further reinforced by perlecan (Behrens et al. 2012; Wijeratne et al. 2015). In extracted BMs, the supramolecular assembly of laminins and collagen IV was visualized with SEM which has revealed that laminins display glomerular bodies (Mestres et al. 2014) while collagen IV exhibits a non-fibrillar arrangement.

There are six different Collagen IV α-chains that can form three collagen IV heterotrimers (Khoshnoodi et al. 2008) α1α1α2, α3α4α5, and α5α5α6 and all of them are exclusively found in BMs. α1α1α2 is found in all tissues, α3α4α5 in the glomerular basement membrane (GBM), kidney, lung, testis and eye, α5α5α6 in skin, smooth muscle and kidney. Especially in the GBM, α1α1α2 is lost after maturation of the GBM. Two NC domains of two collagen IV heterotrimers can join to form a dimer, four 7S domains can join to form a tetramer (see Figure 2.1). The NC domain of all type IV collagens contains interaction sites for integrins, prominently αvβ3 and αvβ5 as well as α1β1, α3β1 and α6β1. The helical repeats of collagen IV α1α1α2 also contain a binding site for the classical collagen integrin α2β1. The 7S domain does not contain integrin binding sites.

The most abundant HSPG in BM are perlecan and agrin, the latter bearing specialized functions in the neuromuscular junction (Iozzo 2005). Perlecan was considered the only BM HSPG (Hassell et al. 1980) until two more BM-associated HSPGs, agrin and collagen XVIII, were identified (Tsen et al. 1995;

Denzer 1995; Halfter et al. 1998; Saarela et al. 1998). Perlecan is a modular proteoglycan with homology to growth factors and proteins involved in lipid metabolism and adhesion (Iozzo 1998). Surprisingly, perlecan co-localizes strongly with laminin in ocular BMs and only interfaces collagen IV but does not overlap. HSPGs are thought to act both pro- and anti-angiogenic (angiogenesis being a process that involves heavy remodelling of existing BMs) through local retention of angiogenic growth factors. In addition, proteolytic processes at the C-terminal can release endostatin and endorepellin, both with angiostatic effect. Based on structure, perlecan is commonly divided into five domains carrying different functions. Domain I, through HS chains, is involved in BM anchoring and can interact with LN-111 and collagen IV. Like domain IV that interacts with nidogen1/2, collagen IV and fibronectin it is also attributed to regulate cell motility and adhesion. Domain V interacts with nidogen-1, laminin-nidogen complexes, α-dystroglycan and integrin α2β1 (through 3 LG domains) (Brown et al. 1997; Talts et al. 1999) which is otherwise the prototypic interaction partner for fibrillary collagens (Iozzo 2005). In this manner, BM that present laminin and perlecan to the basal side of epithelial cells may provoke laminin and collagen-like responses without being in direct contact with collagen (current working hypothesis in our lab). Moreover, 50 % of HSPG2-/- mice die between E10 and E12 due to haemorrhage of the pericardial cavity indicating that BM lacking perlecan are more prone to failure under mechanical stress (Costell 1999).

2.3 BIOLOGICAL ACTIVITY OF BM PROTEINS

Laminin activities can be roughly grouped into (1) matrix assembly, which can be localized to short arms of all three chains and (2) cell interaction that is associated with the N- and C-terminal ends of the α-subunit (Figure 2.1). Laminin polymerization is thought to be mediated by calcium-dependent bonding of three LN domains of laminins 1-4, 10 and 11. The short arm of laminin α1 and α2 is also interacting with integrins α1β1 and α2β1 as well as heparin, while integrin αVβ3 interacts with the short arm of the laminin α5 chain. The five LG domains on the long arm interact with heparins and sulfatides and (Yurchenco et al. 2004). Many of them with the exception of laminin α1 interact with integrin α3, and integrin α6. In addition, these domains have a strong interaction with α-dystroglycan (Durbeej et al. 1999) and the Lutheran glycoprotein (Kikkawa et al. 2002; Kikkawa et al. 2003). The close dependence of cells on BM properties and vice versa became apparent in experiments which showed that the self-polymerization and interaction with

LG-domains is prerequisite for myotube formation and epiblast differentiation (Colognato et al. 1999; Li et al. 2002). Implantation of laminin-deficient mice provides further evidence that laminins are essential for many epithelial functions during development and adulthood. For example, homozygous null mutation of the laminin γ1 chain gene *LAMC1* prevents polymerization of basement membranes and leads to post implantation lethality at E6 (embryo at day 6) of development (Smyth 1999). In this case, there is no presence of basement membranes or Reichert's membrane and the endoderm does not differentiate, leading to the disorganization and massive apoptosis. This is most likely due to a lack of survival signals from the ECM. In contrast, BMs can assemble in absence of collagen IV and mice only die at E10.5, indicating that collagen IV is needed only in later stages (Pöschl et al. 2004). Similar experiments in zebrafish reveal that *LAMC1* or *LAMB1* (laminin β1 chain gene) null embryos survive until a relatively late stage (tailbud stage) because maternal laminin mRNA can be used by the embryo for BM assembly (Parsons et al. 2002). The same is found in mouse trophoblasts which can partially compensate the lack of own laminin by using maternal laminin in the very early stages. Additional insight comes from *LAMA1* (laminin α1 chain gene) null mice, which survive a day longer than *LAMB1* or *LAMC1* null mice. *LAMA1* null mice still lack Reichert's membrane but are able to differentiate their epithelia. Overexpressing *LAMA5* (laminin α5 chain gene) increases survival of these embryoid bodies to a later stage, nevertheless they finally they die due to the absence of Reichert's membrane. This suggests that *LAMA5* would be sufficient for epithelial differentiation (Miner et al. 2004). A dramatic exemplary phenotype of a *LAMA5* knockout is shown in figure 2.2, where the tubular urether is not able to form in the absence of a proper BM.

Mutations of proteins that are irreplaceable for BM assembly cause embryonic death prior to gastrulation (Smyth 1999); hence, vertebrates cannot develop and survive without BMs. Non-lethal mutations in mice and humans lead to a collection of BM-typical phenotypes. These include vascular defects that are particularly prominent in brain and eyes (Costell 1999; Halfter et al. 2002; Halfter et al. 2005; Pöschl et al. 2004; Gould 2005). Common are retinal or cortical ectopias, in which retinal or cortical cells migrate through breaks in the pial (Costell 1999; Halfter et al. 2002; Halfter et al. 2005) or retinal BMs (Lee et al. 2007; Edwards et al. 2010; Labelle-Dumais et al. 2011; Pinzón-Duarte et al. 2010). The cortical/retinal BM defects are associated with a major loss of Cajal-Retzius cells in the cortex and at least 50 % loss of ganglion cells in the retina (Halfter et al. 2002; Halfter et al. 2005). Common phenotypes also include defects in kidney (Miner et al. 1998; Willem et al. 2002) and ear
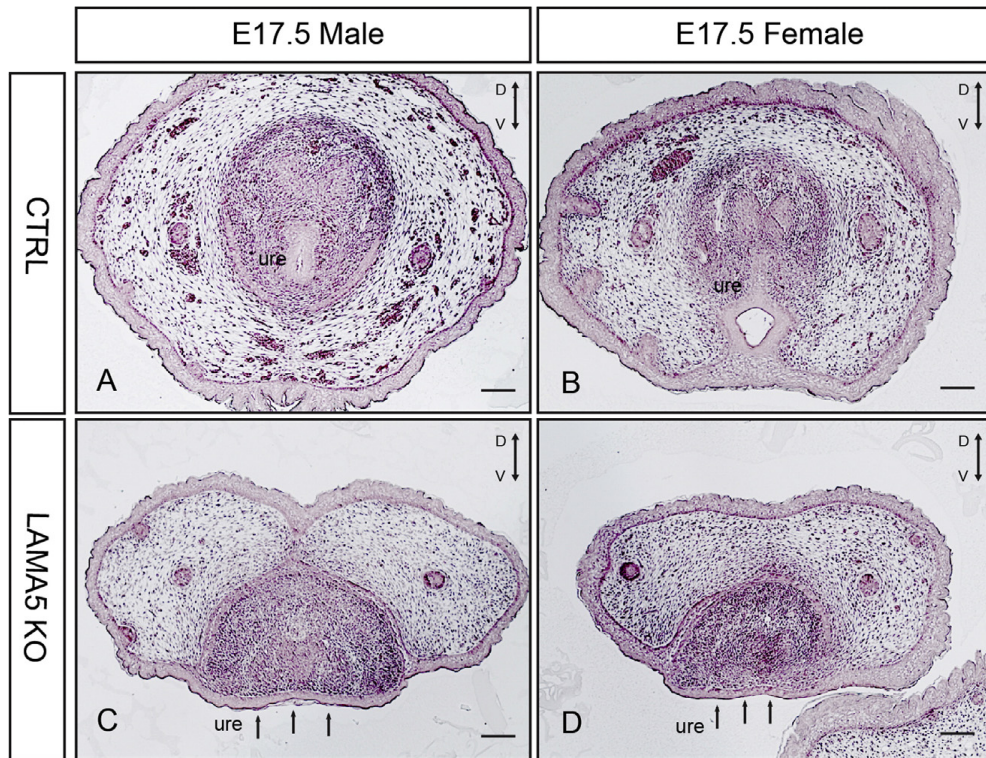
Figure 2.2 Mouse *LAMA5* knockouts do not develop genital tubercles
Haematoxilin & eosin stainings of mouse E17.5 penis (A,C) and clitoris (B,D). The tubular urethra (ure) are located in roughly in the center of the organ in the controls (A,B). In a *LAMA5* (laminin α5 chain) knockout (C,D) the epithelium of the tubuluar urether is missing the support of the basement membrane (BM) and the whole epithelium moves as a plane to the outside of the organ instead of forming a lumen. Adapted from Lin et al. 2016.

development, whereas skin blisters are restricted to mutations of a subset of the epidermal BM proteins (Kiritsi et al. 2013). A common phenotype also includes several forms of congenital muscular dystrophy (Labelle-Dumais et al. 2011; Yoshida et al. 2001; Liu et al. 2006; Lee et al. 2005; Holmberg et al. 2013). Many of these pathologies often co-exist as syndromes and are particularly damaging during embryonic development when tissues and organs are expanding and BMs are under stress. In particular, these phenotypes suggest an essential role of mechanical stability for BM functions and that the integrity of BMs is particularly vulnerable in embryonic and neonatal development. Recent data using mutant mice have emerged demonstrating a key role for integrins and dystroglycan, including the carbohydrate side chain of dystroglycan, in the assembly of many BMs. In particular, mice with defective or no receptors have pathologies that are similar to defects in

humans with BM protein mutations (Stephens et al. 1995; Fassler et al. 1995; Georges-Labouesse et al. 1998; Henry et al. 1998; Graus-Porta et al. 2001; Moore et al. 2002).

2.4 LIMITATIONS OF THE CURRENT BM MODEL

The current model, prominently based on protein binding studies and imaging of isolated BM proteins from mouse tumors, proposes that BMs are composed of two interconnected networks: a laminin polymer, which is found to provide the main cell-binding activity of BMs, and a collagen IV network, considered as the main stabilizing structure (Timpl et al. 1981; Yurchenco et al. 1986). The thickness of BMs is commonly accepted to be in range of 100 nm. Exceptions are the several μm-thick lens capsule, tracheal BM and Descemet's membrane as well as the amnion. For instance, a high-angle shadowing analysis of the amnion BM has demonstrated a more complex arrangement of collagen IV (Yurchenco 1987). This concept of thin BMs poses tight restrictions on making a model to accommodate the various BM proteins in this membrane.

Collagen IV is a trimer with a length of 400 nm and the long axis of laminin heterotrimers measures about 80 nm. The assumption of very thin BMs only allows for a horizontal alignment of the collagen IV in a chicken-wire configuration (Schittny et al. 1988; Yurchenco et al. 2009) and a laminin configuration that is depicted as oblique to the collagen IV network (see Figure 2.3). Such a configuration of thin BMs with extended but flat laminin and collagen IV networks would leave very little flexibility to mechanically expand or shrink the BM, which is an important feature in developing but also adult tissues that are under constant mechanical load. In addition, BM are rich in proteoglycans (Kalluri 2003; Halfter et al. 2013) which are also able the swell and shrink, thereby exerting a lot of mechanical strain on the other BM components. Thus, thicker BMs as shown in our work leave much more room to align the proteins such that further expansion or compression is possible.This configuration enables BMs throughout the body to serve a wide range of purposes while maintaining the same basic constituents. Detailed shortcomings of the current model of BMs are listed below.

- Much of the analysis of BM protein composition was based on studies of reconstituted or mouse BMs and quantitative analysis to measure the ratio of the proteins in the BMs was mostly missing. Recent analysis of *in vivo* derived BMs showed that by far the largest amounts of BM
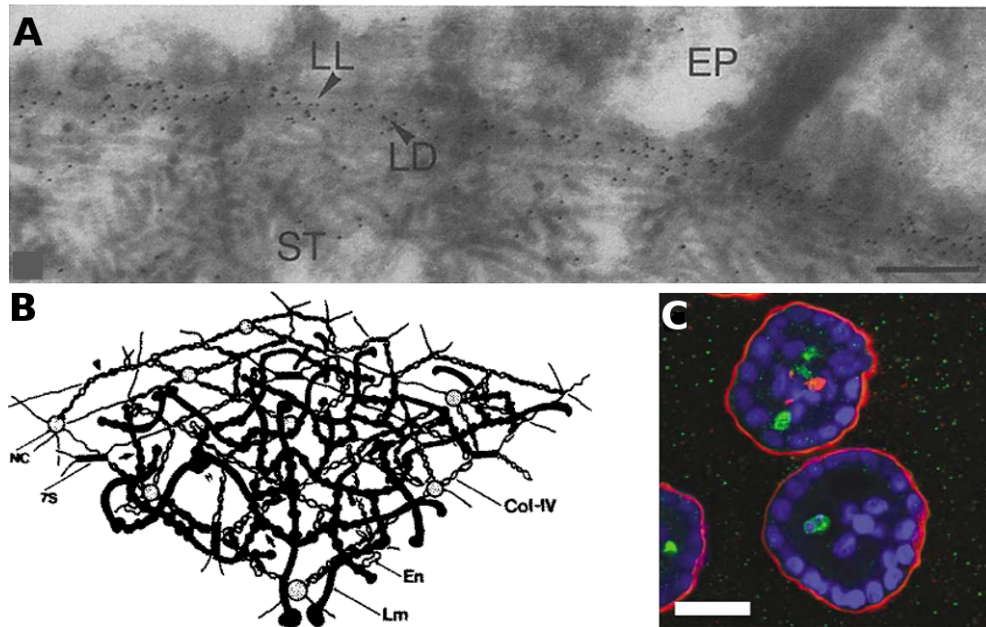
Figure 2.3 Molecular model of the basement membrane
(A) transmission electron microscopy (TEM) micrograph of ultrathin cryosections of mouse cornea with immuno-gold labelling of laminin, showing a basement membrane (BM) with roughly 100 nm thickness. LD, lamina densa, LL, lamina lucida, scale bar 0.3 μm. (B) Widespread working model, depicting the collagen IV (N-terminal 7S, C-terminal NC) in flat a chicken wire configuration and the laminin forming a network tightly connect to the chicken-wire and nidogen (En) associated with laminin. (C) MCF-10A acini grown in matrigel with a fine BM of laminin α3β3γ2 (LN-332) which is secreted by the cells during culture. Probably due to the lack of organized collagen IV and time, the BM does not get thicker, and in addition, LN-332 lacks to possibility to polymerize. Adapted from Yurchenco et al. 1992; Debnath et al. 2003; Schittny et al. 1988.

proteins comprise collagen IV and laminin (Cummings et al. 2014; Balasubramani et al. 2010; Uechi et al. 2014).

- Based on structural assumptions of the collagen IV networks, BMs were regarded as mechanically rigid structures with high tensile strength, yet biomechanical testing of BMs was largely missing except for the case of the LC which was measured in hydrostatic test chambers (Danysh et al. 2008). The data presented in this work based on nanomechanical testing of various BMs with AFM surprisingly reveals that the mechanical properties may be governed by laminin rather than collagen IV (Henrich et al. 2012; Halfter et al. 2013).

- BM research has had a strong focus on rBM, spheroids grown in rBM and short-lived rodents and invertebrate model organisms. As a con-

sequence, the organization and composition of BM in adult humans where age has a major impact on increasing the thickness of BM has been missed (Candiello et al. 2010). In addition, the impact of chronic diseases such as diabetes on BM functional properties could not be studied in these models (To et al. 2013).

- The asymmetrical distribution of BM proteins in many membranes was not known until very recently (Henrich et al. 2012; Behrens et al. 2012; Suleiman et al. 2013). This new aspect completely alters the way ultrastructural organisation of BMs is depicted and raises new questions regarding the role of BMs in tissue organization, since epithelial cells but not fibroblasts show a side preference to stay on the laminin side of the BM (Halfter et al. 2013).

- Finally, the picture describing collagen IV as the main component governing the architecture of thin BMs distorts the assumptions made in case of cancer invasion. Most cancer invasion studies highlight the interaction of cancer cells with stromal components such as fibrillar collagen I (Rowe et al. 2008) and neglect the fact that cells first need to breach the mechanically very rigid laminin of the BM such as in the case of the colon or breast. Data presented in this chapter demonstrate that the initiation of cancer cell invasion is a very slow process and involves physical forces exerted by the cells and reorganization of the BM. These processes are far more complex than described by the simplified model of thin BMs.

2.4.1 *Asymmetry of BMs*

The mechanical and geometrical properties of ocular BMs were measured using AFM and the protein distribution was analyzed with fluorescence microscopy. Contact mode and force spectroscopy imaging both revealed differences between the two sides of ILM, LC and DM and also differences among these three BMs. The ILM shows the most complex topography of all three BMs with a crater-like looking laminin-rich retinal side and a very smooth surface on the collagen IV-rich vitreous body side. The DM on the other hand shows a a coarse-grained endothelial surface and a furrowed stromal side whereas the LC shows a coarse-grained structure on both sides with the vitreous side being wavier than the epithelial side (Figure 2.4). The two sides of the ILM and DM are easily told apart based on topology. On the other hand for the LC this can be challenging. Nevertheless, stiffness values
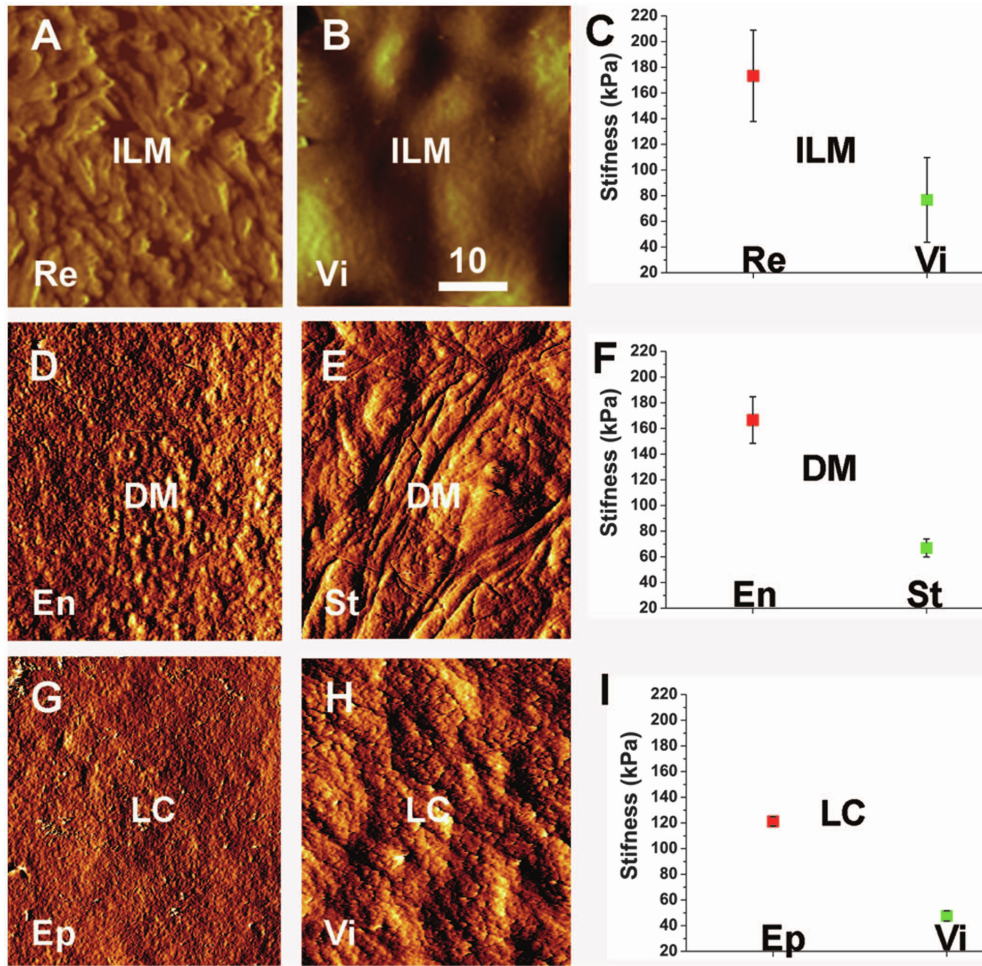
Figure 2.4   Atomic force microscopy (AFM) testing of ocular basement membrane (BM) surfaces
(A-C) AFM testing of the two surfaces of the inner limiting membrane (ILM), (D-F) the Descemet's membrane (DM) (D–F) (G-I) lens capsule (LC). AFM contact imaging shows the topographical differences between the retinal (Re), the epithelial (Ep) and endothelial (En) surfaces on one side and the vitreal (Vi)/stromal (St) surfaces on the other side, of the ILM, DM and the LC. The retinal side of the ILM shows a crater-like structure whereas the endothelial and epithelial sides of the DM and LC are grainy. For all BMs vitreal/stromal side is wavier and varies in appearance from smooth to furrowed. The stiffness graphs (C, F, I) show that the epithelial sides of all tested BM are 2 - 3 times stiffer than the stromal sides. Scale bar: 10 µm. Adapted from Halfter et al. 2013.
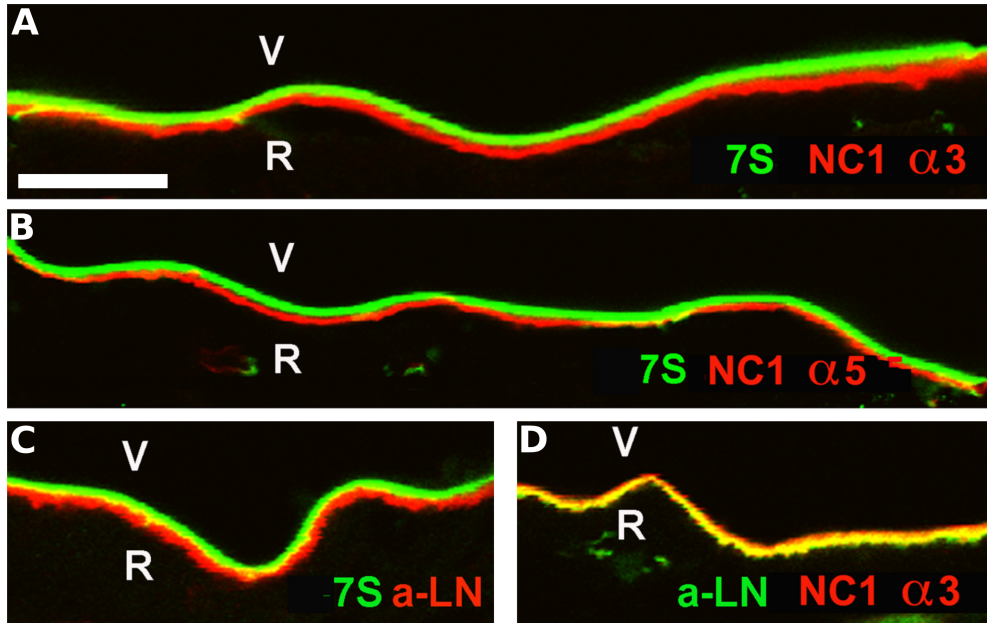
Figure 2.5 Localization of collagen IV and laminin domains in inner limiting membrane (ILM) (A, B) Co-staining of the N-terminal 7S domain and C-terminal NC1 domain of collagen IV α3 and α5 fibrils reveal a clear separation of the two opposite sides of collagen IV within the ILM, contradicting the flat chicken-wire configuration proposed for collagen IV. (C) Co-staining of collagen IV 7S a domain and laminin α-chains show further a clear separation of these two domains (D) Co-staining of laminin α-chains and collagen IV NC1 domain of α3 shows an overlap. Together (C) and (D) suggest that the bulk of laminin is not associated with collagen IV and the interface between the two proteins is at the NC domains of collagen IV. Scale bar is 10 μm. Adapted from Halfter et al. 2013.

measured by nano-indentation and independent of topographical features clearly demonstrate in all cases that the laminin side is two to three times stiffer than the collagen IV side (Figure 2.4 C, F, I).

The reason for this mechanical asymmetry became clear when ILM was stained for collagen IV and laminin (Figure 2.6); laminin was only found in the stiff epithelial side whereas collagen IV is restricted to the softer vitreous body / stromal side. Furthermore, it could be shown that the 7S and NC domains of collagen IV separate within the layer, with the 7S domains that form tetramers facing the stromal surface while the NC domain that joins two free ends of collagen IV is interfacing the laminin α-chains of the laminins present in the ILM. This suggest interaction domains between α-chains of laminin and collagen IV NC domains or adjacent triple helix domains of collagen IV (Yurchenco 2012).

We further analyzed the edge of capsulotomy-derived lens capsules (Lua et al. 2016). The typical thickness of the LC of approximately 30 μm initially
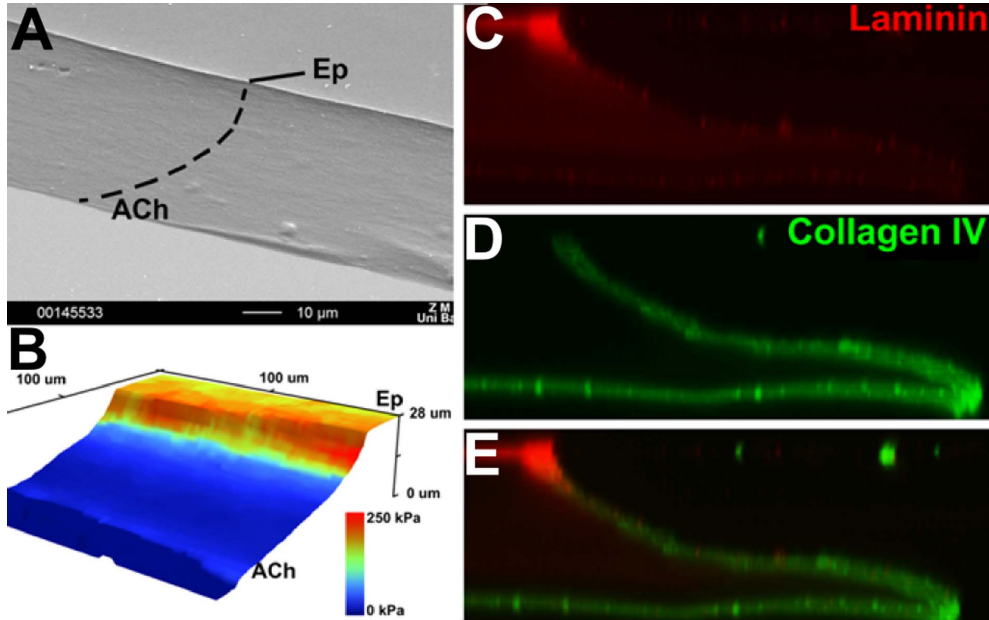
Figure 2.6 Stiffness profile of the lens capsule (LC) after manual capsulotomy
(A) The scanning electron microscopy (SEM) micrograph shows the wedge-shaped edge of the manual capsulotomy sample. (B) Force map measurement performed across the edge of the lens capsule (LC), stiffness is overlayed in color onto the topography. The stiff upper side corresponds to laminin, the soft lower to collagen IV. (C-E) Staining of the LC edge with antibodies to laminin and collagen IV showed that laminin stains only the epithelial side, collagen IV only the anterior chamber (ACh) side. The interior of the specimen remains unstained, probably due to the high density of protein. Fluorescence image size: 30 μm x 80 μm. Adapted from Lua et al. 2016.

posed an issue for force spectroscopy measurements. We solved this problem by using cantilevers with very long tips of 30 μu length (special development prototype, Nanoworld AG, Switzerland) and employing levelling algorithms for the sample stage that allowed us to measure the stiffness of the LC along its edge. Interestingly enough, be SEM does not reveal any differences between the epithalial (Ep) and the vitreous body side (ACh) while AFM stiffness mapping and fluorescence imaging shows clear compositional and mechanical differences between the laminin and the collagen IV layer (Figure 2.6).

This highlights the differences between the highly specialized ocular BMs. In the ILM for instance, the difference between the laminin and collagen IV layers, with the laminin forming globular structures and the collagen IV forming a fibrous network, is clearly visible in the SEM data (Figure 2.7). This is not the case for all BMs and mechanical and immunofluorescence data provide more information in these cases.
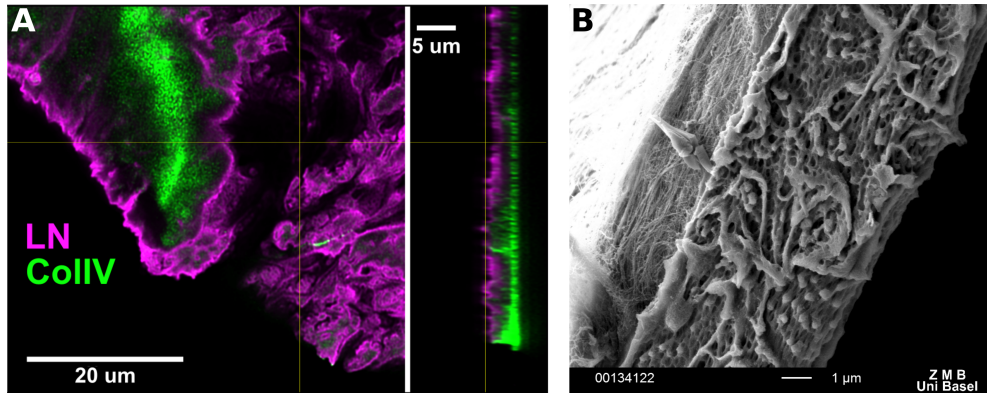
Figure 2.7   Structural and compositional assymetry of the inner limiting membrane (ILM)
(A) Confocal microscopy imaging shows a homogeneous collagen IV distribution and a highly patterned laminin surface of the ILM. The orthogonal yz slice (right) shows a very clear separation of laminin and collagen IV. (B) scanning electron microscopy (SEM) micrograph of an ILM edge confirms the bi-layered organisation of the ILM and displays a fibrous collagen IV network (left side) and a dense structure with globular and rod-like domains on the laminin phase (right side).

2.4.2   *Thickness and rigidity of BM changes with age and diabetes*

Contact mode imaging and force spectroscopy on flat-mounted normal and diabetic ILM show thickness increases with age, and stiffness increases in certain diabetic patients. A linear extrapolation shows that the thickness of ILM increases by 250 nm after puberty, effectively doubling the thickness from 1000 nm at an age of 25 to more than 2000 nm at age 80. Interestingly, onset and progression of diabetes does not not increase the rate at which ILM thickens but simply increases the thickness by about 1000 nm (2.8). Further, mechanical measurements on the ILM show that the laminin side of the ILM stiffens dramatically in a subset of patients, by a factor 4 - 5 as compared to healthy specimens. However, surprisingly enough the collagen IV side remains unaffected, only the laminin stiffness increases. One explanation might be that AGE do not reach into the anterior chamber of the eye to which the collagen IV side of the LC is exposed, while the laminin side is exposed to the lens epithelium that could produce AGE, which are often metabolites (Stitt W Alan 2001).
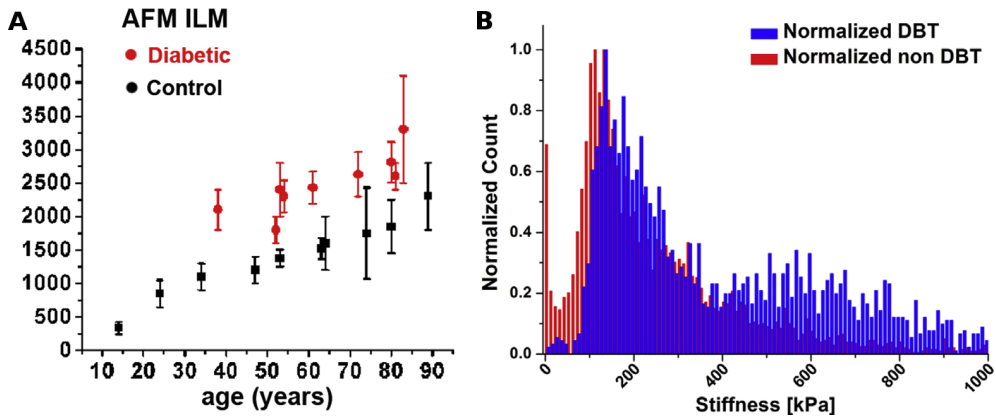
Figure 2.8 Dependence of inner limiting membrane (ILM) thickness and stiffness on age and diabetes (A) Graph of the thickness of ILM measured in atomic force microscope (AFM) contact mode as a function of time. The thickness increases linearly with age and disease, but diabetic ILM are thicker by an offset of approximately 1000 nm. (B) shows force spectroscopy stiffness measurements of the laminin side of healthy and diseased ILM. While healthy ILM always show a peak around 120 kPa, diabetic ILM are slightly stiffer, but more interestingly, show a broad second peak around 500 to 700 kPa which arises from few patients with very stiff ILM. Adapted from To et al. 2013

2.5 DISCUSSION & OUTLOOK

The mechanical stability of BMs *in vivo* is tightly regulated by the composition and organization of its components, hence any deviations in their properties will lead to loss or change of BM function. In this chapter I have gathered evidence from our won work and available literature, which show that the intrinsic asymmetry of BMs is a key requirement for tissue homeostasis. Moreover, breach of this asymmetry could be directly related to pathological states such as cancer or diabetes and ageing. Likely, the alternating arrangement of epithelia and and stroma is a metazoan feature that requires BM asymmetry. the data presented her also show that BM proteins can adopt very diverse ultrastructural organizations and that for example mesentery membrane is not a classical epithelial BM like the ones encompassing epithelia in breast, colon or kidney (see chapter 3). An important outstanding question is what the function of asymmetry is in morphogenesis and organogenesis; Here further studies are necessary to elucidate at which timepoint in development BMs acquire asymmetry and a certain thickness that allows for asymmetry. In epithelial BMs, the laminin and collagen IV layers form extremely dense sheets which appear as solid masses of protein without cavities, indicating that these proteins have been continuously added from the epithelial and stromal side over many years.

The observed increase in ILM thickness confirms findings that other BMs also thicken with age (Danysh et al. 2008; Neumann et al. 2004; Vázquez et al. 1996). However, it remains to be elucidated if the thickness increase stems from an increase of secretion of BM proteins with age, a decrease of catabolic activity or if it is simply the live-long steady secretion of BM proteins. At the same time, age-dependent thickening does not have an impact on the stiffness of the ILM. On the other hand, diabetes induced thickening first of all leads to a higher thickness than age-induced thickening and increases the stiffness of ocular BMs. Diabetic patients usually carry increased levels of advanced glycation endproducts (AGE), proteins or lipids that become glycated when exposed to sugars. Contradicting evidence exists in the literature if AGE increase cross-linking (Singh et al. 2001) or decrease polymerization (Brownlee 1995) of BM proteins in diabetes. Our finding that the stiffness increases in diabetes hints towards an increase in cross-linking. In summary, diabetes seems to induce an accelerated and pre-mature ageing of BMs and changes in the mechanics of BM might be very important in diabetic retinopathies and nephropathies where malfunctions of blood vessels, the GBM or Henle's loop occur (Tsilibary 2003).

REFERENCES

Bader, B. L. et al. (July 2005). „Compound Genetic Ablation of Nidogen 1 and 2 Causes Basement Membrane Defects and Perinatal Lethality in Mice." In: *Molecular and Cellular Biology* 25.15, pp. 6846–6856. DOI: 10.1128/mcb.25.15.6846-6856.2005.

Balasubramani, Manimalha et al. (July 2010). „Molecular interactions in the retinal basement membrane system: A proteomic approach." In: *Matrix Biology* 29.6, pp. 471–483. DOI: 10.1016/j.matbio.2010.04.002.

Beck, K et al. (1993). *Ionic interactions in the coiled-coil domain of laminin determine the specificity of chain assembly.* DOI: 10.1006/jmbi.1993.1284.

Behrens, D. T. et al. (Apr. 2012). „The Epidermal Basement Membrane Is a Composite of Separate Laminin- or Collagen IV-containing Networks Connected by Aggregated Perlecan, but Not by Nidogens." In: *Journal of Biological Chemistry* 287.22, pp. 18700–18709. DOI: 10.1074/jbc.m111.336073.

Brown, Judith C et al. (1997). „The C-terminal domain V of perlecan promotes pl integrin-mediated cell adhesion , binds heparin , nidogen and fibulin-2 and can be modified by glycosaminoglycans." In: *European Journal of Biochemistry* 250, pp. 39–46.

Brownlee, M (1995). „Advanced protein glycosylation in diabetes and aging.“ In: *Annual review of medicine* 46, pp. 223–234. DOI: 10.1146/annurev.med.46.1.223.

Burgeson, Robert E. et al. (1994). „A new nomenclature for the laminins.“ In: *Matrix Biology* 14.3, pp. 209–211. DOI: 10.1016/0945-053X(94)90184-8.

Candiello, Joseph, Gregory J. Cole, and Willi Halfter (June 2010). „Age-dependent changes in the structure, composition and biophysical properties of a human basement membrane.“ In: *Matrix Biology* 29.5, pp. 402–410. DOI: 10.1016/j.matbio.2010.03.004.

Carlin, Barry et al. (1981). „Entactin, a novel basal lamina-associated sulfated glycoprotein.“ In: *Journal of Biological Chemistry* 256.10, pp. 5209–5214.

Chong, N H Victor et al. (2005). „Molecular Pathogenesis of Genetic and Inherited Diseases Decreased Thickness and Integrity of the Macular Elastic Layer of Bruch's Membrane Correspond to the Distribution of Lesions Associated with Age- Related Macular Degeneration.“ In: *The American Journal of Pathology* 166.1, pp. 241–251. DOI: 10.1016/S0002-9440(10)62248-1.

Chung, Albert E. et al. (Feb. 1979). „Properties of a basement membrane-related glycoprotein synthesized in culture by a mouse embryonal carcinoma-derived cell line.“ In: *Cell* 16.2, pp. 277–287. DOI: 10.1016/0092-8674(79)90005-9.

Chung, Albert E, Ian L Freeman, and Janina E Braginski (1977). „A novel extracellular membrane elaborated by a mouse embryonal carcinoma-derived cell line.“ In: *Biochemical and biophysical research communications* 79.3, pp. 859–868.

Colognato, H and P D Yurchenco (1999). „The laminin alpha2 expressed by dystrophic dy(2J) mice is defective in its ability to form polymers.“ In: *Current biology : CB* 9.22, pp. 1327–1330. DOI: 10.1016/S0960-9822(00)80056-1.

Costell, M. (Nov. 1999). „Perlecan Maintains the Integrity of Cartilage and Some Basement Membranes.“ In: *The Journal of Cell Biology* 147.5, pp. 1109–1122. DOI: 10.1083/jcb.147.5.1109.

Cummings, Christopher F. and Billy G. Hudson (Jan. 2014). „Lens capsule as a model to study type IV collagen.“ In: *Connective Tissue Research* 55.1, pp. 8–12. DOI: 10.3109/03008207.2013.867337.

Danysh, Brian P. et al. (Dec. 2008). „Contributions of Mouse Genetic Background and Age on Anterior Lens Capsule Thickness.“ In: *Anat Rec* 291.12, pp. 1619–1627. DOI: 10.1002/ar.20753.

Debnath, Jayanta, Senthil K. Muthuswamy, and Joan S. Brugge (July 2003). „Morphogenesis and oncogenesis of MCF-10A mammary epithelial acini grown in three-dimensional basement membrane cultures." In: *Methods* 30.3, pp. 256–268. DOI: 10.1016/S1046-2023(03)00032-X.

Denzer, A. J. (Dec. 1995). „An amino-terminal extension is required for the secretion of chick agrin and its binding to extracellular matrix." In: *The Journal of Cell Biology* 131.6, pp. 1547–1560. DOI: 10.1083/jcb.131.6.1547.

Durbeej, Madeleine and Kevin P Campbell (1999). „Biochemical Characterization of the Epithelial Dystroglycan Complex." In: 371.5, pp. 207–219.

Edwards, M. M. et al. (Jan. 2010). „Mutations in Lama1 Disrupt Retinal Vascular Development and Inner Limiting Membrane Formation." In: *Journal of Biological Chemistry* 285.10, pp. 7697–7711. DOI: 10.1074/jbc.m109.069575.

Erickson, A. C. and J. R. Couchman (Oct. 2000). „Still More Complexity in Mammalian Basement Membranes." In: *Journal of Histochemistry & Cytochemistry* 48.10, pp. 1291–1306. DOI: 10.1177/002215540004801001.

Fassler, R and M Meyer (Aug. 1995). „Consequences of lack of beta 1 integrin gene expression in mice." In: *Genes & Development* 9.15, pp. 1896–1908. DOI: 10.1101/gad.9.15.1896.

Ferrigno, O et al. (1997). „Murine Laminin a3A and a3B Isoform Chains are Generated by Usage of Two Promoters and Alternative Splicing." In: *J. Biol. Chem.* 272.33, pp. 20502–20507.

Fox, JW et al. (1991). „Recombinant nidogen consists of three globular domains and mediates binding of laminin to collagen type IV." In: *The EMBO Journal* 10.11, p. 3137.

Fukai, N. (Apr. 2002). „Lack of collagen XVIII/endostatin results in eye abnormalities." In: *The EMBO Journal* 21.7, pp. 1535–1544. DOI: 10.1093/emboj/21.7.1535.

Gagnoux-Palacios, Laurent et al. (2001). „The short arm of the laminin γ2 chain plays a pivotal role in the incorporation of laminin 5 into the extracellular matrix and in cell adhesion." In: *Journal of Cell Biology* 153.4, pp. 835–849. DOI: 10.1083/jcb.153.4.835.

Gautam, Medha et al. (May 1996). „Defective Neuromuscular Synaptogenesis in Agrin-Deficient Mutant Mice." In: *Cell* 85.4, pp. 525–535. DOI: 10.1016/s0092-8674(00)81253-2.

Georges-Labouesse, Elisabeth et al. (Aug. 1998). „Essential role of α6 integrins in cortical and retinal lamination." In: *Current Biology* 8.17, 983–S1. DOI: 10.1016/s0960-9822(98)70402-6.

Gould, D. B. (May 2005). „Mutations in Col4a1 Cause Perinatal Cerebral Hemorrhage and Porencephaly." In: *Science* 308.5725, pp. 1167–1171. DOI: 10.1126/science.1109418.

Graus-Porta, Diana et al. (Aug. 2001). „β1-Class Integrins Regulate the Development of Laminae and Folia in the Cerebral and Cerebellar Cortex." In: *Neuron* 31.3, pp. 367–379. DOI: 10.1016/s0896-6273(01)00374-9.

Hainsworth, D P et al. (2002). „Retinal capillary basement membrane thickening in a porcine model of diabetes mellitus." In: *Comp Med.* 52.6, pp. 523–529.

Halfter, W. et al. (Sept. 1998). „Collagen XVIII Is a Basement Membrane Heparan Sulfate Proteoglycan." In: *Journal of Biological Chemistry* 273.39, pp. 25404–25412. DOI: 10.1074/jbc.273.39.25404.

Halfter, Willi, Michael Willem, and Ulrike Mayer (Mar. 2005). „Basement Membrane–Dependent Survival of Retinal Ganglion Cells." In: *Investigative Opthalmology & Visual Science* 46.3, p. 1000. DOI: 10.1167/iovs.04-1185.

Halfter, Willi et al. (2002). „A critical function of the pial basement membrane in cortical histogenesis." In: *The Journal of neuroscience* 22.14, pp. 6029–6040.

Halfter, Willi et al. (Jan. 2013). „The bi-functional organization of human basement membranes." In: *PloS one* 8.7, e67660. DOI: 10.1371/journal.pone.0067660.

Hassell, J. R. et al. (Aug. 1980). „Isolation of a heparan sulfate-containing proteoglycan from basement membrane." In: *Proceedings of the National Academy of Sciences* 77.8, pp. 4494–4498. DOI: 10.1073/pnas.77.8.4494.

Henrich, Paul B. et al. (June 2012). „Nanoscale Topographic and Biomechanical Studies of the Human Internal Limiting Membrane." In: *Investigative Opthalmology & Visual Science* 53.6, p. 2561. DOI: 10.1167/iovs.11-8502.

Henry, Michael D and Kevin P Campbell (Dec. 1998). „A Role for Dystroglycan in Basement Membrane Assembly." In: *Cell* 95.6, pp. 859–870. DOI: 10.1016/s0092-8674(00)81708-0.

Ho, Matthew S P et al. (May 2008). „Nidogens-extracellular matrix linker molecules." In: *Microscopy Research and Technique* 71.5, pp. 387–395. DOI: 10.1002/jemt.20567.

Holmberg, Johan and Madeleine Durbeej (Jan. 2013). „Laminin-211 in skeletal muscle function." In: *Cell Adhesion & Migration* 7.1, pp. 111–121. DOI: 10.4161/cam.22618.

Hutter, Harald et al. (2000). „Cell Adhesion and Extracellular Matrix Genes." In: 287.February, pp. 989–995. DOI: 10.1126/science.287.5455.989.

Iozzo, Renato V (1998). „Matrix proteoglycans: from molecular design to cellular function." In: *Annual review of biochemistry* 67, pp. 609–52. DOI: 10.1146/annurev.biochem.67.1.609.

Iozzo, Renato V. (Aug. 2005). „Basement membrane proteoglycans: from cellar to ceiling." In: *Nature Reviews Molecular Cell Biology* 6.8, pp. 646–656. DOI: 10.1038/nrm1702.

Kalluri, Raghu (2003). „Angiogenesis: Basement membranes: structure, assembly and role in tumour angiogenesis." In: *Nature Reviews Cancer* 3.6, pp. 422–433. DOI: 10.1038/nrc1094.

Kashtan, Clifford (1998). „Alport Disease Syndrome and Thin Glomerular Basement Membrane." In: *Journal of the American Society of Nephrology* 9.9, pp. 1736–1750.

Khoshnoodi, Jamshid, Vadim Pedchenko, and Billy G. Hudson (2008). „Mammalian collagen IV." In: *Microscopy Research and Technique* 71.5, pp. 357–370. DOI: 10.1002/jemt.20564.

Kikkawa, Yamato, Ismo Virtanen, and Jeffrey H. Miner (2003). „Mesangial cells organize the glomerular capillaries by adhering to the G domain of laminin α5 in the glomerular basement membrane." In: *Journal of Cell Biology* 161.1, pp. 187–196. DOI: 10.1083/jcb.200211121.

Kikkawa, Yamato et al. (2002). „Identification of the binding site for the Lutheran blood group glycoprotein on laminin α5 through expression of chimeric laminin chains in vivo." In: *Journal of Biological Chemistry* 277.47, pp. 44864–44869. DOI: 10.1074/jbc.M208731200.

Kiritsi, Dimitra, Cristina Has, and Leena Bruckner-Tuderman (Jan. 2013). „Laminin 332 in junctional epidermolysis bullosa." In: *Cell Adhesion & Migration* 7.1, pp. 135–141. DOI: 10.4161/cam.22418.

Kleinman, Hynda K. et al. (Nov. 1982). „Isolation and characterization of type IV procollagen, laminin, and heparan sulfate proteoglycan from the EHS sarcoma." In: *Biochemistry* 21.24, pp. 6188–6193. DOI: 10.1021/bi00267a025.

Kleinman, Hynda K and George R Martin (2005). „Matrigel: basement membrane matrix with biological activity." In: *Seminars in cancer biology*. Vol. 15. 5. Elsevier, pp. 378–386.

Koch, M et al. (1999). „Characterization and expression of the laminin gamma3 chain: a novel, non-basement membrane-associated, laminin chain." In: *The Journal of cell biology* 145.3, pp. 605–18.

Labelle-Dumais, Cassandre et al. (May 2011). „COL4A1 Mutations Cause Ocular Dysgenesis, Neuronal Localization Defects, and Myopathy in Mice

and Walker-Warburg Syndrome in Humans." In: *PLoS Genetics* 7.5. Ed. by Nancy B. Spinner, e1002062. DOI: 10.1371/journal.pgen.1002062.

Lee, Jiwoon and Jeffrey M. Gross (June 2007). „Laminin β1 and γ1 Containing Laminins Are Essential for Basement Membrane Integrity in the Zebrafish Eye." In: *Investigative Opthalmology & Visual Science* 48.6, p. 2483. DOI: 10.1167/iovs.06-1211.

Lee, Yongsuk et al. (Oct. 2005). „Ocular abnormalities in Largemyd and Largevls mice, spontaneous models for muscle, eye, and brain diseases." In: *Molecular and Cellular Neuroscience* 30.2, pp. 160–172. DOI: 10.1016/j.mcn.2005.07.009.

Lennon, Rachel, Michael J Randles, and Martin J Humphries (Jan. 2014). „The importance of podocyte adhesion for a healthy glomerulus." In: *Frontiers in endocrinology* 5.October, p. 160. DOI: 10.3389/fendo.2014.00160.

Li, Shaohua et al. (2002). „Matrix assembly, regulation, and survival functions of laminin and its receptors in embryonic stem cell differentiation." In: *Journal of Cell Biology* 157.7, pp. 1279–1290. DOI: 10.1083/jcb.200203073.

Lin, Congxing et al. (2016). „Requirement for basement membrane laminin α5 during urethral and external genital development." In: *Mechanisms of Development*. DOI: 10.1016/j.mod.2016.05.004.

Liu, Jianmin et al. (Mar. 2006). „A genetic model for muscle–eye–brain disease in mice lacking protein O-mannose 1,2-N-acetylglucosaminyltransferase (POMGnT1)." In: *Mechanisms of Development* 123.3, pp. 228–240. DOI: 10.1016/j.mod.2005.12.003.

Lua, Magaly Reyes et al. (2016). „Superior Rim Stability of the Lens Capsule Following Manual Over Femtosecond Laser CapsulotomyThe Lens Capsule After Manual or Laser Capsulotomy." In: *Investigative Ophthalmology & Visual Science* 57.6, pp. 2839–2849.

McCarthy, Kevin J (2015). *The Basement Membrane Proteoglycans Perlecan and Agrin: Something Old, Something New.* Vol. 76, pp. 255–303. DOI: 10.1016/bs.ctm.2015.09.001.

Mestres, Pedro et al. (2014). „The basement membrane of the isolated rat colonic mucosa. A light, electron and atomic force microscopy study." In: *Annals of Anatomy - Anatomischer Anzeiger* 196.2–3, pp. 108–118. DOI: http://dx.doi.org/10.1016/j.aanat.2014.01.001.

Michele, Daniel E et al. (2002). „Post-translational disruption of dystroglycan – ligand interactions in congenital muscular dystrophies." In: *Nature* 418.July, pp. 417–422. DOI: 10.1038/nature00892.1..

Miner, J H, R M Lewis, and J R Sanes (1995). „Molecular cloning of a novel laminin chain, a5, and widespread expression in adult mouse tissues." In: *J.Biol.Chem.* 270.48, pp. 28523–28526.

Miner, Jeffrey H., Jeanette Cunningham, and Joshua R. Sanes (Dec. 1998). „Roles for Laminin in Embryogenesis: Exencephaly, Syndactyly, and Placentopathy in Mice Lacking the Laminin α5 Chain." In: *J Cell Biol* 143.6, pp. 1713–1723. DOI: 10.1083/jcb.143.6.1713.

Miner, Jeffrey H. and Joshua R. Sanes (1994). „Collagen IV a3, a4, and a5 chains in rodent basal laminae: Sequence, distribution, association with laminins, and developmental switches." In: *Journal of Cell Biology* 127.3, pp. 879–891. DOI: 10.1083/jcb.127.3.879.

Miner, Jeffrey H. and Peter D. Yurchenco (Jan. 2004). „Laminin functions in tissue morphogenesis." In: *Annual review of cell and developmental biology* 20.M, pp. 255–84. DOI: 10.1146/annurev.cellbio.20.010403.094555.

Moore, Steven A. et al. (July 2002). „Deletion of brain dystroglycan recapitulates aspects of congenital muscular dystrophy." In: *Nature* 418.6896, pp. 422–425. DOI: 10.1038/nature00838.

Morrissey, Meghan a and David R Sherwood (2015). „An active role for basement membrane assembly and modification in tissue sculpting." In: *Journal of cell science*, pp. 1661–1668. DOI: 10.1242/jcs.168021.

Neumann, Klaus H et al. (2004). „Age-dependent thickening of glomerular basement membrane has no major effect on glomerular hydraulic conductivity." In: *Nephrology, dialysis, transplantation : official publication of the European Dialysis and Transplant Association - European Renal Association* 19.4, pp. 805–11. DOI: 10.1093/ndt/gfh067.

Nishiuchi, Ryoko et al. (2006). „Ligand-binding specificities of laminin-binding integrins: A comprehensive survey of laminin-integrin interactions using recombinant a3b1, a6b1, a7b1 and a6b4 integrins." In: *Matrix Biology* 25.3, pp. 189–197. DOI: 10.1016/j.matbio.2005.12.001.

Orkin, RW et al. (1977). „A murine tumor producing a matrix of basement membrane." In: *The journal of experimental medicine* 145.1, pp. 204–220.

Parsons, Michael J et al. (2002). „Zebrafish mutants identify an essential role for laminins in notochord formation." In: *Development (Cambridge, England)* 129.13, pp. 3137–3146.

Pinzón-Duarte, Germán et al. (Mar. 2010). „Defective Formation of the Inner Limiting Membrane in Laminin β2- and γ3-Null Mice Produces Retinal Dysplasia." In: *Investigative Opthalmology & Visual Science* 51.3, p. 1773. DOI: 10.1167/iovs.09-4645.

Pöschl, Ernst et al. (2004). „Collagen IV is essential for basement membrane stability but dispensable for initiation of its assembly during early development." In: *Development (Cambridge, England)* 131.7, pp. 1619–1628. DOI: 10.1242/dev.01037.

Rowe, R. Grant and Stephen J. Weiss (Nov. 2008). „Breaching the basement membrane: who, when and how?" In: *Trends in Cell Biology* 18.11, pp. 560–574. DOI: 10.1016/j.tcb.2008.08.007.

Saarela, Janna et al. (Aug. 1998). „The Short and Long Forms of Type XVIII Collagen Show Clear Tissue Specificities in Their Expression and Location in Basement Membrane Zones in Humans." In: *The American Journal of Pathology* 153.2, pp. 611–626. DOI: 10.1016/s0002-9440(10)65603-9.

Schittny, J C, R Timpl, and J Engel (1988). „High resolution immunoelectron microscopic localization of functional domains of laminin, nidogen, and heparan sulfate proteoglycan in epithelial basement membrane of mouse cornea reveals different topological orientations." In: *The Journal of cell biology* 107.4, pp. 1599–610. DOI: 10.1083/jcb.107.4.1599.

Shimizu, Hiroshi et al. (2002). „Epithelial morphogenesis in hydra requires de novo expression of extracellular matrix components and matrix metalloproteinases." In: *Development (Cambridge, England)* 129.6, pp. 1521–1532.

Singh, R. et al. (2001). „Advanced glycation end-products: A review." In: *Diabetologia* 44.2, pp. 129–146. DOI: 10.1007/s001250051591.

Smyth, N. (Jan. 1999). „Absence of Basement Membranes after Targeting the LAMC1 Gene Results in Embryonic Lethality Due to Failure of Endoderm Differentiation." In: *The Journal of Cell Biology* 144.1, pp. 151–160. DOI: 10.1083/jcb.144.1.151.

Spenle, Caroline et al. (2013). „Laminin a5 guides tissue patterning and organogenesis." In: *Cell Adhesion and Migration* 7.1, pp. 90–100. DOI: 10.4161/cam.22236.

Stephens, L E et al. (Aug. 1995). „Deletion of beta 1 integrins in mice results in inner cell mass failure and peri-implantation lethality." In: *Genes & Development* 9.15, pp. 1883–1895. DOI: 10.1101/gad.9.15.1883.

Stitt W Alan (2001). „Advanced glycation, an important pathological event in diabetic and age related ocular disease." In: *Br J Ophthalmol* 85.(6), pp. 746–753. DOI: 10.1136/bjo.85.6.746.

Sugawara, Koji et al. (June 2008). „Laminin-332 and -511 in skin." In: *Experimental Dermatology* 17.6, pp. 473–480. DOI: 10.1111/j.1600-0625.2008.00721.x.

Suleiman, Hani et al. (Oct. 2013). „Correction: Nanoscale protein architecture of the kidney glomerular basement membrane." In: *eLife* 2. DOI: 10.7554/elife.01663.

Talts, Jan F. et al. (1999). „Binding of the G domains of laminin α1 and α2 chains and perlecan to heparin, sulfatides, α-dystroglycan and several extracellular matrix proteins." In: *EMBO Journal* 18.4, pp. 863–870. DOI: 10.1093/emboj/18.4.863.

Timpl, Rupert and Judith C. Brown (Feb. 1996). „Supramolecular assembly of basement membranes." In: *Bioessays* 18.2, pp. 123–132. DOI: 10.1002/bies.950180208.

Timpl, Rupert et al. (1979). „Laminin–a glycoprotein from basement membranes." In: *Journal of Biological Chemistry* 254.19, pp. 9933–9937.

Timpl, Rupert et al. (Nov. 1981). „A Network Model for the Organization of Type IV Collagen Molecules in Basement Membranes." In: *Eur J Biochem* 120.2, pp. 203–211. DOI: 10.1111/j.1432-1033.1981.tb05690.x.

Timpl, Rupert et al. (Dec. 1983). „Nidogen: a new, self-aggregating basement membrane protein." In: *European Journal of Biochemistry* 137.3, pp. 455–465. DOI: 10.1111/j.1432-1033.1983.tb07849.x.

To, Margaret et al. (Nov. 2013). „Diabetes-induced morphological, biomechanical, and compositional changes in ocular basement membranes." In: *Experimental Eye Research* 116, pp. 298–307. DOI: 10.1016/j.exer.2013.09.011.

Tsen, Guoshan et al. (1995). „Agrin is a heparan sulfate proteoglycan." In: *Journal of Biological Chemistry* 270.7, pp. 3392–3399.

Tsilibary, Effie C. (2003). „Microvascular basement membranes in diabetes mellitus." In: *Journal of Pathology* 200.4, pp. 537–546. DOI: 10.1002/path.1439.

Uechi, Guy et al. (July 2014). „Proteomic View of Basement Membranes from Human Retinal Blood Vessels, Inner Limiting Membranes, and Lens Capsules." In: *Journal of proteome research*. DOI: 10.1021/pr5002065.

Vázquez, Francisco et al. (Nov. 1996). „Changes of the basement membrane and type IV collagen in human skin during aging." In: *Maturitas* 25.3, pp. 209–215. DOI: 10.1016/s0378-5122(96)01066-3.

Wijeratne, Sithara S. et al. (2015). „Single molecule force measurements of perlecan/HSPG2: A key component of the osteocyte pericellular matrix." In: *Matrix Biology* 50, pp. 27–38. DOI: 10.1016/j.matbio.2015.11.001.

Willem, Michael et al. (2002). „Specific ablation of the nidogen-binding site in the laminin γ1 chain interferes with kidney and lung development." In: *Development* 129.11, pp. 2711–2722.

Xi, Yu-Ping et al. (Aug. 1982). „Age-related changes in normal human basement membrane." In: *Mechanisms of Ageing and Development* 19.4, pp. 315–324. DOI: 10.1016/0047-6374(82)90015-x.

Yoshida, Aruto et al. (Nov. 2001). „Muscular Dystrophy and Neuronal Migration Disorder Caused by Mutations in a Glycosyltransferase, POMGnT1." In: *Developmental Cell* 1.5, pp. 717–724. DOI: 10.1016/s1534-5807(01)00070-3.

Yurchenco, P. D. (Dec. 1987). „Basement membrane structure in situ: evidence for lateral associations in the type IV collagen network." In: *The Journal of Cell Biology* 105.6, pp. 2559–2568. DOI: 10.1083/jcb.105.6.2559.

Yurchenco, P. D. et al. (Jan. 1986). „Models for the self-assembly of basement membrane." In: *Journal of Histochemistry & Cytochemistry* 34.1, pp. 93–102. DOI: 10.1177/34.1.3510247.

Yurchenco, Peter D (2012). „Basement Membranes : Cell Scaffoldings and Signaling Platforms." In: pp. 1–28.

Yurchenco, Peter D., Peter S. Amenta, and Bruce L. Patton (2004). „Basement membrane assembly, stability and activities observed through a developmental lens." In: *Matrix Biology* 22.7, pp. 521–538. DOI: 10.1016/j.matbio.2003.10.006.

Yurchenco, Peter D, Yi-shan Cheng, and Holly Colognato (1992). „Laminin forms an independent network in basement membranes [published erratum appears in J Cell Biol 1992 Jun;118(2):493]." In: *The Journal of cell biology* 117.5, pp. 1119–1133. DOI: 10.1083/jcb.117.5.1119.

Yurchenco, Peter and Bruce Patton (Apr. 2009). „Developmental and Pathogenic Mechanisms of Basement Membrane Assembly." In: *CPD* 15.12, pp. 1277–1294. DOI: 10.2174/138161209787846766.

Zipser, B. D. et al. (2007). „Microvascular injury and blood-brain barrier leakage in Alzheimer's disease." In: *Neurobiology of Aging* 28.7, pp. 977–986. DOI: 10.1016/j.neurobiolaging.2006.05.016.

3

NATIVE BASEMENT MEMBRANES ENFORCE EPITHELIAL MECHANOPHENOTYPE

Native basement membranes enforce epithelial mechanophenotype

Philipp Oertle[1], Daphne Asgeirsson[1], Willi Halfter[2], Serenella Eppenberger[3], Ellen Obermann[3], Roderick YH Lim[1], Marija Plodinec[1,3]

[1]Biozentrum and Swiss Nanoscience Institute, University of Basel, Switzerland

[2]Eye Hospital, University Hospital Basel, Switzerland

[3]Institute of Pathology, University Hospital Basel, Switzerland

IN BRIEF   Oertle et al. show that epithelial formation depends on composition, architecture and mechanical properties of native human basement membranes (BMs) substrate. Such native substrates facilitate authentic BM interactions with living cells in situ. Results of the study demonstrate that the activation of laminin (Ln) $\alpha 5 - \beta 1/4$ integrin signaling by the BM specific properties regulates epithelial mechanophenotype in physiological tissues.

HIGHLIGHTS

- Determining architecture and mechanical properties of human native BMs

- Developing an in vitro tissue model whereby culturing epithelial cells on native BMs

- Identifying spatial, chemical and mechanical interactions between cells and native BMs in a physiological setting

- Identifying Ln $\alpha 5 - \beta 1$ integrin signaling pathway as the key regulator of epithelial stiffness on native human BMs

SUMMARY   BM represent a specialized form of extra-cellular matrix (ECM) that defines epithelial structure and function. Yet, how the physical and biochemical determinants of native BMs regulate the mechanobiology of epithelial cells remains poorly understood. Here, we show that isolated native human BMs exhibit a composition-specific multi-layered architecture and stiffness that concomitantly establish the mechanophenotype of epithelial cells. As a key feature, native BMs expose an ECM-facing collagen IV (ColIV)-rich side and a Ln-rich cellular interface that activates the Ln α5-β1/β4 integrin signaling pathway. In comparison to in vitro systems, this enables native BMs to mediate apico-basal polarity, tissue barrier formation and cell plasticity, being physiological hallmarks of human epithelia. In conclusion, our results underscore the role of BMs in tissue development and highlights possible links to cancer progression.
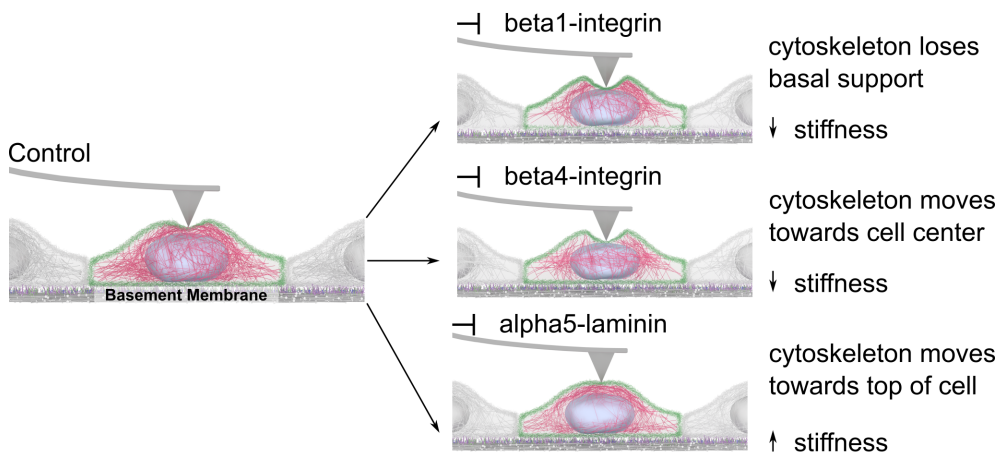
Graphical Abstract.
(Left) Cantilever indenting an epithelial cell growing on a basement membrane (BM). (Right) When β1-integrin is blocked, the cellular cytoskeleton is disorganized at the basal side and under the same force as in the control, the cantilever indents deeper into the cell. Upon blocking β-4 integrin, the cytoskeleton relocates from the apical face towards the cell center, also making the cell apparently softer. Finally, when blocking laminin (Ln) -α5 of the BM, the cytoskeleton moves towards the apical face, leading to an increase in apparent stiffness.

3.1 INTRODUCTION

The basement membrane (BM) is a specialized extra-cellular matrix (ECM) that plays a fundamental role in epithelial development and tissue function (Kalluri 2003). To do so, BMs promote cell adhesion as well as polarity, and compartmentalize tissue by separating the epithelium from the stroma (Morrissey et al. 2015; Sherwood 2015). BMs are composed of laminins (Lns), collagens and proteoglycans (PGs). Defects in this composition lead to early embryonic death prior to gastrulation (Smyth 1999). In cancer, the BM acts as a crucial physical barrier that hinders the dissemination of cancer cells (Kelley et al. 2014). However, it remains poorly understood how BM composition, organization and stiffness impact epithelial function.

In comparison to stromal ECM (Gilbert et al. 2017), in situ BM analysis is challenging due to the surrounding stroma, whose removal requires extensive decellularization procedures (Mayorca-Guiliani et al. 2017). To circumvent this, most studies reconstitute BM components in vitro. For example, Matrigel ®, a reconstituted basement membrane (rBM) consisting of components isolated from mouse ascites (Barcellos-Hoff et al. 1989) is commonly used in three-dimensional (3D) cell cultures (REFs). This has led to a Matrigel-based model (Gudjonsson et al. 2003), where BMs are depicted as a largely interconnected network (Yurchenco et al. 1986). In comparison, human BMs such as the inner limiting membrane (ILM) isolated from the eye reveal a bi-functional organization with distinct alternating layers of Ln and collagen IV (ColIV) (Halfter et al. 2013). Moreover, BMs vary in thickness and stiffness amongst different mammals (Laurie et al. 1984). Hence, the extent by which in vitro models recapitulate native tissue remains unresolved.

TISSUE ARCHITECTURE STRONGLY DEPENDS ON BM COMPOSITION   As a major BM component, Lns form at least 15 tissue-specific heterotrimeric isoforms that combine five αchains, four βchains, and three γchains (Yurchenco 2011). They facilitate cell adhesion and establish apico-basal polarity by ligating cell surface receptors (Gudjonsson et al. 2002; Weir et al. 2006) and hemidesmosomes (Mercurio et al. 2001). In particular, Miner et al. systematically demonstrated that Ln-α5 is necessary for maintaining glomerular filtration barrier integrity, distal epithelial maturation in the developing murine lung and the architecture of murine small intestine mucosa (Goldberg et al. 2010; Mahoney et al. 2008; Miner 2005; Nguyen et al. 2005). As the second major BM component, ColIV is composed of six different α-chains that

assemble into three linear ColIV heterotrimers (Khoshnoodi et al. 2008) to stabilize BM structure (McKee et al. 2009; Timpl et al. 1981).

By ensuring tissue architecture, BM components mediate essential biochemical signaling networks that guide cellular fate and function (Inman et al. 2015). This includes mechanical and biochemical signals, stromal derived growth factors and cytokines (Frantz et al. 2010). The key cell surface receptors that underlie these interactions are the integrins (Streuli 2009), which consist of at least 16 α- and 8 β-subunits that organize into 20 different heterodimers (Plopper et al. 1998; Paszek et al. 2004). Integrins typically cluster and associate with cytoplasmic molecules to form specialized adhesion sites such as focal adhesions (i.e., vinculin) and hemidesmosome (i.e., plectin) complexes (Austen et al. 2015). In doing so, integrins sense ECM rigidity to regulate cell proliferation (Lo et al. 2000), to drive differentiation into different lineages (Engler et al. 2006) and to regulate cell mechanophenotype.

By binding Ln, β1-integrins, such as α3β1 and α6β1, are required for epithelial polarity (lumen formation), apoptosis and functional stem cell maintenance (Taddei et al. 2008). Separately. β4-integrins are thought to be essential given the lack of mechanical resilience of tissues in epidermolysis bullosa patients (Vidal et al. 1995). As such, integrin α6β4 is required for hemidesmosome formation, cell adhesion and cell survival (Wilhelmsen et al. 2006). the role of β4-subunit for tissue stability has been suggested based on the lack of mechanical resilience of tissues from epidermolysis bullosa patients (Vidal et al. 1995). Nevertheless, the direct role of β1- and β4-integrins in determining cellular mechanophenotype has not been investigated in situ on native BMs. The involvement of each accompanying α-integrin is even more ambiguous. For example, α6 and α3 knockouts in a mouse model exhibited normal mammary morphogenesis, which suggests the existence of a compensatory mechanism involving other integrins (Klinowska et al. 2001; Klinowska et al. 1999). Interestingly, rBM-cultured 3D cysts of MDCK cells suggests a substrate-dependent role for different integrins with respect to polarity and lumen formation (Myllymäki et al. 2011; Rodriguez-Fraticelli et al. 2014).

In this study, we asked how native BMs trigger downstream integrin signaling followed by cytoskeleton rearrangements to regulate epithelial mechanophenotype. To address this question, we first isolated and characterized native BMs from the following human organs: mammary gland, kidney, colon and retina. Next, we correlated the mechano-cellular attributes of the BM/epithelium interface to its biochemical and structural properties using atomic force microscope (AFM) together with other high-resolution

microscopies. To validate the role of native BMs, we further demonstrated that MDCK cells cultured on isolated ILMs recapitulate tissue mechano-phenotype in vitro. This requires the activation of β1 and β4 integrins by the Ln-α5 chain. However, Ln-α5 coated artificial substrates of adequate stiffness were insufficient to recapitulate such physiological characteristics. Likewise, MDCK cells cultured in Matrigel did not recapitulate such physiological characteristics. Taken together, our work shows that native BM composition, architecture and stiffness concomitantly activates Ln-α5 to β1 -integrin signaling to establish physiologically relevant epithelia.

3.2 MATERIAL AND METHODS

3.2.1 *Substrate Preparation*

ILM PREPARATION   Human ILMs, kindly provided by Prof. W. Halfter, had been isolated from human cadaver eyes obtained from the Center for Organ Recovery and Education in Pittsburgh (IRB protocol number: 0312072;) according to previously published protocols (Candiello et al. 2010). Isolated ILMs were permanently stored at 4 °C in PBS supplemented with 5 % Penicillin-Streptomycin (PenStrep, Gibco 15140-122, LuBio Science GmbH, Switzerland) until further use. For confocal microscopy, ILMs were mounted on glass coverslips, while ILMs intended for AFM experiments were placed on cell culture dishes. In order to improve the adherence of the ILM to the substrate, both coverslips and cell culture dishes were pretreated with poly-L-lysine (PLL) (Sigma-Aldrich P4707, Switzerland). After 15 minutes of incubation at room temperature (RT), PLL was aspirated and the ILM was transferred to the substrate using a pipette and arranged such that the desired surface of the membrane was exposed. Excess medium was gently aspirated and subsequently the ILM was firmly attached to the substrate by centrifugation at 3500 rcf for 10 minutes. After preparation, the mounted ILMs were stored in PBS/PenStrep solution at 4 °C until further use.

LAMININ COATING   Glass coverslips and cell culture dishes were incubated with Ln solution, diluted 1:15 in PBS to yield 1 μg/cm² (BioLamina AB, LN-521 and LN-111, Sweden, kindly provided by Dr. E. Melo), for minimally 4 hours at 37 °C or overnight at 4 °C.

2D GEL SUBSTRATE PREPARATION   Following gel substrates were prepared for cell culturing: polydimethylsiloxane (PDMS), poly-acrylamide (PA),

poly-L-lysine coated poly-acrylamide (PLL-PA), reconstituted basement membrane coated poly-acrylamide (rBM-PA), rBM and laminin-521 coated poly-acrylamide (LN521-PA). Gels were applied to individual coverslips or coverslips glued on cell culture dishes using UV curing glue.

PDMS gels were prepared using the SYLGARD 184 Elastomer kit (SYLGARD, USA), mixing monomer and curing agent with a ration of 80:1. PDMS was thoroughly mixed, degassed and stored at -20 °C. Subsequently, the mixture was spin coated for 30 seconds at 5000 rpm and cured at 80 °C for 3 days. Prior to cell seeding, the mixture was sterilized in UV/Ozone for 10 minutes.

Proper attachment of PA to glass was ensured using 'bind silane'. Bind silane is mixed from 714 µl Silane A174 (Sigma-Aldrich 440159, Switzerland) and 714 µl of acetic acid (Fluka Analytical, Switzerland) and filled up to 5 ml with 96 % ethanol (Sigma Aldrich, Switzerland). The glass surface was incubated with bind silane for 10 minutes, then rinsed 3 times with pure ethanol and dried using a nitrogen stream. Subsequently, 570 µl of 30 % Acrylamide/Bis solution (BIO RAD #161-0158) was mixed on ice with 130 µl of 2 % Bis solution (Bio-Rad #161-0142, Switzerland). For biologically active rBM-PA or LN521-PA, 300 µl growth-factor rBM (Corning, #354230, Netherland) or 300 µl LN-521 or LN-111 was added. For biologically inert PA gels, PLL-PA, 300 µl of PLL was added. The mixture was vortexed, then 1 µl of TEMED (Sigma-Aldrich T7024, Switzerland) and 10 µl 10 % APS (Sigma-Aldrich 215589, Switzerland) were added and vortexed again. Consequently, 20 µl of the PA solution was pipetted onto the previously silanized glass surface and covered by a 18 mm diameter coverslip for 1 hour. The coverslip was subsequently removed and the PA substrate washed using at least 500 ml Milli-Q water overnight in order to remove excess acrylamide monomers prior to cell seeding. PA containing Ln was incubated with additional Ln as described in the previous section.

3.2.2 *Cell culture*

MDCK cells (type II, clone T23) kindly provided by I.S. Näthke, University of Dundee, were grown in minimum essential medium (MEM, Sigma-Aldrich M4655) supplemented with 10 % fetal bovine serum (Gibco 26140-079; LuBioScience GmbH, Switzerland) at 37 °C in a humidified atmosphere containing 5 % CO_2. Cells were split once a week, rinsed with PBS (Sigma Aldrich, Switzerland) and detached with 1X Trypsin-EDTA (Sigma-Aldrich T3924, 15 min incubation in the incubator).

POLYMER AND BM CULTURE   For experiments on polymer substrates or basement membrane, cell passages 3 to 15 were used. Cells were counted (NucleoCounter NC-3000, Chemometec A/S, Denmark) prior to seeding and plated at a density of 30'000 cells/cm² for time series measurements and 150'000 cells/cm² for blocking assays.

MDCK CYST CULTURE   For the formation of MDCK cysts, 48 µl of cell suspension containing 96'000 cells was mixed with 96 µl rBM . 12 µl drops of mixture were placed onto coverslips and allowed to solidify for 1 h at 37 °C before the culture medium was added. Cysts were cultured for 12 days until a hollow lumen was completely formed and the cysts reached a reproducibly diameter of roughly 60 µm.

3.2.3 *Tissue preparation and frozen sections*

Frozen mammary gland and kidney tissues, kindly provided by Dr. E. Obermann, were removed during surgery in accordance with ethical guidelines and approval by the institutional review board (Ref. no. EKBB 86/13). Fresh mammary gland, kidney and gut tissue was received from University hospital Basel through Tumor Bank (internal study ID 253). Tissue samples were used for confocal microscopy and AFM. Samples for confocal microscopy were fixed in 4 % formaldehyde solution (Formaldehyde 32 %, EM grade, EMS, USA) for 3 hours and then incubated in modified Hank's buffer (MHB) (Hank's buffer without Ca²⁺, containing 2mM EGTA, 5mM 2-(N-morpholino) ethane-sulfonic acid, pH 6.2–6.4) supplemented with 20 % sucrose for at least 12 hours. Samples for AFM were not treated prior to freezing to avoid stiffening through fixation. All samples were then embedded in Tissue-Tek (Sakura , Finetek, USA), frozen and stored at -20 °C. Frozen sections were prepared prior to subsequent experiments with a Leica cryostat with a cutting thickness of 10 to 20 µm.

3.2.4 *Antibody Blocking*

For Ln blocking, the ILM or PA-substrate was incubated with either laminin α1β1γ1 (LN-111) - or Ln-α5 (SAB4501720) antibody at a dilution of 1:100 at 4 °C overnight and subsequently rinsed with PBS. For short-term experiments (1 day incubation with cells), cells were seeded in growth medium at a concentration of 150'000 cells/cm². 2 hours post seeding, non-adherent cells

were removed by washing with growth medium. For long-term experiments (up to 11 days incubation with cells), cells were seeded at a concentration of 30'000 cells/cm². After cell fixation, samples were incubated with secondary antibodies against Ln for 3 hours to verify the antibody activity.

Integrin blocking was only performed short-term. The substrate was incubated with serum free medium containing 1 % bovine serum albumin (BSA) in the incubator for 1 hour. Cells were trypsinized, centrifuged and resuspended in serum-free medium containing 1 % BSA. The cells were diluted to 150'000 cells/cm² and 0.5 µl of antibody was added per 150'000 cells in solution. Cells were then kept in suspension on ice for 30 minutes and vortexed every 5 minutes to avoid aggregation of the cells. Excess medium was removed from the prepared substrates, cells pipetted onto the sample and incubated at 37 °C for two hours. In order to remove non-adherent cells, samples were rinsed 3x with serum free medium containing 1 % BSA and then normal growth medium was added.

3.2.5 *Confocal microscopy*

All confocal images were recorded at the Biozentrum Imaging Core Facility using a Zeiss LSM 700 upright microscope, 63x, 1.4 NA immersion oil objectives. Images were deconvolved using Huygens Remote Control (SVI, Netherlands) software and further analyzed with Fiji/ImageJ (Rasband, NIH, USA), Imaris (Bitplane AG, Switzerland), Python (Python Software Foundation, version 3.4.), Matplotlib (Hunter, J.D.) and CellProfiler, for cell counting (Broad Institute, USA). If not stated differently, primary and secondary antibodies, as well as dyes were diluted in MHB supplemented with 1 % BSA and 0.01 % sodium azide. The standard staining procedure consisted of application of the primary antibody, washing the sample 3x with MHB for at least 15 minutes before application of the secondary antibodies for 1 hour and washing again 3 times with MHB for at least 15 minutes.

CELL CULTURE SAMPLES   For immunofluorescence assays, cells were first permeabilized and fixed in MHB containing either 0.2 % TritonX-100 and 0.5 % formaldehyde or 2 % Octyl-POE and 0.125 % glutaraldehyde (the latter is used only for tubulin staining) for 5 minutes. After three washes with MHB, samples were further fixed with 4 % formaldehyde or 1 % glutaraldehyde, respectively for 20 minutes and stored at 4 °C until further use. For integrin staining, cells were fixed with 1 % formaldehyde in MHB for 10 minutes and then permeabilized with 0.5 % TritonX-100 in MHB for another 10 minutes. In

order to quench background fluorescence, samples fixed with glutaraldehyde were additionally treated with ice-cold MHB containing 5 mg/ml NaBH4, two times 10 minutes on ice. MDCK cysts in rBM were fixed in 4 % formaldehyde for 45 minutes until the rBM was dissolved and the sample then stored in MHB at least overnight. Individual cysts were pipetted individually onto glass holders that had been incubated with PLL for 30 minutes and incubated with 0.5 % TritonX-100 in MHB for 10 minutes. Samples grown on Ln- or ColIV-containing substrates were incubated overnight at 4 °C with the respective Ln or ColIV antibodies. Samples were then further stained using various primary antibodies against cellular components (see Table 3.1) at RT for 1 hour. Washing with the respective buffer was performed 3 times for at least 15 minutes. Subsequently, samples were incubated with secondary antibodies for 1 hour at RT. The following secondary antibodies were used: Alexa 488, 568 and 647 anti-mouse, rabbit, rat, goat and guinea pig (1:400, Invitrogen Life Technologies, Switzerland). Samples were then mounted on a glass slides using Vectashield (Vector Laboratories, USA)

BASEMENT MEMBRANES   Pristine ILM and rBM (gelled in the incubator for 30 minutes) were treated with blocking buffer (1 % BSA in MHB) at 4 °C overnight prior to staining. Samples were incubated with primary antibodies at 4 °C overnight, washed three times with MHB for at least 15 minutes, then incubated with secondary antibodies for 3 hours at RT, followed by washing in MHB for 3 hours at RT and mounted in Vectashield on glass slides.

TISSUES   Frozen sections of tissue specific thickness, 10 μm (kidney), 15 μm (breast), and 20 μm (gut) were stained for basement membrane components and polarity markers. To stain BM components, frozen sections were treated with blocking buffer (1 % BSA, 0.05 % Triton and 0.01 % sodium azide) for 5 minutes. Aspiration of the blocking buffer was followed by application of the primary antibody (dilution 1:100 in blocking buffer) and incubation for 1 hour at RT. After three washes with blocking buffer, samples were incubated with the secondary antibody (dilution 1:100 in blocking buffer) for 1 hour at RT. For polarity markers, frozen sections were first fixed and permeabilized with 0.5 % formaldehyde and 0.2 % Triton diluted in MHB for 5 minutes, followed by 20 minutes incubation with 4 % formaldehyde.

After fixation, the tissue sections were rinsed three times in excess with MHB and then incubated with the primary antibody at RT. After three washes with MHB, the secondary antibody combined with DAPI was applied and

Table 3.1 Antibodies/stains used to investigate cell-BM and cell-cell interactions.
Species: Mouse (Ms), Rat (Rt), Human (Hu), Rabbit (Rb), Guinea Pig (Gp)

Target/dye	Function	Spieces (Clone) / dye	Source
Z0-1	Tight junction	Ms (1A12)	Invitrogen
GP135	Glycoprotein	Ms (P3U-1)	DSHB
β4-integrin	Polarity	Ms (M126)	ab29042
α6-integrin	Polarity	Rt (GoH3)	ab95703
β1-integrin	Polarity	Rt (AIIB2)	DSHB
α3-integrin	Polarity	Ms (158A3)	BM6023P
Vinculin	Focal adhesion	Ms (hVIN-1)	V9131
Cytokeratin	Cytoskeleton	Ms (AE1/AE3 + 5D3)	ab86734
F-Actin	Cytoskeleton	Phalloidin	Invitrogen
β-Tubulin	Cytoskeleton	Ms (KMX-1)	MAB3408
Plectin	Cytoskeleton	GP	gift by H.H*
Laminin-111	GP, BM	Rb	L9393
Laminin α1	BM	Go	sc-6017
Laminin-332	BM	Rb	ab14509
Laminin α3	BM	Rb (EPR8266)	ab151715
Laminin α5	GP, BM	Rb	SAB4501720
Laminin α5	GP, BM	Ms (4C7)	MAB1924
CollagenIV	BM	Ms (J3-2)	SAB4200500
Collagen IV	BM	Rb	ab6586
Perlecan	HSPG, BM	Rt (A7L6)	MAB1948P
Nidogen	BM	Ms	ab77179
Nidogen	BM	Rb	ab14511
DNA	Nuclear Stain	DAPI	D9542

incubated for 1 hour at RT in the dark. Subsequently samples were rinsed three times with MHB and mounted with Mowiol.

ANTIBODIES

APICO-BASAL INTENSITY QUANTIFICATION   The apico-basal intensity distribution of actin and cytokeratin was quantified by a customized Python / ImageJ software. Confocal stacks of areas showing 30 to 50 cells were recorded and the nuclei detected automatically. On each z-slice, a band of 2.5 μm width was drawn around the nucleus of each cell and the intensity of actin or cytokeratin was quantified within this band. This quantification was repeated for each cell from the basal to the apical end of the cell. Actin or cytokeratin intensity was plotted in arbitrary units in an interval between

0 and 1 as a function of the z-stack position, averaged over all cells in the image (see Suppl. Figure 3.S1).

3.2.6 *Atomic Force Microscopy (AFM)*

ILM IMAGING   AFM imaging was only performed on bare ILMs prior to cell seeding in order to determine whether the LN-ILM or collagen IV side of inner limiting membrane (ColIV-ILM) would be exposed towards cells. Images were recorded at a frame size of 30 x 30 µm, with a setpoint of 1 Volt, line speed of 0.7 seconds/line and 5 % overscan.

FORCE MAPPING   Indentation testing experiments on substrates, cells and tissues were carried out using custom made AFM, ARTIDIS (ARTIDIS AG, Switzerland) and JPK Nanowizard I (Berlin, Germany), mounted on inverted microscopes. Standard triangular silicon nitride cantilevers with a spring constant between 0.07 and 0.09 N/m and a nominal tip radius of 10 nm and tip height of 5 µm were used for substrate testing and cell measurements (DNP-S10, Bruker AFM Probes, Camarillo, USA). Rectangular silicon nitride cantilevers with a spring constant around 0.09 N/m and a nominal tip radius of 35 nm and a tip height of 15 µm was used for tissue measurements (HQ-CSC38, MikroMasch, Nanoworld AG, Switzerland). The spring constant of each cantilever was determined using thermal tune and the Sader method (Sader et al. 1999) prior to each measurement. All measurements were performed with an indentation speed of 16 µm/s.

SUBSTRATE STIFFNESS TESTING   All ILMs used for force mapping were mapped before cell seeding in order to determine which areas corresponded to ColIV-ILM or LN-ILM and cells were seeded accordingly. Polymer substrates from each batch were tested by AFM to ensure that their stiffness matched the stiffness of LN-ILM. Basement membranes and substrates were characterized with force maps of 30 µm x 30 µm at a resolution of 32 x 32 points and a load of 3.1 nN.

CELL STIFFNESS MEASUREMENTS   Cells were measured at three time points (day 1; 60 % confluency), day four (day 4; confluent) and day eleven (day 11; maximum density). Cells on substrates where characterized using following settings: 80 µm x 80 µm at a resolution of 64 x 64 points and a load of 1.8 nN. For each condition, 3 dishes were prepared; 4 maps were recorded

per dish at different locations within the dish in order to account for inter-cell and inter-batch differences.

TISSUE STIFFNESS MEASUREMENTS   Frozen sections of 10 μm thickness from unfixed tissue were mounted on glass slides and measured in MHB. Maps of 40 μm x 40 μm up to 100 μm x 100 μm with a resolution of 100 x 100 pixels were recorded at 3.1 nN to locate and resolve the BM.

FORCE MAP ANALYSIS   Force maps were analyzed using the "ARTIDIS OfflineReader" analysis software (ARTIDIS AG, Switzerland). Force curves were analyzed using the modified Oliver and Pharr method as described previously (Loparic et al. 2010). The stiffness values calculated from curves were spatially plotted to yield color-coded stiffness maps and summarized into histograms using the ARTIDIS Offline Reader. For further data analysis, maps and histograms were processed as shown in Figure 3.S1. Using two automatically defined threshold stiffness values and a visual feedback, maps where split into nuclear, perinuclear and junctional regions. From the resulting histogram, a mean value μ, an amplitude A and the standard deviation σ were immediately displayed for each of the three regions. These parameters were set to obtain a triple Gaussian fit and only the resulting fit values were used for data interpretation and further statistical analysis. In addition, high-resolution of the stiffness maps allowed us to quantify cell density per surface area. Stiffness measurements for short-term blocking experiments are reported in arbitrary units (a.u.) rather than kPa when cells from different seeding conditions are compared to the different preparation of the cells which influences the stiffness of the controls. All values were normalized to the respective control which is by definition 1 a.u.

3.2.7 *Trans-epithelial resistance (TER) measurements*

TER measurements were performed using a customized support (Figure 3.S1C) that was fabricated using a 3D printer technology (envisionTec, μPerfactory, US). In contrast to standard transwell-membranes, this support has no micropores but one central hole of 1 mm radius that can be entirely covered with ILM. As a control, the resistance of each device is measured in a cell culture medium at RT prior to ILM mounting. To measure the resistance of the ILM, the membrane was mounted via centrifugation step on the support as described earlier and the resistance measurement was repeated. To follow cell-membrane barrier formation, time-lapse resistance measurements were

performed daily from cell seeding until the trans-epithelial resistance (TER) reached maximum value that remained constant.

3.2.8 *Scanning electron microscopy (SEM)*

ILMs attached to glass coverslips according to the protocol described above were fixed overnight in a freshly prepared solution of 4 % glutaraldehyde (EM grade) in MHB and then stored in 200-proof ethanol (Sigma-Aldrich-E7023, Switzerland) until further dehydration with a graded ethanol series. After critical point drying, samples were sputter-coated with platinum to a nominal thickness of 3 - 5 nm and examined with a Hitachi S4800 FEG scanning electron microscope at an accelerating voltage of 5 keV.

3.2.9 *Statistical Analysis*

Error bars in stiffness graphs show the standard error of the mean, non-overlapping error bars indicate a significant difference. The statistical significance of differences in mean values was assessed with the paired Student's t-test in OriginPro 8.5. The exact p-value for each data set is indicated in the corresponding figure with the asterisk ($* = p < 0.05, ** = p < 0.01, *** = p < 0.001$).

3.3 RESULTS

3.3.1 *The asymmetric layering of human basement membranes (BMs)*

Native BMs embedded within tissue sections of human colon, retina, mammary gland and kidney are characterized in Figure 3.1. Thin sections were assessed for their surface topography and mechanical stiffness by AFM under physiological buffer conditions followed by post-AFM confocal microscopy (Figure 3.1A). This allowed us to identify BM components being correlated to BM stiffness at the epithelial (Ep) or stromal (St) surfaces (for technical details Suppl. Figure 3.S1A).

AFM measurements performed revealed spatial and mechanical asymmetry based on a 3D overlay of topography and stiffness data for all examined BMs (Figure 3.1B, left). For example, the Ep side was significantly rougher and stiffer when directly compared with the St side. Post-AFM high-resolution fluorescence has revealed compositional asymmetry where all Ep sides were
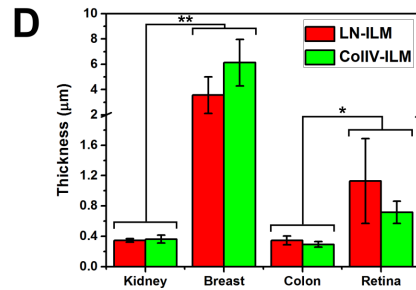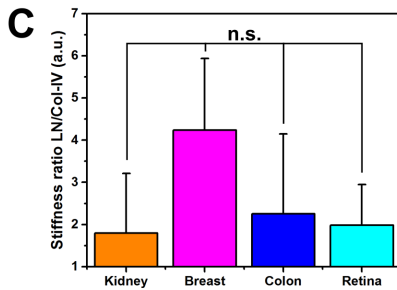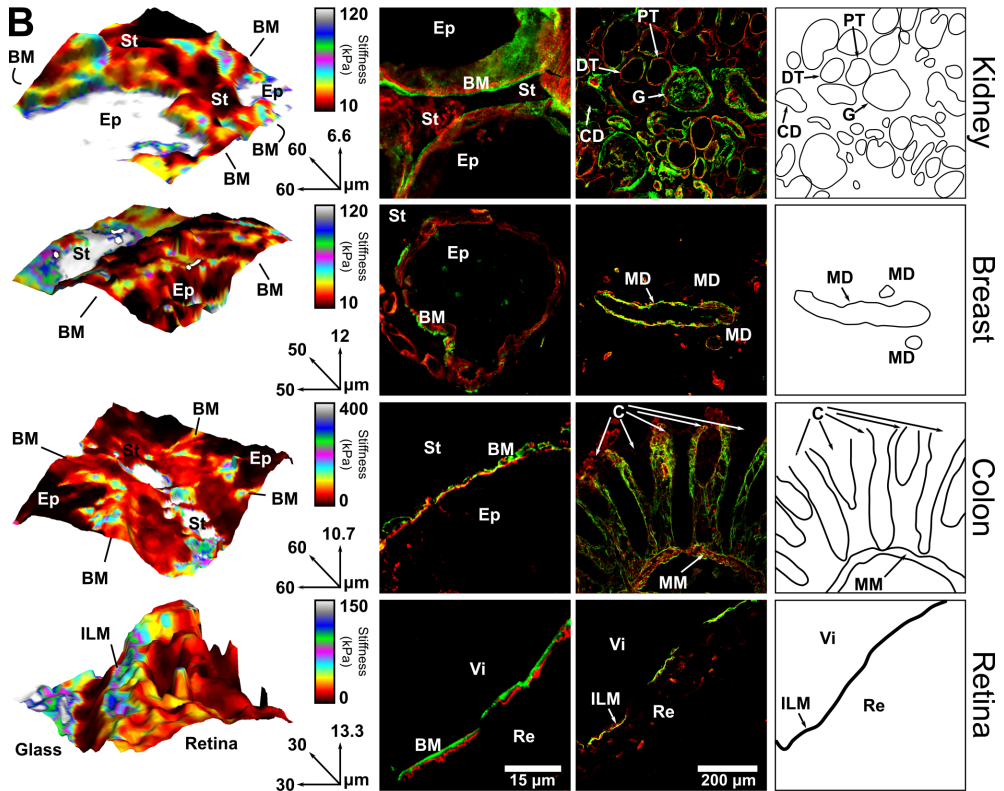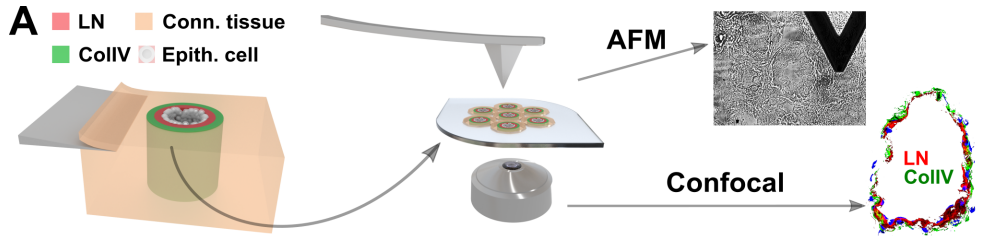
Figure 3.1 *(previous page)* The architecture and stiffness asymmetry of human basement membranes (BMs).

(A) Schematics shows experimental approach using combined fluorescence and atomic force microscope (AFM) for measurements of native human basement membranes.

(B) 1st column: 3D AFM overlay (topography and stiffness) showing BM spatial-mechanical asymmetry in kidney DT, breast MD, colon crypts and retinal inner limiting membrane (ILM). 2nd, 3rd column: Confocal fluorescence images displaying BM compositional asymmetry in kidney, breast, colon and retina. 4th column: Schematics highlight the outline of the organ specific basement membranes.

(C) Stiffness ratio of laminin (Ln) and collagen IV (ColIV)-side for kidney DT, breast MD, colon crypts and retinal ILM measured on a representative duct or membrane. All ratios are above 1, indicating that the Ln-side is consistently stiffer than the ColIV-side across tissues. Stiffness ratios are not significantly different between tissues.

(D) Thickness values of representative membranes of human kidney DT, breast MD, colon crypt and retinal ILM assessed from confocal imaging and labelled for Ln and ColIV. The thickness was measured on 10 different positions along the membrane. Breast MD BMs are significantly thicker than retina, colon or kidney BMs. Retinal BM is thicker than kidney and colon BM, while kidney and colon do not differ significantly in thickness.

G = glomerulus, PT = proximal tubule, DT = distal tubule, CD = collecting duct, A = alveoli, MD = mammary duct, BrM = Bruch's membrane, ILM = Inner Limiting Membrane, Vi = vitreal side, Re = retinal side, Ep = epithelial / luminal side, St = stromal side

All data are represented as means $\pm$ SD. $***p < 0.001, **p < 0.01, *p < 0.05$; two-tailed unpaired t-test.

predominantly comprised of Ln based on Ln-γ1 staining, while St sides were mainly composed of ColIV based on tissue specific staining (Figure 3.1B, middle). In addition, fluorescence data showed compositional asymmetry of different BMs specific to each organ (Figure 3.1B, middle, 2nd column), which was additionally outlined for a better orientation in the schematics (Figure 3.1B, right). Quantitative analysis of stiffness measurements has confirmed significant differences in stiffness between the Ep and St side.

In particular, the stiffness ratio between St predominantly expressing ColIV versus Ep expressing Ln was for all membranes in the similar range of 1:2.5 (Figure 3.1C). This is also in agreement with the data we published previously for ILM isolated from human retinas ((Halfter et al. 2013), Suppl. Figure 3.S2).

The AFM topography measurements (Figure 3.1B, left and Suppl. Figure 3.2) have indicated that native human BMs might be significantly thicker than considered previously. Therefore, we specifically measured the thickness of all BMs in native hydrated conditions. Surprisingly, the results have revealed that all BMs exhibited thicknesses in the range of micrometers (Figure 3.1D). More specifically, the kidney proximal distal tubules were thinnest with values around one micrometer, followed by colon and then thickest membranes; breast and retinal membranes as for example ILM that were ranging up to 5 micrometers (Figure 3.1D, Suppl. Figure 3.S2A and 3.S2B). The high resolution confocal images have confirmed the bi-layered structure

of ILM (Suppl. Figure 3.S2B, left) and also stiffness sensitivity of the LN-ILM to changes of the buffer ionic strength (Suppl. Figure 3.S2B, right) additionally confirming the direct association of proteoglycan charged sugar chains to Ln but not to ColIV-ILM which did not exhibit any stiffness alterations as a function of ionic strength of the buffer (Suppl. Figure 3.S2B, right, (Halfter et al. 2013)). Importantly, the thickness of all BMs did not correlate with stiffness measurements, therefore excluding possible side effects of underlying glass substrate on thinner membranes. In contrast to native BMs, an rBM substitute that is mainly used to mimic BMs in vitro exhibited amorphous, unstructured mixture of BM components (Suppl. Figure 3.S2C, left) with significant viscoelastic response due to high water content and stiffness values that are up to 100-folds lower than for all native BMs (Suppl. Figure 3.S2C). We conclude that different BMs isolated from human epithelial organs exhibit a significant degree of similarity with predominant compositional, organizational and stiffness asymmetry that might be critical for functions performed by cells that attach specifically either to the Ep or St side of the same BM.

3.3.2 *Determining expression of Ln α-chains in human BMs*

The Ln face of BMs is thought to be the main platform for biochemical and mechanical transmission between epithelial cells and their microenvironment. In this context, Ln α-chains are known to interact specifically with cell surface integrin receptors (Nielsen et al. 2001; Nishiuchi et al. 2006). To determine the presence of specific Ln α-chains in the tissue sections from human kidney proximal distal tubule, breast, colon and retina we performed high-resolution confocal microscopy of stained sections with antibodies that allowed for direct visualization of specific Lns within each BM (Figure 3.2).

Ln-α5 chain is known to comprise laminin α5β1γ1 (LN-511) and laminin α5β2γ1 (LN-521) and was also the predominant α-chain found in the ILM (Uechi et al. 2014). Our data showed that Ln-α5 chain and LN-111 are abundantly present in all examined BMs (Figure 3.2A). In addition LN-332, a typical constituent of the epidermis that originates from the ectoderm (Kiritsi et al. 2013) was detected abundantly in kidney and breast BMs, scarcely in colon and none in retina (Figure 3.2B). Interestingly, Ln-α3 chain was predominantly expressed in the regions populated by epithelial cells but not localized to BM (Figure 3.2C). We also observed the similar expression pattern lacking Ln-α1 chain expression at the BM, whereas localized to the inlaying cells across all examined tissues (Figure 3.2D). In contrast, to native BMs in rBM only LN-111 was present, but not Ln-α5 (Suppl. Figure 3.S2D). These results indicate that
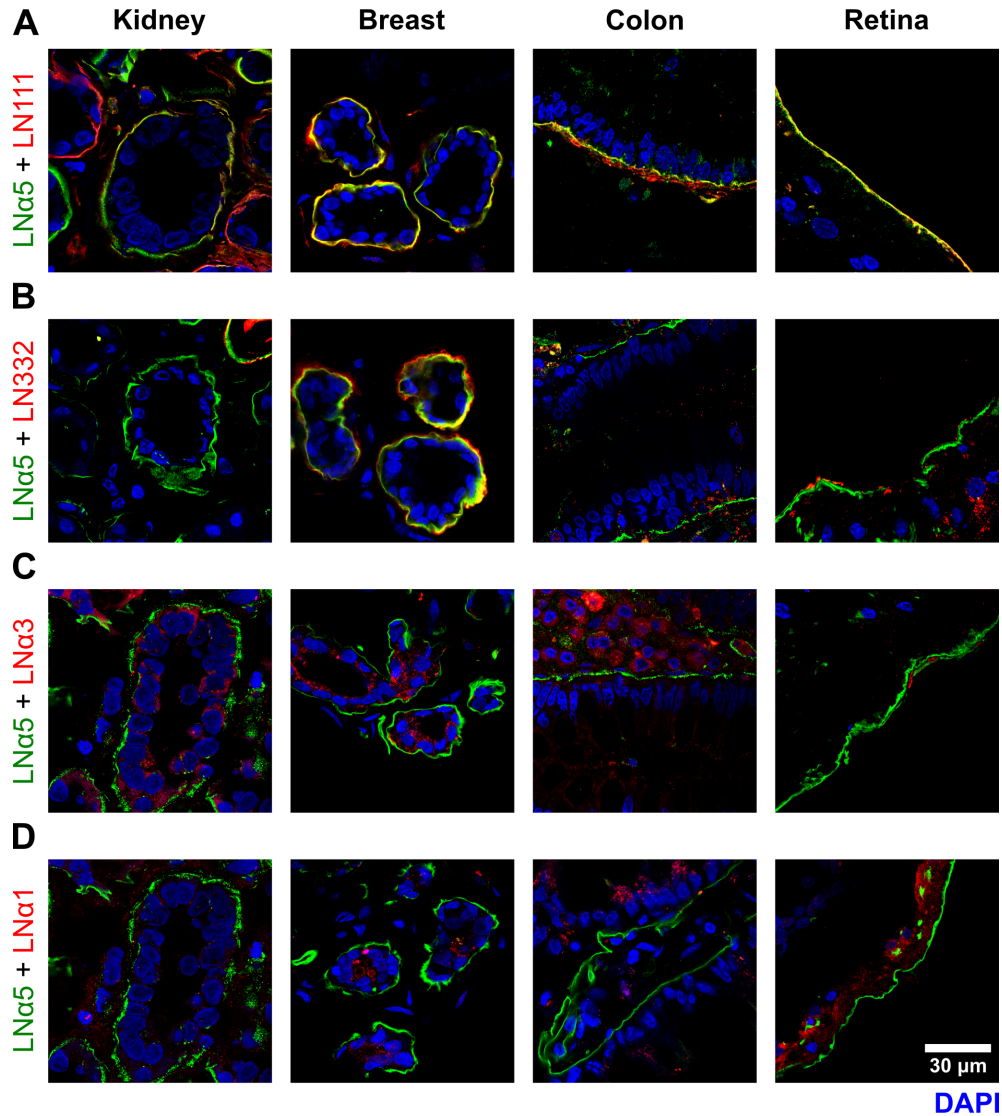
Figure 3.2 Laminin (Ln) α-chain distribution in human basement membranes (BMs).
Confocal images reveal distribution of (A) laminin α1β1γ1 (LN-111) and Ln-α5, (B) laminin α3β3γ2 (LN-332) and Ln-α5, as well as (C) Ln-α1 and Ln-α3, (D) Ln-α1 and Ln-α5 chains in kidney (column 1), breast (column 2), colon (column 3) and retina (column 4).

the expression of the Ln-α5 chain is a predominant shared feature of human epithelial BMs while other Ln chains were expressed in an organ specific manner as suggested previously reviewed in (Yurchenco 2011)

3.3.3 *Culturing epithelial cells on native BM promotes tissue-like physiological properties in vitro*

ILM exhibits great similarity in terms of asymmetrical composition, architecture and stiffness to other BMs from kidney, colon and breast. Therefore, our key objective was to assess the suitability of retinal ILM as a native BM substrate for culturing epithelial MDCK cells in vitro. Also, in contrast to other BMs, ILM membranes were most efficiently isolated devoid of cells and cellular debris from the original organ. Although not of human origin, MDCK cells extracted from the proximal distal tubules of dog kidney establish typical epithelial morphology even under standard 2D culturing conditions in vitro (Rodriguez-Fraticelli et al. 2014; Trepat et al. 2007).

We have cultured MDCKs on top of human ILMs (Figure 3.3A, left) up to 14 days to examine the role of native BM in epithelial tissue formation in vitro (Figure 3.3). Fluorescence microscopy visualization of the LN-ILM as well as DAPI staining showed that cells on ILM were significantly denser than cells on the adjacent artificial culture dish (Figure 3.3A, right). This was also quantified by monitoring the cell proliferation over a 14-day period. Results revealed that MDCK cells on ILM exhibit 75% higher density and strong substrate adherence, i.e. cannot be easily detached by trypsin than cells on glass substrate. The comparison of cells cultured on top of LN-ILM versus ColIV-ILM showed a clear side-dependence of proliferation behaviour. For example, exposure to LN-ILM promoted stronger cell-substrate adherence and higher proliferation than for cells on ColIV-ILM (Figure 3.3B, left panel). Furthermore, even at full confluence, MDCKs cultured on top of ILM did not exhibited domes; specific structures that appear overt time when these cells are cultured on artificial hard substrates. MDCKs cultured on ILM established a functional barrier that was assessed by the TER measurements (Figure 3.3B, right, Suppl. Figure 3.S1C).TER values measured in this setup were orders of magnitude higher than ones reported for MDCK cells when cultured in trans-well plates (Stevenson et al. 1988), indicating that LN-ILM provides the means for MDCK cells to establish a tight functional barrier. We assessed this further by examining provision of signals that are involved in epithelial polarization and architecture (Figure 3.3C).

We compared the reference sections from human kidney presenting distal tubules (Figure 3.3C, top) to MDCK cysts cultured in rBM and MDCK cells cultured on top of an ILM. Fluorescence imaging was used to detect specific markers, such as ZO-1 (tight junctions), E-Cadherin (adherens junctions), Na+/K+ -ATPases (constituting intercellular ion channels, localized laterally

at the intercellular space between single cells) and GP135/podocalyxin (a major component of podocyte glycocalyx), as well as to examine the level of apico-basal cell polarity and epithelial organization (Figure 3.3C, bottom). Optical cross-sections of the epithelial layer revealed apical localization of ZO-1 and GP135, while E-Cadherin and Na+/K+ ATPases expression appeared orthogonally to the substrate in the intercellular space (Figure 3.3C, left). These results were in agreement with the localization of the same markers in the human tissue sections (Suppl. Figure 3.S4) visualized both longitudinally and perpendicular to examine different regions and more specifically areas of proximal distal tubules of human kidney (Figure 3.3C, middle). In contrast, when the MDCK cells were cultured as cysts in rBM over an equal period of time (14 days), which is sufficient to complete cyst formation (Wang et al., 1990a, b), the polarity markers were only partially expressed and the junctions were not correctly localized (Figure 3.3C, right). These results demonstrated the dependency of cell proliferation, apico-basal polarity and functional barrier formation with regards to the underlying substrate where only the native BMs were capable of recapitulating the physiologically relevant BM microenvironment in vitro.
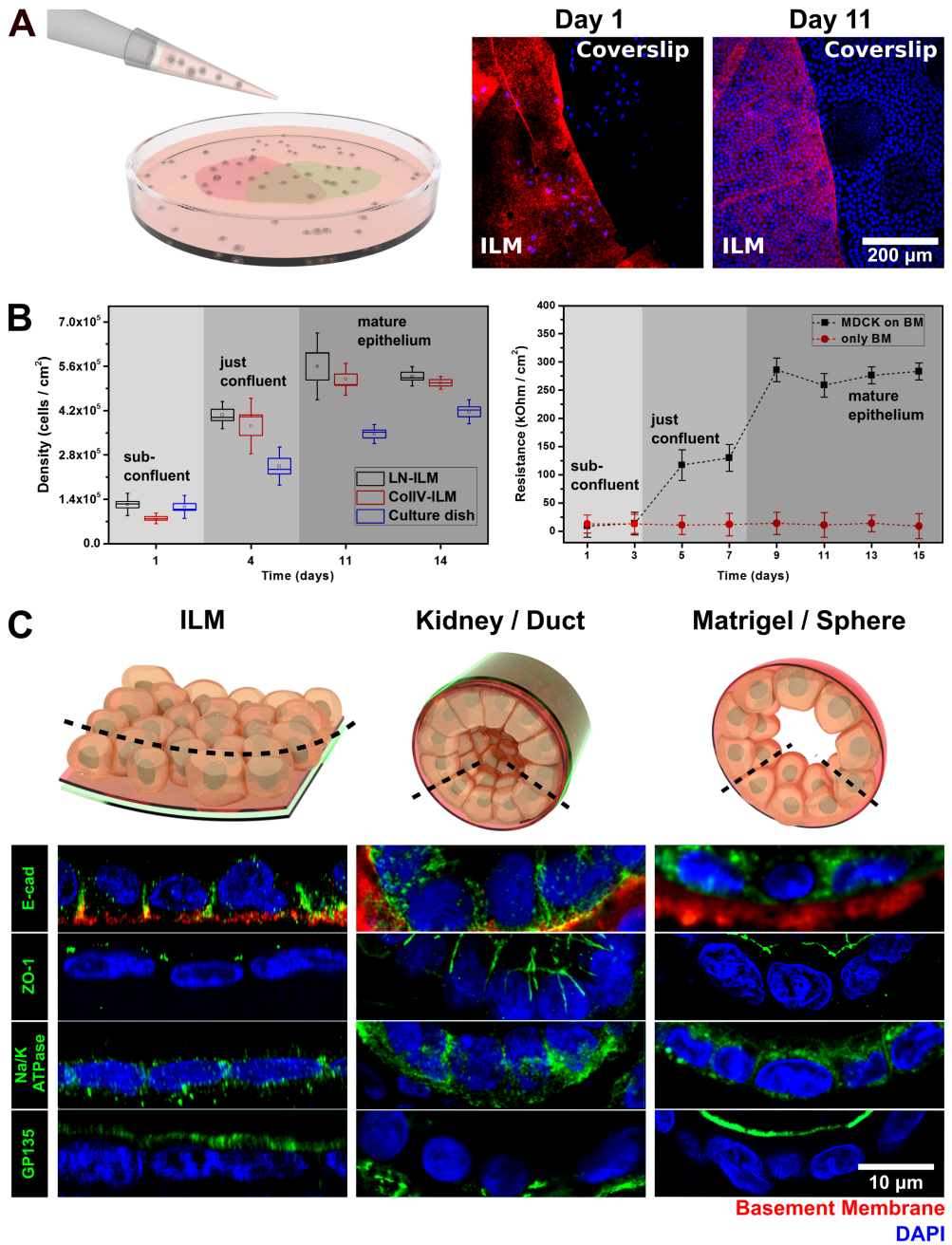
Figure 3.3

Figure 3.3 *(previous page)* MDCK cells establish apical-basal polarity and an electro physical barrier on inner limiting membrane (ILM).

(A) (Left) Schematics describing experimental procedure of seeding epithelial MDCK cells on laminin-side of inner limiting membrane (LN-ILM) (red) or collagen IV side of inner limiting membrane (ColIV-ILM) (green) of a flat mounted native basement membrane (BM). (Right) Confocal images of MDCK cells (DAPI, blue) on ILM (LN-111, red) and coverslip (no staining), 24 hours post seeding and 11 days post seeding.

(B) (Left) Cell density increases significantly for cells cultured on LN-ILM or ColIV-ILM when compared to bare coverslip. (Right) Trans-epithelial resistance (TER) values of MDCK cells on ILM and bare ILM over a course of 15 days reveal formation of a tight electro physical barrier.

(C) (Top) Schematic depicting planes of optical sections for (left) cells on ILM, (middle) kidney duct and (right) and an epithelial cyst of MDCKs cultured in reconstituted basement membrane (rBM), i.e Matrigel. (Bottom) Orthogonal (x-z) sections of confocal stacks of (left) of MDCK cells cultured for 11 days on ILM, (center) kidney tissue sections and (right) MDCK cysts cultured in Matrigel for 11 days. Fluorescence imaging of polarity markers E-cadherin, Na/K-ATPases and GP135/Podocalyxin (green), BM (LN111, red) and nuclei (DAPI, blue) enables direct verification and cross-comparison of epithelial architecture and barrier formation after 11 days in culture.

3.3.4 *MDCK cells on LN-ILM recapitulate tissue-like mechanophenotype and cytoarchitecture*

Currently it is not well understood how BMs contribute to mechanophenotype of epithelia (Lecuit et al. 2017). To address this question, we have cultured MDCK cells on LN-ILM and ColIV-ILM for a period of 11 days (Figure 3.4A), since we determined no significant difference in cellular characteristics between 11 and 14 days as illustrated in Figure 3.3. We used AFM to perform stiffness mapping of epithelial layers at defined time points from 24 hours post seeding (Day 1) until day 11 in cell culture (Figure 3.4B, Suppl. Figure 3.S1B). The AFM stiffness maps revealed distinct differences in mechanical response between cells cultured on LN-ILM when compared to cells cultured on ColIV-ILM. For example, within 24 hours post seeding MDCK cells cultured on LN-ILM or ColIV-ILM exhibited similar stiffness properties. However, over time stiffness differences became more apparent. In particular, MDCKs on LN-ILM have maintained their stiffness after four days.

In contrast, cells on the ColIV-ILM exhibited fluctuations in stiffness with 20 % higher stiffness values than on LN-ILM (Figure 3.4C) and appeared more similar in stiffness to cells cultured on bare dish. In contrast cells cultured in rBM were 2-fold softer than cells on LN-ILM (Suppl. Figure 3.S3A). Taken together, AFM stiffness measurements have revelaed distinct epithelial mechanophenotype of MDCK cells on LN-ILM that is similar to stiffness of human epithelia measured in situ (Plodinec et al. 2012)

MDCK cells cultured for 11 days on LN-ILM exhibited very distinct stiffness values for cell body (soft - dark colour on the map, Figure 3.4B left) and
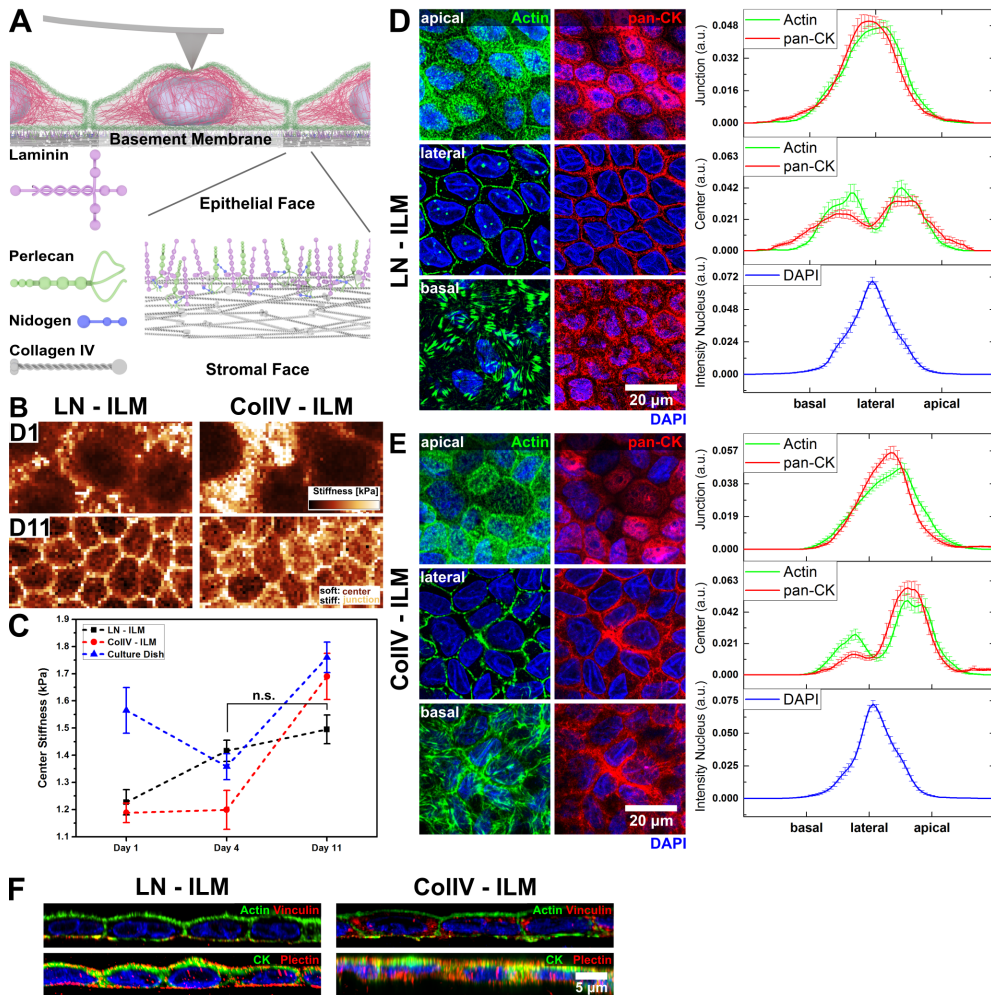
cellular junctions (stiff - bright colour on map, Figure 3.4B left). In comparison, cells on COLIV-ILM displayed significantly smaller differences between cell body and junctions (Figure 3.4B, right). These data corroborated distinct epithelial stiffness corresponding to barrier formation as already indicated by TER data (Figure 3.3B, right) and polarity and junctional markers (Figure 3.3C).

Distinct alterations in stiffness between MDCK cells cultured on LN-ILM and COLIV-ILM prompted us to examine the organization of the cytoskeleton since it has a major impact on cellular mechanics (Fletcher et al. 2010). Confluent layers of MDCK cells cultured for 11 days on native LN-ILM exhibited mature actin bundles and a solid lateral cytokeratin expression (Figure 3.4D).

Figure 3.4 *(previous page)* The architecture and stiffness asymmetry of human BMs differentially impacts cytoarchitecture and mechanophenotype of epithelia.

(A) Schematics displays confluent cells on native BM. (Top) BM signaling at the basal side influences the apical cytoskeleton and consequently mechanical properties as measured by atomic force microscope (AFM). (Bottom left) Renderings illustrate four main components of human BM; laminin (Ln), perlecan, collagen IV (ColIV) and nidogen. (Bottom right) Structural representation of the BM architecture.

(B) Atomic force microscopy (AFM) force maps of MDCK cells on laminin-side of inner limiting membrane (LN-ILM), collagen IV side of inner limiting membrane (ColIV-ILM) and culture dish cultured for 24 hours (upper panel) and eleven days (lower panel). 80 μm x 40 μm, 64 x 32 pixel, load 1.8 nN.

(C) Stiffness time-lapse of MDCK cells on LN-ILM, ColIV-ILM and culture dish.

(D) (Left) Confocal projections of MDCK cells cultured in LN-ILM stained for actin (left column) and cytokeratin (right column), from basal to apical side. (Right) Apical-basal fluorescence intensity distribution of MDCK on LN-ILM. In the central area, below and above the nucleus, actin and cytokeratins are distributed evenly along the basal-apical axis on the LN-ILM at 11 days of culture.

(E) (Left) Confocal projections of MDCK cells cultured in ColIV-ILM and stained for actin (left column) and cytokeratin (right column), from basal to apical side. (Right) Apical-basal fluorescence intensity distribution of MDCK on ColIV-ILM. The actin and cytokeratin intensities are drastically shifted towards apical side for cells cultured on ColIV-ILM for 11 days.

(F) (Left) Confocal orthogonal x-z projections of MDCK cells reveal focal adhesions and hemidesmosome formation based on the localization of actin, vinculin and DAPI (upper panel) and (lower panel) cytokeratin, plectin and DAPI for cells cultured on LN-ILM or (Right) ColIV-ILM for 11 days.

Both proteins were detected throughout the cell, traversing the entire apico-basal space. A dominant trait expressed by these cells was the formation of thick actin bundles at the basal side, located between the cell membrane and the nucleus (Figure 3.4D, left). Actin filaments closely lined the regions of cellular junctions, located laterally of epithelial cells, stretching up to the apical side where they eventually converged into a so-called actin cap (Esue et al. 2008). In contrast to actin, that is intimately associated with the cell membrane, cytokeratin spanned the whole cytoplasm from the basal to the apical side, forming a nucleus-embracing structure while connecting the basolateral portion of the cell membrane with its apical side (Figure 3.4D, right) (Herrmann et al. 2007). This specific phenotype is only found in the epithelia from native tissues and embryonic tissue sections (Cetera et al. 2015; Horne-Badovinac 2014) (Suppl. Figure 3.S5), but not for cells cultured in/on artificial substrates such as rBM (Suppl. Figure 3.S3B) in vitro.

To be able to quantitatively correlate changes in cell stiffness with alterations in the cytoskeleton architecture we have developed an algorithm to correlate and accurately evaluate changes in fluorescence intensity for cells cultured on native BM. We compared the organization of actin and cytokeratin networks from basal to apical side under influence of either Ln (Figure 3.4D) or ColIV (Figure 3.4E). On the LN-ILM, the cytoskeleton was evenly distributed from basal to apical surface and the specific stiffness properties of MDCK cells on LN-ILM could be directly attributed to an evenly distributed cytoskeleton

network (Figure 3.4D, right). Moreover, on the LN-ILM we detected a distinct localization of focal adhesions as shown by vinculin and actin co-staining (Figure 3.4F, top). Hemidesmosome formation was identified from basolateral localization of cytokeratin and plectin (Figure 3.4F, bottom). In contrast, on the ColIV substrate actin and cytokeratin were significantly shifted towards apical surface in the central area of the cell thus leading to a 20 % stiffness increase for MDCK cells after 11 days in culture (Figure 3.4E, right).

3.3.5   *Reconstituted BM matrices in vitro evoke cellular mechanophenotypes distinct from ILM or native tissues*

We have thus far demonstrated that epithelial cells experience an input of mechanics, structural and biochemical information provided by the underlying BM. In order to uncouple these aspects we sought to examine epithelial behaviour on artificial substrates (Figure 3.5). Using the analogy to native BMs, we tested matrices of defined stiffness but with varying composition and surface properties. For this purpose, we prepared a set of gel-based substrates (Figure 3.5A, left), all of them tuned to a LN-ILM characteristic stiffness of 100 kPA (Figure 3.5A, right). Homogeneous gel substrates, based either on PDMS, or PA, served as models representing solely the stiffness aspect of the native ILM.

Next, PA was either coated with PLL-PA to provoke unspecific reaction or with LN521-PA that represented a crucial BM component, i.e. Ln-α5 chain. These preparations were designed with the intention to provide biochemical information. We performed time-lapse stiffness mapping to quantify changes in cell stiffness on each specific substrate (Figure 3.5B, left). Evidently, substrates that lacked biological signals did not evoke the physiological stiffness response of MDCK cells. Stiffness values measured for cells grown on PDMS or PLL coated polymers were significantly lower over time despite high substrate stiffness than for cells exposed to LN-ILM or LN521-PA (Figure 3.5B, right). In particular, cells cultured on physiologically more relevant LN-521 were 25 % stiffer than cells on LN-ILM, while cells cultured on PLL-PA and PDMS were approximately 50 % softer under same substrate stiffness conditions.

In epithelial tissues, focal adhesions and hemidesmosomes play a fundamental role in conveying signals from ECM to cell cytoskeleton (Herrmann et al. 2007; Leube et al. 2015). Therefore, we asked how cell adhesive properties and organization of the cytoskeleton alter as a consequence of artificial substrates versus cells cultured on native ILM (Figure 3.5C,). We found that the localization of focal adhesions was considerably different between ILM

and all artificial substrates. For instance, the vinculin expression was prominent on the basal side of cells cultured on ILM and was lacking stress fibres (Figure 3.5C, left), while on the LN-521 coated plastic it was only localized to the tip ends of actin stress fibres (Figure 3.5C, middle). Similar observation was made for cells cultured on LN521-PA. Interestingly, the co-localization between actin and vinculin has demonstrated a good degree of co-localization for LN-521 and LN521-PA specifically at the actin tips (LN-521) and cell junctions (LN521-PA). However on native ILM co-localization of actin-vinculin was significantly more prominent and spatially spanning the cells (Figure 3.5C, bottom row). Quantification of fluorescence colocalization, i.e. Mander's coefficients plot (Figure 3.5D) has revealed that in case of LN-521 and LN521-PA vinculin increasingly co-localized with actin, while actin decreasingly co-localized with vinculin. These data additionally corroborated distinct vinculin localization to stress-fiber tips in case of artificial Ln substrates as opposed to a homogeneous distribution of both the actin and vinculin on physiological LN-ILM.

Our data demonstrated that cellular substrate perception is not only restricted to surface chemistry or substrate stiffness. Moreover, cellular responses in terms of stiffness and cytoskeleton reorganization are regulated by the microarchitecture of the matrix substrate (Shakouri-Motlagh et al. 2017).
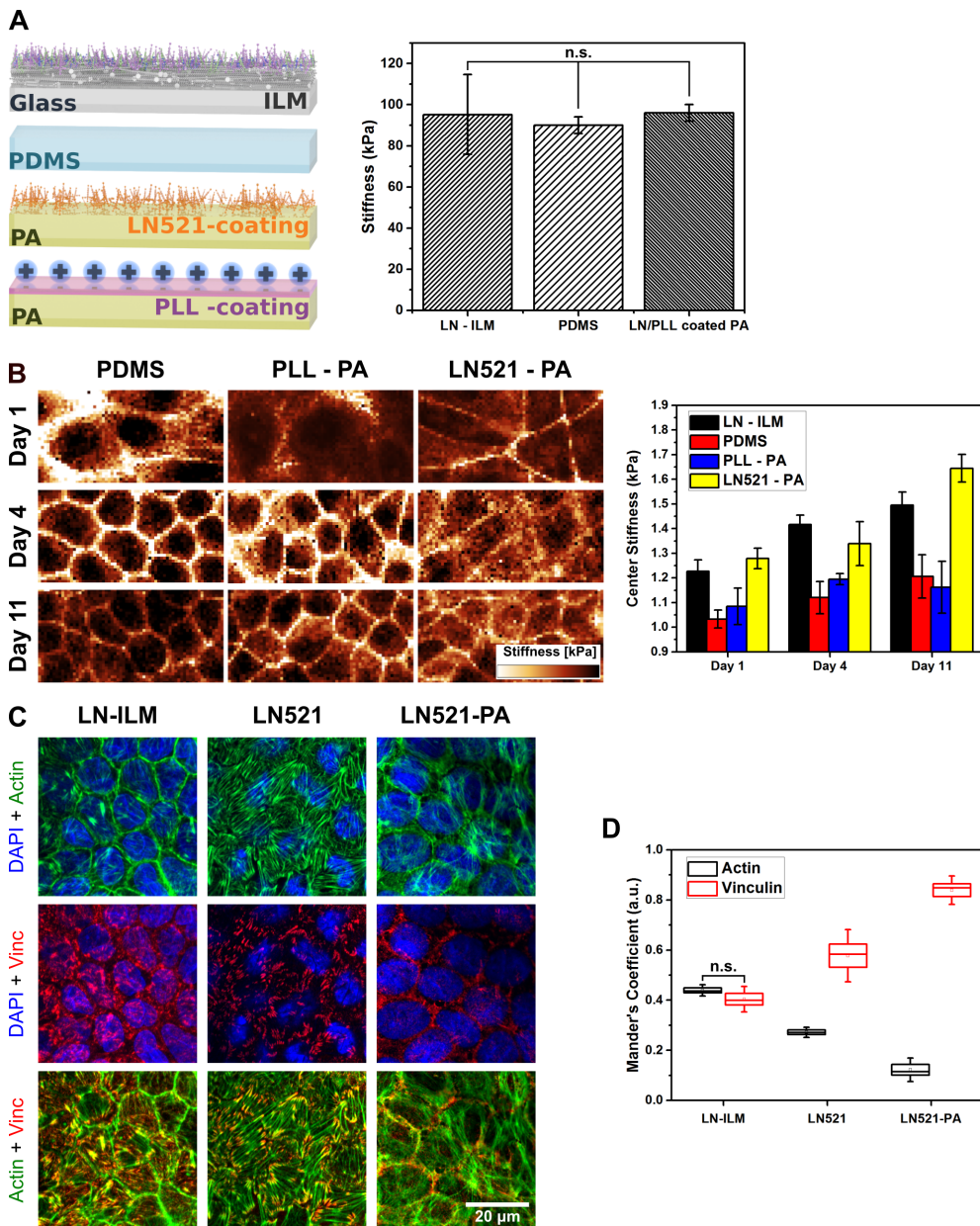
Figure 3.5

Figure 3.5 *(previous page)* Basement membrane (BM) composition and stiffness jointly regulate mechanophenotype of epithelial cells.

(A) (Left) Schematics illustrates biochemical composition of polymer substrates used to mimic BM properties. polydimethylsiloxane (PDMS) is hydrophobic polymer that bears no biological function. polyacrylamide (PA) can be coated with either laminin α5β2γ1 (LN-521) to gain biologically relevant activity for epithelial cells or with poly-L-lysine (PLL) that negatively charges the surface and primes it for nonspecific cell adherence. (Right) Substrate stiffness was measured by AFM at force load of 3.1 nN. Stiffness of all substrates was tuned to the stiffness of LN-ILM. PLL or LN-521 coating of PA substrates has no influence on stiffness properties.

(B) (Left) atomic force microscope (AFM) stiffness maps of cells cultured on PDMS, poly-L-lysine coated poly-acrylamide (PLL-PA) and laminin-521 coated poly-acrylamide (LN521-PA) for one day (top row), four days (center row) and eleven days (bottom row) at 80 μm x 40 μm, 64 x 32 pixel, load 1.8 nN. (Right) Quantification of the stiffness response of MDCK cells cultured for 11 days on the artificial substrates versus ILM reveals significant differences in stiffness between cells cultured on native BM vs. artificial substrates, even in the case of physiologically relevant LN-521 coated PA.

(C) Confocal projections of the basal face of MDCK cells on laminin-side of inner limiting membrane (LN-ILM) cultured for 11 days (left column), LN-521-coated coverslips (center column) or LN521-PA (right column). The actin stress-fibers are distinctly present on LN-521 and LN521-PA, however, not on the LN-ILM even though all substrates exhibit similar stiffness of 100 kPA. The fluorescence staining reveals vinculin spread across the basal side of cells on LN-ILM, while it associates only to the tips of actin stress fibers on LN-521 or strongly to the junctional regions on LN521-PA substrate.

(D) Visual data are further corroborated by quantification in a Mander's coefficients plot.

3.3.6 *The Ln-α5 to integrin β-signaling determines the epithelial mechanophenotype on native human BMs*

Various aspects of BMs, such as molecular composition and stiffness are involved in the activation of integrins (Huebsch et al. 2011). We inquired the relationship between BM composition, integrin activation and cell stiffness with the aim to elucidate the contribution of individual molecular components that regulate epithelial mechanophenotype. Here, we have established a procedure adapted from earlier studies (Alcaraz et al. 2008; Weaver et al. 1997) studies to specifically block selected interaction partners that are known to establish cell-BM contacts (Figure 3.6A).

We blocked the Ln-α5 by incubating the LN-ILM with the specific antibody and consequently detected a 30 % stiffness increase in comparison to cells cultured on control LN-ILM with Ln-α5 chain being accessible to cell surface integrins (Figure 3.6B, left). In contrast, when LN-111 was blocked no significant change in cell stiffness occurred. The quantification of cytoskeleton fluorescence (Suppl. Figure 3.S1D) revealed significant shift of cytokeratin and in particular actin intensity towards apical surface at the cell center (Figure 3.6B, right) that correlated well with a distinct increase in cell stiffness assessed from the apical surface.
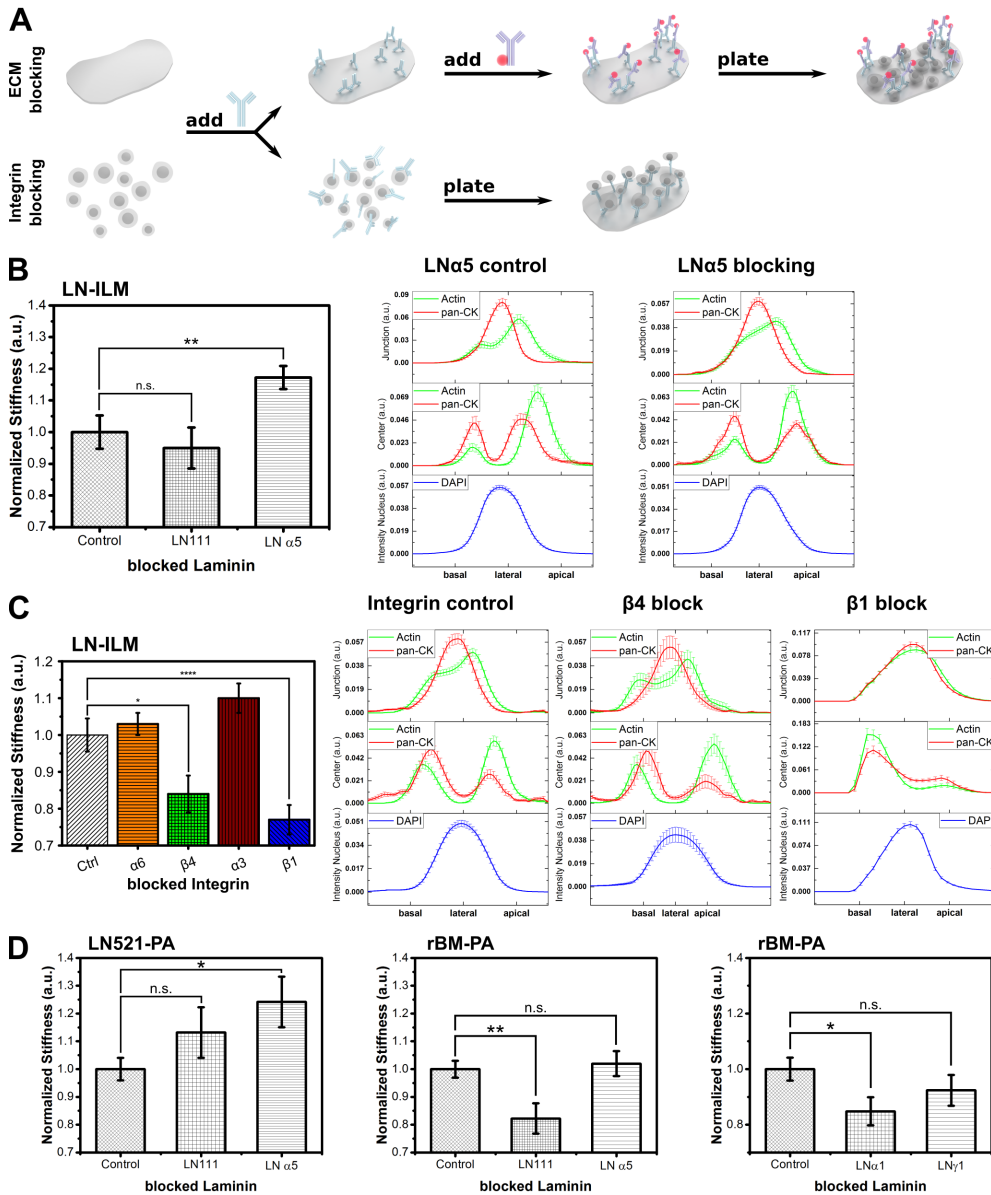
Figure 3.6

Complementary to the LN-blocking from the BM side, we inhibited BM specific integrin subunits at the cellular surface (Figure 3.6C). According to the standard protocol (Weaver et al. 1997) blocking was performed on cells in suspension prior to seeding on ILM and the subsequent stiffness mapping was conducted immediately after cells settled on the substrate (Figure 3.6A).

Figure 3.6 *(previous page)* Laminin (Ln)-α5 to β1 integrin signaling regulates mechanical properties of epithelial cells on native basement membranes (BMs).

(A) Schematics illustrating the experimental procedure of blocking (top) Ln activity or (bottom) specific integrin activation with monoclonal antibodies on inner limiting membrane (ILM).

(B) (Left) Atomic force microscopy (AFM) stiffness measurements on amino-terminal laminin globule (LN) reveal mechanical response of MDCK cells to Ln-α5 block by significant stiffness increase. Blocking of LN-111 does not induce changes in mechanical response of cells. (Right) Normalized fluorescence intensity distribution from basal to apical side of DAPI, actin and cytokeratin for control cells (left distributions) and Ln-α5 blocked ILM (right). For cells on top of Ln-α5 blocked ILM, the actin shifts towards the apical side in the junctional region and in the center-region around the nucleus, while the cytokeratin shifts from a lateral to a more apical position thereby correlating to the increase in cell stiffness.

(C) (Left) AFM stiffness measurements of MDCK cells cultured on upon blocking of integrin activity using specific antibodies against integrin subunits α3, β1, α6 or β4 measured at force load 1.8 nN, 20 < n < 30 cells show significant stiffness decrease of MDCKs when integrins β1 and β4 are blocked, most prominenetly for β1, while blocking of α3 and α6 integrin has no influence on MDCK mechanophenotype. (Right) Normalized fluorescence intensity distribution from basal to apical side of DAPI, actin and cytokeratin for control cells (left distributions) and cells with blocked integrin β4 (center distributions), and β1 (right distributions). In the case of β4 blocking there is a slight but not significant trend in cytokeratin shift from apical to basal region in the central area of cells. For β1 blocked cells, the actin fully shifts towards a lateral position in the junction region, whereas in the central region there is a drastic shift of both cytoskeleton components from the apical to the basal side. 30 < n < 40 cells, corroborates decrease in stiffness when measured from the apical side by AFM

(D) (Left) AFM stiffness measurements of MDCK cells cultured on laminin-521 coated poly-acrylamide (LN521-PA). Blocking was performed using either LN-111 or LNα5 antibodies. Blocking of Ln-α5 but not LN111 significantly increases cell stiffness. Stiffness measurements of cells cultured on PA coated with reconstituted basement membrane coated poly-acrylamide (rBM-PA) that where prior to measurements blocked with (center) either LN-111 or Ln-α5 antibodies or (right) or with antibodies specifically targeting Ln-α1 or Ln-γ1 chain of LN-111 that is present in rBM-PA. Blocking of LN-111 results in significant decrease of cell stiffness, while blocking LNα5 has no effect. Moreover, specific blocking Ln-α1 chain significantly decreases MDCK stiffness, while Ln-γ1 blocking has no effect on their mechanophenotype.

Plotted means are $\pm$ SEM, $*p < 0.05, **p < 0.01, ***p < 0.005, ****p < 0.0001$.

The resulting cell stiffness data revealed that α-integrin subunits α6 and α3 did not alter the stiffness of MDCK cells on native ILM. Interestingly, previous findings showed the effect of α-integrin blocking on cell functions for cells cultured on artificial substrates (Manninen 2015).
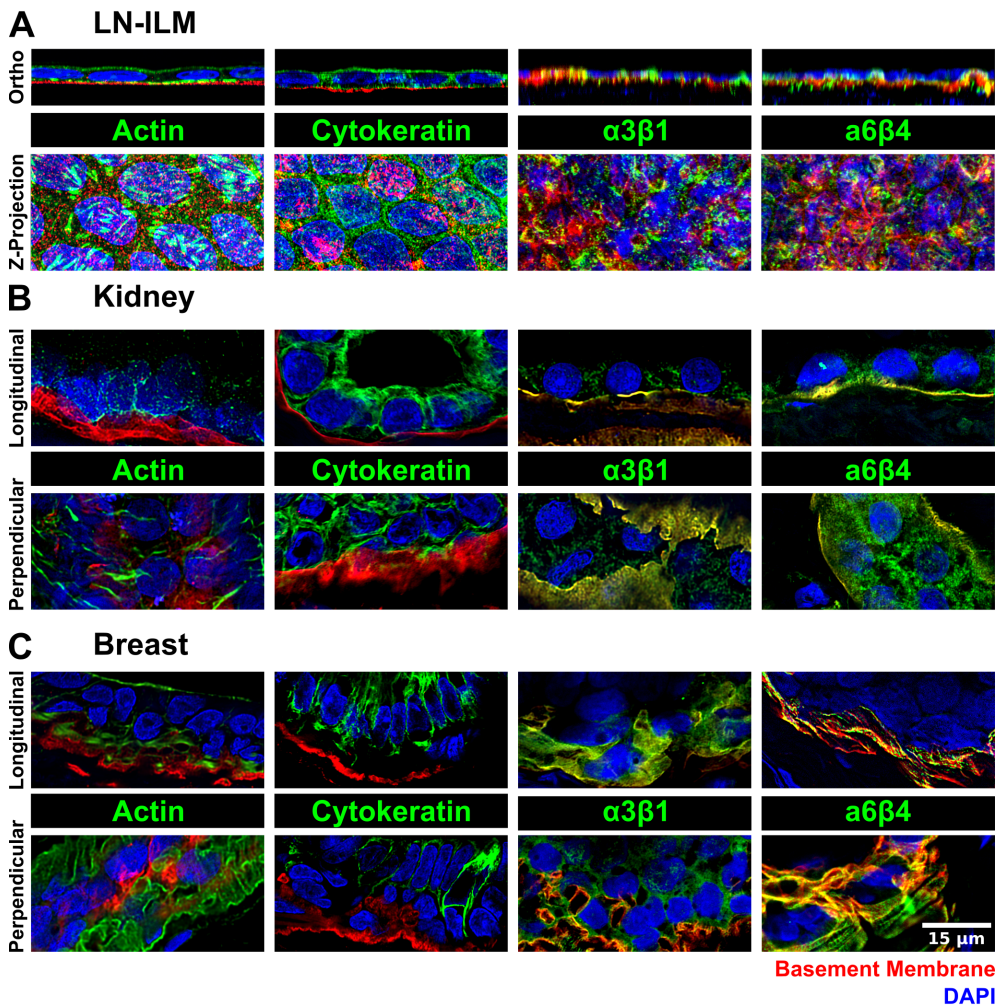
Figure 3.7 Basement membranes (BMs) in human tissue organize epithelial cells.
(A) Orthogonal- (top) and z-projections (bottom) of MDCK cultured on laminin-side of inner limiting membrane (LN-ILM) for 11 days.
(B) Confocal images of longitudinal and perpendicular sections of frozen tissue sections show human kidney tubules and reveal tissue cytoarchitecture and localization of BM-specific integrins.
(C) Similarly, confocal images of longitudinal and perpendicular sections of human breast frozen sections show mammary duct with similar cytoarchitecture and integrin expression as in kidney.

When we blocked either β4 or β1 integrin subunits, cells exhibited significant decrease in cell stiffness from 25 to 40 % for β4 and β1 respectively (Figure 3.6C). Furthermore, the fluorescence intensity data of actin and cytokeratin networks corroborated AFM results, indicating a significant shit of the overall cytoskeleton intensity towards basal surface leaving the apical space more devoid of cytoskeleton networks and thus softer (Figure 3.6C, right). This was particularly prominent upon β1 integrin blocking. Moreover, the cytoskeleton shift towards the basal portion of a cell enabled much deeper indentation of the AFM probe (i.e more than 1 μm) into soft, viscoelastic and water rich cellular space resulting in significant cell softening similarly to malignant cells in native tissues (Plodinec et al. 2012). Finally, we examined specific Ln and integrin α6, α3, β4 and β1 expression for native LN-ILM (Figure 3.7A) and compared these to native kidney (Figure 3.7B) and breast tissue sections (Figure 3.7C). The expression of LN specific integrins was most prominent for cells cultured on LN-ILM, which corresponded well with expression and spatial organization of the same integrins on native kidney and breast tissues (Figure 3.7). Integrin expression on LN-521 (Suppl. Figure 3.S5B) and LN521-PA (Suppl. Figure 3.S5C) was localized to cell edges on the basal side and was not present throughout the cells. In contrast, integrins on ColIV were expressed in a diffuse and unspecific manner throughout as comparable to unspecific substrates (Suppl. Figure 3.S5A). In addition, we have also examined the integrin expression in the formed MDCK cysts, where all integrins were found to be poorly expressed at the interface and significantly more localized to cells rather than BM (Suppl. Figure 3.S3B). In conclusion, these data further strengthened argumentation that BM composition, architecture and stiffness need to act jointly to regulate cell adhesion and mechanophenotype in physiologically relevant conditions. Artificial substrates that either recapitulate native BMs in terms of chemical composition or stiffness or both but lack correct architecture of BM components are not able to epitomize functionality of native BMs.

3.4 DISCUSSION

We have extracted and characterized human BMs from different organs such as retina, breast, kidney and colon under near physiological conditions. Biophysical measurements in situ revealed an unprecedented degree of similarity in composition, structural organization and stiffness for these BMs. For example, all BMs exhibit bi-layered architecture with distinctive epithelial (Ln) and stromal (ColIV) sides, while the thickness of native unfixed specimens

was in the order of micrometers, which is up 10-fold higher than thought previously (LeBleu et al. 2007). The specific architecture Ep versus St side correlated well with the 2.5 -fold higher stiffness for the BM side expressing Ln versus ColIV. These results provided new insights into the currently accepted model of BMs being described as thin sheets of interconnected Ln and ColIV meshwork (Dunn et al. 2012) and demonstrated that current BM model needs to be amended for most human BMs.

To address the biological relevance of asymmetric BM organization and side specific mechanical properties, we have specifically examined how stiffness, composition and architecture of human BM modulates the behavior of adherent cells, and in which manner are these properties distinct from BMs reconstituted in vitro (Page-McCaw 2008). For this purpose ILMs isolated from human retinas served to act as native substrates for culturing epithelial MDCK cells in vitro. This enabled us specifically address the responsiveness of epithelial cells with respect to 1) composition, 2) organization and 3) stiffness of native BM. MDCK cells on ILMs for 14 days revealed similarities in markers such as proliferation, polarity (Figure 3.3, Suppl. Figure 3.S4). On the other hand, marked differences were observed between native tissues and cysts cultured in rBMs for the same time period (Suppl. Figure 3.S3).

Thus far, BM matrices reconstituted in vitro have been extensively used to provide substrate characteristics for in vitro cell cultures that better simulate conditions in vivo. In fact, integrins were the first receptors identified to mediate the interactions between epithelial cells and BM components in studies using the Engelbreth-Holm-Swarm (EHS) derived LN-111 and ColIV (α1 and α2 chains) (Lochter et al. 1999; Muschler et al. 1999). Also, recent studies have shown that in an assembled form BM components bind to one set of integrins, but when the BM is structurally altered, additional sets of integrins are activated (Lu et al. 2011). An example of such integrin activation was observed with ColIV (Neely et al., 1999). For example, studies have shown that denatured ColIV can bind αVβ3 integrin, whereas folded ColIV binds only α1β1 and α2β1 integrins (Xu et al. 2001). Similar observations could be reported for Ln integrin receptors α6β4 and α3β1 implying that rigidity of BM, protein composition and spatial organization of its components might trigger differential signals to the adhering epithelia (Li et al. 2005; Weaver et al. 2002; Zahir et al. 2002). Here we show that rBMs only partially recapitulate living tissues in terms of mechanobiological functions. For example, we measured stiffness of the rBM in the range of 0.1 − 1 kPa (Suppl. Figure 3.S2C). The stiffness dramatically varied due to extreme sample viscoelasticity arising from high water content as shown previously by Soofi and co-workers (Soofi

et al. 2009). In particular, measured rBM stiffness was approximately 50-fold softer and significantly more viscoelastic than native BMs. Accordingly, such substrates might not be appropriate for reflecting biological functions of epithelia and examining the influence of microenvironment on cell stiffness properties (Melzak et al. 2013; Miller 2017).

In living tissues, cell stiffness is regulated by the organization and composition of its cytoskeletal structures; actin, microtubules and tissue specific intermediate filaments, i.e cytokeratins (Hesse et al. 2004) activate those specific cytoskeleton structures to adhere to an underlying substrate (Case et al. 2015; Gardel et al. 2010) or to neighboring cells (Perez et al. 2008; Sim et al. 2017; Yamada et al. 2007). Any modification in the chemical or physical properties of the substrate, will undoubtedly lead to downstream modulation of adhesion/cytoskeleton systems (Owen et al. 2017; Parsons et al. 2010). Interestingly, when we compared adhesion/cytoskeleton system and cell stiffness properties of MDCK cells cultured on physiologically relevant LN-ILM; specific differences were observed in comparison to cells cultured on ColIV-ILM. For example, stiffness of epithelial cells attached to the LN-ILM correlated well stiffness values measured for native healthy epithelia in situ ((Plodinec et al. 2012)). On the other hand, stiffness of cells cultured on ColIV was increased by 30 % similarly to cells cultured on stiff artificial substrates. More surprisingly, even though LN-ILM of the BM exhibited stiffness values in the range of 100 kPa we did not detect actin stress fibers - typically observed for such stiff substrates in vitro (Gupta et al. 2015; Walcott et al. 2010).

To specifically evaluate cytoarchitecture of cells cultured on different BM substrates, we have developed a set of digital tools that enabled us to quantify fluorescence intensities of different cell regions (apical, lateral, basal). This enabled us to quantitatively correlate changes in the cell cytoarchitecture with stiffness for cells cultured either on native BMs or artificial substrates. In particular, LN-ILM side we observed cells exhibiting cage like homogeneous distribution of cytoskeleton structures from the basal to apical side with distinct baso-apical actin (Rodriguez-Boulan et al. 2014). Cells cultured on ColIV-ILM displayed cytoskeleton that was concentrated at the apical side and correlated well with the significant increase in stiffness. Similar behavior to cells on ColIV was observed for cells cultured on plastic. Interestingly, cells cultured on polymer based substrates that were artificially tuned both in terms of surface coating and substrate stiffness to resemble native BMs (Figure 3.5A) also were not able to recapitulate physiological cytoarchitecture and mechanical phenotype measured on native BMs
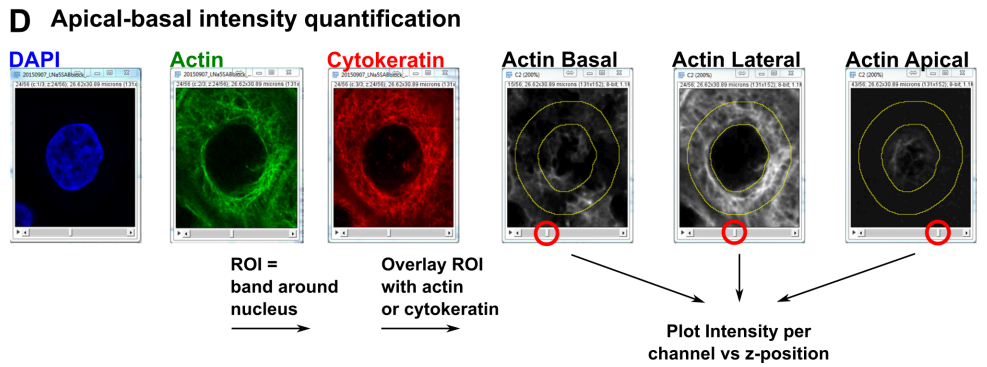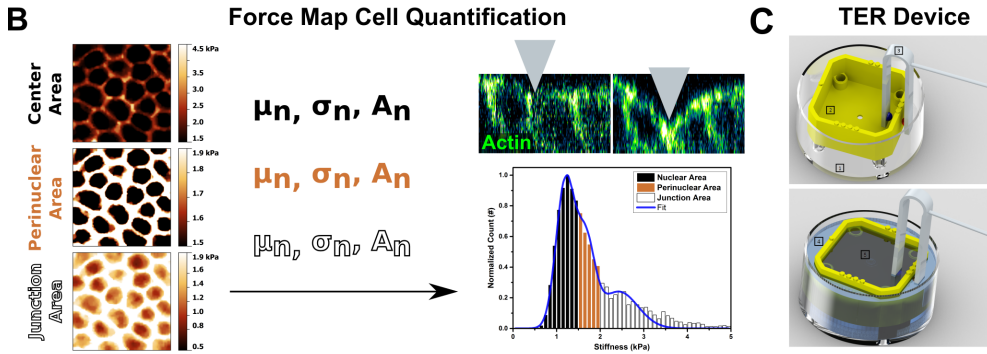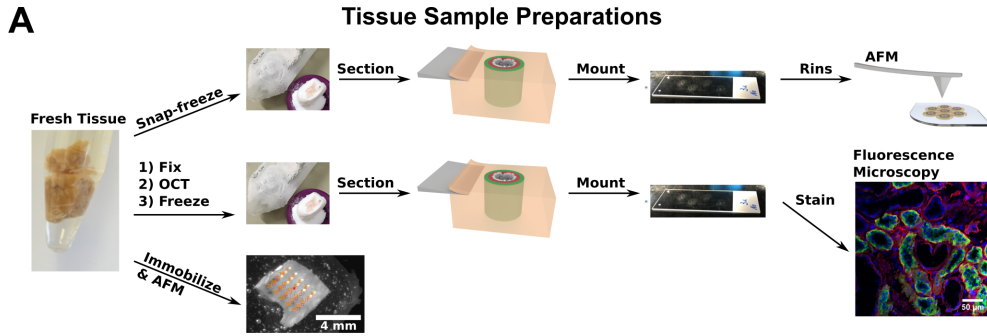
Native human BMs exhibit architecture composition and stiffness properties that profoundly regulate cytoarchitecture and stiffness of the inlying epithelia. Biochemical characterization of LN-ILM has revealed that Ln-α5 chain expression is as a common feature among different tissues (Figure 3.2). This was surprising since it was long considered that for example mammary gland BMs contain predominantly Ln-α1 (Bissell et al. 2003). Moreover, LN-111 was shown previously to act as a regulator of cellular elasticity and functional differentiation of mammary epithelia in vitro (Alcaraz et al. 2008; Fiore et al. 2017). On the other hand, previous research data indicated that Ln-α5 has a critical role in regulating: 1) urethral and external genital development, (Lin et al. 2016), 2) architecture of the mouse small intestine mucosa (Mahoney et al. 2008) and 3) in guiding tissue patterning and organogenesis, (Spenle et al. 2013). Altogether, previous observations and our expression data in human tissues (Figure 3.2) pointed towards Ln α5 being a potential external regulator of cell and tissue mechanical properties that in turn give rise to tissue formation and organ sculpting in vivo.

In this regard, cellular integrins α6β4 and α3β1 are known to be interaction partners of Ln substrates as shown both in vivo and in vitro (Stipp, 2010). Moreover, specific role of integrins in physiological and pathological conditions such as cancer (Chaudhuri et al. 2014; Paszek et al. 2005; Weaver et al. 2002) or kidney disease (Joly et al. 2003) has long been debated. Our work sheds new light onto the role of Ln-α5 in regulating cell stiffness under physiological conditions with native BMs acting as native substrate to mimic much of the 3D mechano-chemical environment found in vivo. In particular, we found that compromising Ln-α5 to β1 / β4 integrin signalling with function blocking antibodies was sufficient to inhibit effect of native BM on cellular stiffness. An increase in cellular stiffness was accompanied by a significant shift in cytoskeleton intensity towards apical surface. In contrast, for cells cultured in rBM substrates there was no effect of Ln-α5 blocking on cell stiffness. This was expected since rBM does not contain Ln-α5 (Benton et al. 2014). However, functional blocking of Ln-α1 lead to cell softening which was in agreement with previous observations (Alcaraz et al. 2008). Consistent with this notion it has been also shown previously that blocking α6 integrin in SCp2 cells had only a week effect on cell mechanics and changes in cell shape (Muschler et al. 1999).

Functional blocking of the cellular counterparts of Ln-α5; i.e. β1 and β4 integrins resulted in a decreased cellular stiffness on native BM which is consistent with stiffness phenotypes observed in malignant mouse and human tissues (Plodinec et al. 2012). Moreover, this stiffness change has correlated

strongly with a shift in cytoskeleton intensity towards basal cell surface. One might speculate, that such a shift could contribute to increased traction forces exerted on a stiff substrate and consequently increased migration potential associated with early development (Aman et al. 2010) and cancer cell migration (Paul et al. 2017). The effect was significantly more pronounced both in terms of stiffness and cytoskeleton changes for β1 blocking than for β4 indicating a more significant role for α5 - β1 signaling in regulating the cell mechanophenotype. Interestingly, in a seminal article introducing MMTV –PyMT mouse model for breast cancer, Lin et al. (Lin et al. 2003) have shown that loss of β1 integrin has indeed accompanied breast cancer progression to a late stage. Our data also provide new mechanistic insights with regards to previous findings where downstream signals of β1 integrin were implicated in controlling the cytoskeleton in various cell types (Galbraith et al. 2002; Hammer et al. 2005; Kwong et al. 2003; Wakatsuki et al. 2002; Wang et al. 1994).

Taken together, we have provided a mechanism by which composition, microarchitecture and stiffness of native human BMs act together to define physical properties of epithelia which are relevant to healthy and diseased states of living epithelia. More specifically, we have demonstrated that α5 - β1 signaling pathway specifically regulates cell mechanophenotype in physiological tissues. Finally, we also provide tools and assays to explore BM properties in situ, that could be in future extended for investigating BMs from human organs in various pathological conditions. Numerous human diseases such as diabetes, hypertension, Alzheimer's and cancer (Morrissey et al. 2015) are caused by mutations of BM components that in turn impair mechano-chemical signaling between cells and the underlying substrate. Understanding these processes might help to utilize novel treatment options based on modulating the mechanobiological properties of tissues in vivo.

3.5 SUPPLEMENTARY FIGURES

A **Tissue Sample Preparations**

B **Force Map Cell Quantification**

C **TER Device**

D **Apical-basal intensity quantification**

Supplementary Figure 3.S1

Supplementary Figure 3.S1 *(previous page)*   Schematic visualizing key experimental procedures used to analyze native basement membranes (BMs) and their interactions with adherent epithelia.

(A) Workflow shows experimental procedure used to prepare native tissues for atomic force microscope (AFM) and confocal microscopy. (Top) Preparation of BMs from native human tissues from retina, kidney, breast and colon. (Middle) Sample preparation for fluorescence imaging; unfixed BM specimens were incubated with primary and secondary antibodies and protein expression vas visualized using confocal scanning fluorescence microscopy. (Bottom) Experimental sequence of AFM measurements on fresh tissue. Post –AFM, fresh tissue can be used for further experimentation.

(B) AFM stiffness maps are analyzed using custom made software in Labview and semi-automatically divided into three areas, cell center (nuclear region), the perinuclear (between nucleus and junction) and the junctional region. Initial guesses for a triple Gaussian fit are extracted from the split histogram and the fit is performed to obtain mean values and standard deviations for each of the three specific areas. The image above the histogram displays an orthogonal projection of cells before loading and under the load, the cantilever tip is drawn to scale.

(C) Custom-made mount for native BMs used to measure trans-epithelial resistance (TER). The ILM is centrifuged on the hole of the mount. Measurements are performed by applying an electrical current at point 3.

(D) Apical-basal intensities are quantified from confocal images using the actin and cytokeratin channels. Nuclei are detected automatically using DAPI signal. Subsequently a band of given width around the nucleus is used as a region of interest (ROI) and within cytokeratin and actin signals are measured. Finally, cytokeratin and actin intensity is plotted as function of z-position normalized to an area of one.

A

B

C

D
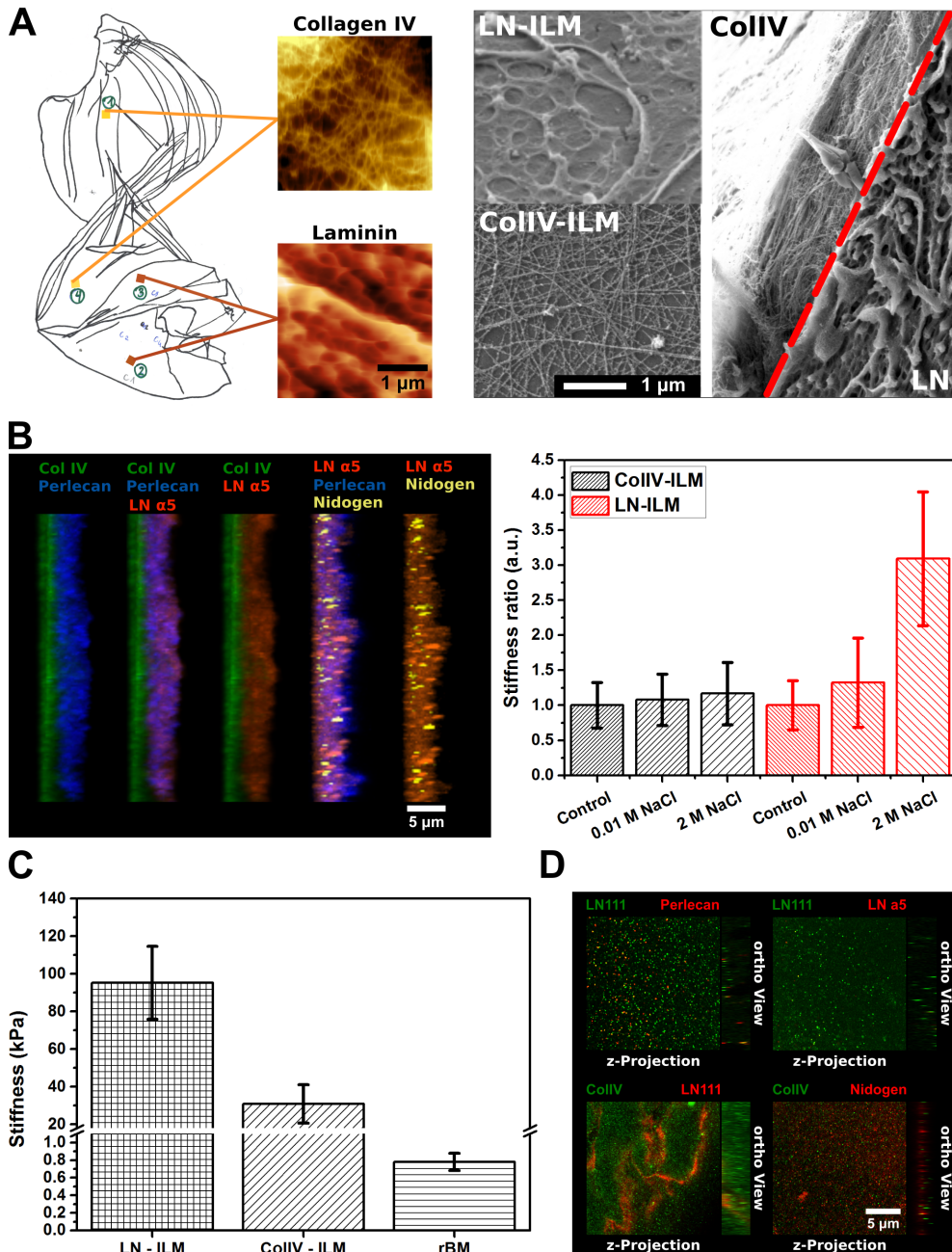
Supplementary Figure 3.S2

Supplementary Figure 3.S2 *(previous page)* The inner limiting membrane (ILM) acts as a basement membrane (BM) model for culturing epithelial cells.

(A) (Left) Sketch illustrates extracted human ILM mounted on a flat surface. atomic force microscope (AFM) measurements of the exposed surfaces reveal distinct topographies for laminin (Ln) and collagen IV (ColIV). (Right) SEM micrographs corroborate the sidedness of ILM, the laminin-side of inner limiting membrane (LN-ILM) shows a rough surface with a crater-like topography, while collagen IV side of inner limiting membrane (ColIV-ILM) exhibits smooth fibrilar structures. The cross-section reveals the interface between the two sides.

(B) (Left) Confocal stacks of the predominant BM proteins: Ln, ColIV, perlecan and nidogen in ILM reveal distinct localization and sidedness of BM. (Right) In contrast to ColIV-ILM, AFM measurements show stiffness changes of LN-ILM after incubation with 0.01 and 2 M NaCl due to modification of proteoglycan chains under hypotonic vs. hypertonic conditions indicating direct association of proteoglycans to Ln but not collagen side of ILM. Both controls are normalized to 1 and the ratios calculated to the control of the respective side.

(C) The mean stiffness of the LN-ILM are 100 kPa and ColIV-ILM exhibits stiffness values at 30 kPa In contrast, reconstituted basement membrane (rBM) is approximately 100 –fold softer with values around 0.8 kPa.

(D) Confocal imaging of rBM reveal amorphous gelatinous material with diffusely distributed BM proteins: ColIV, perlecan and nidogen.

A

B Cytoskeleton   **C** Integrins

DAPI
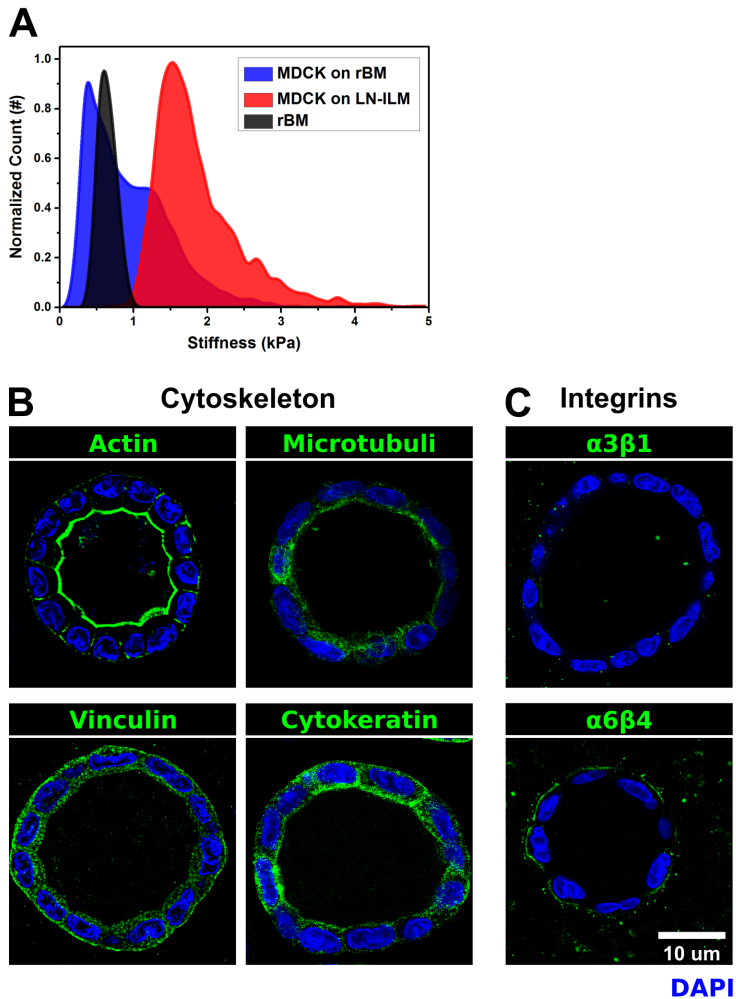
Supplementary Figure 3.S3 Analysis of MDCK cysts cultured in reconstituted basement membrane (rBM) shows partially established tissue barrier and polarity markers.
(A) Comparison of atomic force microscope (AFM) stiffness measurements for MDCK cells cultured on rBM or laminin-side of inner limiting membrane (LN-ILM) reveals 2-fold stiffness differences between two systems indicating that reconstituted basement membrane (rBM) cannot recapitulate mchanophenotype of native basement membrane (BM).
(B) Confocal images of MDCK cytoarchitecture reveal cytoskeleton apical-basal polarization.
(C) BM relevant integrins are only sparsely expressed at the basal side of MDCK cysts.
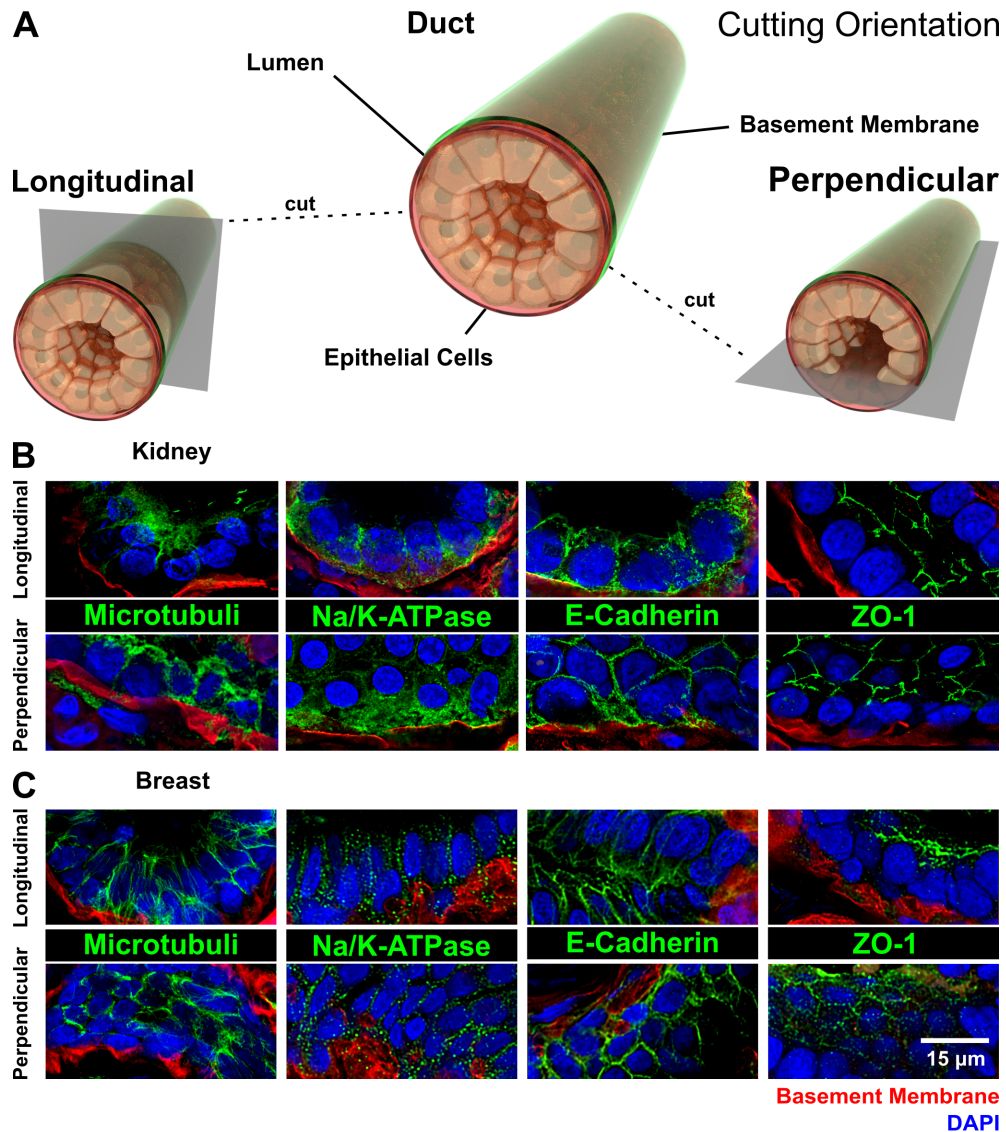
Supplementary Figure 3.S4 Visualization of expression of cytoskeleton, polarity, barrier and integrins markres in distal tubules of human kidney and mammary ducts of human breast based on the field of view.

A) Schematics shows preparation of sections where ducts in human tissue (breast, kidney) are cut longitudinally (along the apical-basal axis of cells) or perpendicular (across the planar layer of an epithelium) to provide the differential view on tissue architecture from the basal to apical side.

(B) Confocal images of longitudinal and perpendicular sections of ducts in frozen sections of human kidney.

(C) Confocal images of longitudinal and perpendicular sections of ducts in frozen sections of human breast.
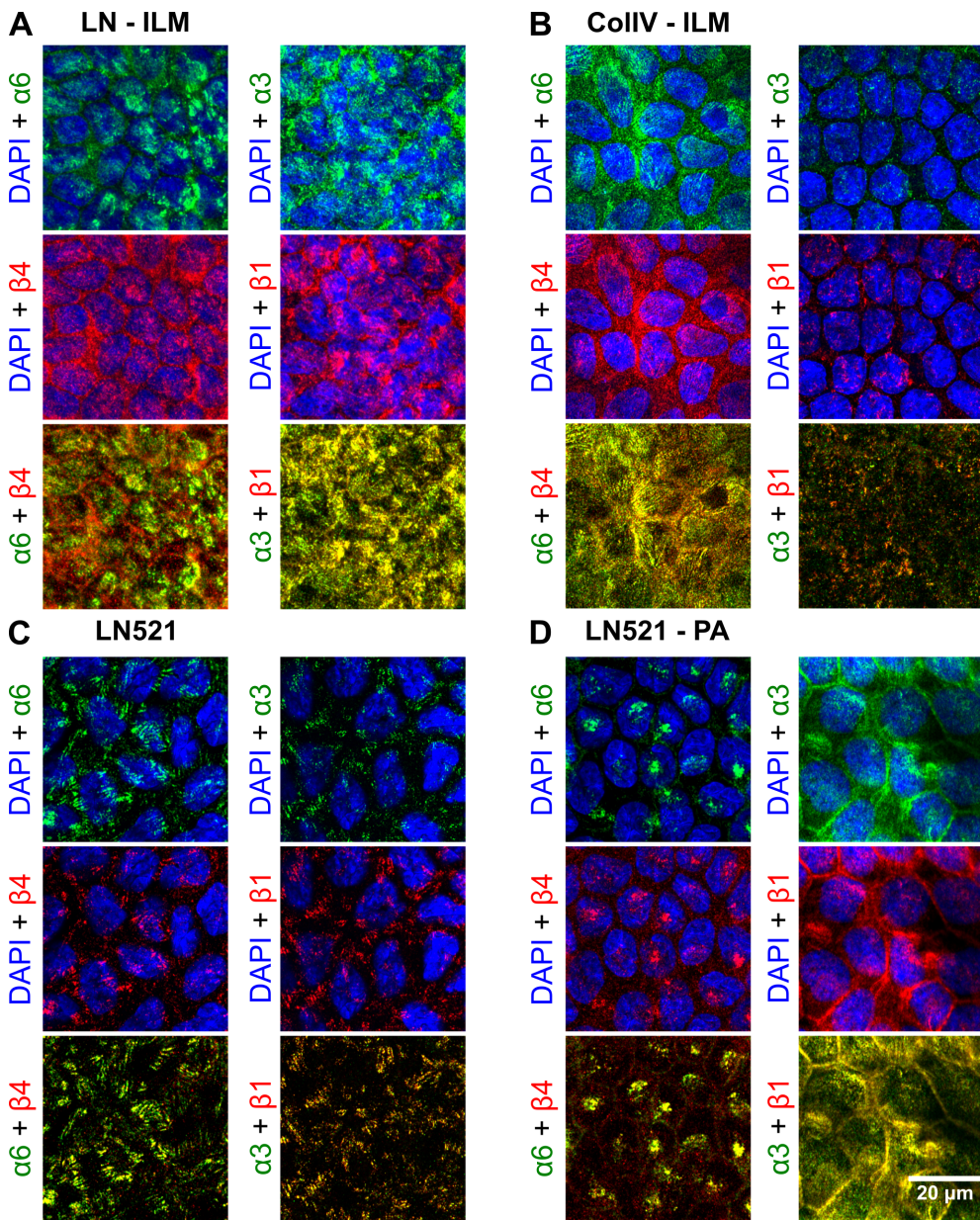
Supplementary Figure 3.S5

Supplementary Figure 3.S5 *(previous page)*   Comparison of cellular integrin receptors α6β4 and α3β1 and their expression on native and artificial substrates.

(A) On laminin-side of inner limiting membrane (LN-ILM) both α6β4 and α3β1 display strong signal distinctive at the junctions versus the nuclear region of the basal cell surface. α3β1 exhibit stronger co-localization than α6β4.

(B) In contrast, MDCK cells cultured on collagen IV side of inner limiting membrane (ColIV-ILM) display very strong diffuse signal spanning the entire basal surface, but most prominently at the junctions. Here, α6β4 exhibit stronger co-localization than α3β1

(C) On laminin α5β2γ1 (LN-521) coated substrates cells exhibit less integrins distinctly localized at specific junctional areas. α6β4 do not co-localize, while α3β1 associate strongly similarly to LN-ILM but with significantly lower integrin recruitment.

(D) on laminin-521 coated poly-acrylamide (LN521-PA) substrate α6β4 are both strongly localized to the basal side of the nuclear region, however they do not co-localize, while α3β1 are strongly localized and expressed to the junctional regions of cells. α3β1 associate well along the cell junctions.

REFERENCES

Alcaraz, Jordi et al. (2008). „Laminin and biomimetic extracellular elasticity enhance functional differentiation in mammary epithelia." In: *The EMBO journal* 27.21, pp. 2829–2838. DOI: 10.1038/emboj.2008.206.

Aman, Andy and Tatjana Piotrowski (2010). „Cell migration during morphogenesis." In: *Developmental biology* 341.1, pp. 20–33.

Austen, Katharina et al. (2015). „Extracellular rigidity sensing by talin isoform-specific mechanical linkages." In: *Nature cell biology* 17.12, p. 1597.

Barcellos-Hoff, MH et al. (1989). „Functional differentiation and alveolar morphogenesis of primary mammary cultures on reconstituted basement membrane." In: *Development* 105.2, pp. 223–235.

Benton, Gabriel et al. (2014). „Matrigel: from discovery and ECM mimicry to assays and models for cancer research." In: *Advanced drug delivery reviews* 79, pp. 3–18.

Bissell, Mina J and David Bilder (2003). „Polarity determination in breast tissue: desmosomal adhesion, myoepithelial cells, and laminin 1." In: *Breast cancer research* 5.2, p. 117.

Candiello, Joseph, Gregory J. Cole, and Willi Halfter (June 2010). „Age-dependent changes in the structure, composition and biophysical properties of a human basement membrane." In: *Matrix Biology* 29.5, pp. 402–410. DOI: 10.1016/j.matbio.2010.03.004.

Case, Lindsay B and Clare M Waterman (2015). „Integration of actin dynamics and cell adhesion by a three-dimensional, mechanosensitive molecular clutch." In: *Nature cell biology* 17.8, p. 955.

Cetera, Maureen and Sally Horne-Badovinac (2015). „Round and round gets you somewhere: collective cell migration and planar polarity in elongating Drosophila egg chambers." In: *Current Opinion in Genetics & Development* 32, pp. 10–15. DOI: 10.1016/j.gde.2015.01.003.

Chaudhuri, Ovijit et al. (2014). „Extracellular matrix stiffness and composition jointly regulate the induction of malignant phenotypes in mammary epithelium." In: *Nature Materials* 13.June, pp. 1–35. DOI: 10.1038/nmat4009.

Dunn, Sara-Jane et al. (2012). „Modelling the role of the basement membrane beneath a growing epithelial monolayer." In: *Journal of theoretical biology* 298, pp. 82–91.

Engler, Adam J et al. (2006). „Matrix elasticity directs stem cell lineage specification." In: *Cell* 126.4, pp. 677–689.

Esue, Osigwe et al. (2008). „The filamentous actin cross-linking/bundling activity of mammalian formins." In: *Journal of molecular biology* 384.2, pp. 324–334.

Fiore, Ana Paula Zen Petisco et al. (2017). „Laminin-111 and the Level of Nuclear Actin Regulate Epithelial Quiescence via Exportin-6." In: *Cell reports* 19.10, pp. 2102–2115.

Fletcher, Daniel a. and R. Dyche Mullins (2010). „Cell mechanics and the cytoskeleton." In: *Nature* 463.7280, pp. 485–492. DOI: 10.1038/nature08908.

Frantz, Christian, Kathleen M Stewart, and Valerie M Weaver (2010). „The extracellular matrix at a glance." In: *J Cell Sci* 123.24, pp. 4195–4200.

Galbraith, Catherine G, Kenneth M Yamada, and Michael P Sheetz (2002). „The relationship between force and focal complex development." In: *J Cell Biol* 159.4, pp. 695–705.

Gardel, Margaret L et al. (2010). „Mechanical integration of actin and adhesion dynamics in cell migration." In: *Annual review of cell and developmental biology* 26, pp. 315–333.

Gilbert, Penney M and Valerie M Weaver (2017). „Cellular adaptation to biomechanical stress across length scales in tissue homeostasis and disease." In: *Seminars in cell & developmental biology*. Vol. 67. Elsevier, pp. 141–152.

Goldberg, Seth et al. (2010). „Maintenance of glomerular filtration barrier integrity requires laminin α5." In: *Journal of the American Society of Nephrology* 21.4, pp. 579–586.

Gudjonsson, Thorarinn et al. (2002). „Normal and tumor-derived myoepithelial cells differ in their ability to interact with luminal breast epithelial cells for polarity and basement membrane deposition." In: *Journal of cell science* 115.1, pp. 39–50.

Gudjonsson, Thorarinn et al. (2003). „To create the correct microenvironment: three-dimensional heterotypic collagen assays for human breast epithelial morphogenesis and neoplasia." In: *Methods* 30.3, pp. 247–255.

Gupta, Mukund et al. (2015). „Adaptive rheology and ordering of cell cytoskeleton govern matrix rigidity sensing." In: *Nature communications* 6, p. 7525.

Halfter, Willi et al. (Jan. 2013). „The bi-functional organization of human basement membranes." In: *PloS one* 8.7, e67660. DOI: 10.1371/journal.pone.0067660.

Hammer, DA et al. (2005). „Traction force microscopy reveals basic mechanochemical principles of cell adhesion, speading and cell-cell organization." In: *ABSTRACTS OF PAPERS OF THE AMERICAN CHEMICAL SOCIETY*.

Vol. 229. AMER CHEMICAL SOC 1155 16TH ST, NW, WASHINGTON, DC 20036 USA, U648–U648.

Herrmann, Harald et al. (2007). „Intermediate filaments: from cell architecture to nanomechanics." In: *Nature Reviews Molecular Cell Biology* 8.7, pp. 562–573. DOI: 10.1038/nrm2197.

Hesse, Michael et al. (2004). „Comprehensive analysis of keratin gene clusters in humans and rodents." In: *European journal of cell biology* 83.1, pp. 19–26.

Horne-Badovinac, Sally (2014). „Cell–cell and cell–matrix interactions." In: *Molecular biology of the cell* 25.6, pp. 731–731.

Huebsch, Nathaniel and David J Mooney (2011). „A Role for Integrin-ECM Bonds as Mechanotransducers that Modulate Adult Stem Cell Fate." In: *Mechanobiology of Cell-Cell and Cell-Matrix Interactions*. Springer, pp. 23–46.

Inman, Jamie L et al. (2015). „Mammary gland development: cell fate specification, stem cells and the microenvironment." In: *Development* 142.6, pp. 1028–1042.

Joly, Dominique et al. (2003). „β4 integrin and laminin 5 are aberrantly expressed in polycystic kidney disease: role in increased cell adhesion and migration." In: *The American journal of pathology* 163.5, pp. 1791–1800.

Kalluri, Raghu (2003). „Angiogenesis: Basement membranes: structure, assembly and role in tumour angiogenesis." In: *Nature Reviews Cancer* 3.6, pp. 422–433. DOI: 10.1038/nrc1094.

Kelley, Laura C. et al. (Feb. 2014). „Traversing the basement membrane in vivo: A diversity of strategies." In: *J Cell Biol* 204.3, pp. 291–302. DOI: 10.1083/jcb.201311112.

Khoshnoodi, Jamshid, Vadim Pedchenko, and Billy G. Hudson (2008). „Mammalian collagen IV." In: *Microscopy Research and Technique* 71.5, pp. 357–370. DOI: 10.1002/jemt.20564.

Kiritsi, Dimitra, Cristina Has, and Leena Bruckner-Tuderman (Jan. 2013). „Laminin 332 in junctional epidermolysis bullosa." In: *Cell Adhesion & Migration* 7.1, pp. 135–141. DOI: 10.4161/cam.22418.

Klinowska, T C et al. (1999). „Laminin and beta1 integrins are crucial for normal mammary gland development in the mouse." In: *Developmental biology* 215.1, pp. 13–32. DOI: 10.1006/dbio.1999.9435.

Klinowska, T C et al. (2001). „Epithelial development and differentiation in the mammary gland is not dependent on alpha 3 or alpha 6 integrin subunits." In: *Developmental biology* 233.2, pp. 449–467. DOI: 10.1006/dbio.2001.0204.

Kwong, Lina et al. (2003). „R-Ras promotes focal adhesion formation through focal adhesion kinase and p130Cas by a novel mechanism that differs from integrins." In: *Molecular and cellular biology* 23.3, pp. 933–949.

Laurie, GW et al. (1984). „Fine structure of the glomerular basement membrane and immunolocalization of five basement membrane components to the lamina densa (basal lamina) and its extensions in both glomeruli and tubules of the rat kidney." In: *Developmental Dynamics* 169.4, pp. 463–481.

LeBleu, Valerie S, Brian MacDonald, and Raghu Kalluri (2007). „Structure and function of basement membranes." In: *Experimental biology and medicine* 232.9, pp. 1121–1129.

Lecuit, Thomas and L Mahadevan (2017). *Morphogenesis one century after On Growth and Form*.

Leube, Rudolf E, Marcin Moch, and Reinhard Windoffer (2015). „Intermediate filaments and the regulation of focal adhesion." In: *Current opinion in cell biology* 32, pp. 13–20. DOI: 10.1016/j.ceb.2014.09.011.

Li, Na et al. (2005). „$\beta 1$ integrins regulate mammary gland proliferation and maintain the integrity of mammary alveoli." In: *The EMBO journal* 24.11, pp. 1942–1953.

Lin, Congxing et al. (2016). „Requirement for basement membrane laminin $\alpha 5$ during urethral and external genital development." In: *Mechanisms of Development*. DOI: 10.1016/j.mod.2016.05.004.

Lin, Elaine Y et al. (2003). „Progression to malignancy in the polyoma middle T oncoprotein mouse breast cancer model provides a reliable model for human diseases." In: *The American journal of pathology* 163.5, pp. 2113–26. DOI: 10.1016/S0002-9440(10)63568-7.

Lo, Chun-Min et al. (2000). „Cell movement is guided by the rigidity of the substrate." In: *Biophysical journal* 79.1, pp. 144–152.

Lochter, André et al. (1999). „$\alpha 1$ and $\alpha 2$ integrins mediate invasive activity of mouse mammary carcinoma cells through regulation of stromelysin-1 expression." In: *Molecular biology of the cell* 10.2, pp. 271–282.

Loparic, Marko et al. (June 2010). „Micro- and Nanomechanical Analysis of Articular Cartilage by Indentation-Type Atomic Force Microscopy: Validation with a Gel-Microfiber Composite." In: *Biophysical Journal* 98.11, pp. 2731–2740. DOI: 10.1016/j.bpj.2010.02.013.

Lu, Pengfei et al. (2011). „Extracellular matrix degradation and remodeling in development and disease." In: *Cold Spring Harbor perspectives in biology* 3.12, a005058.

Mahoney, Zhen X, Thaddeus S Stappenbeck, and Jeffrey H Miner (2008). „Laminin α5 influences the architecture of the mouse small intestine mucosa." In: *Journal of cell science* 121.15, pp. 2493–2502.

Manninen, Aki (Jan. 2015). „Epithelial polarity - generating and integrating signals from the ECM with integrins." In: *Experimental cell research*, pp. 1–13. DOI: 10.1016/j.yexcr.2015.01.003.

Mayorca-Guiliani, Alejandro E et al. (2017). „ISDoT: in situ decellularization of tissues for high-resolution imaging and proteomic analysis of native extracellular matrix." In: *Nature medicine* 23.7, p. 890.

McKee, Karen K, Stephanie Capizzi, and Peter D Yurchenco (2009). „Scaffold-forming and adhesive contributions of synthetic laminin-binding proteins to basement membrane assembly." In: *Journal of Biological Chemistry* 284.13, pp. 8984–8994.

Melzak, KA, S Moreno-Flores, and JL Toca-Herrera (2013). „Mechanical cues for cell culture." In: *Handbook of biofunctional surfaces. Singapore: Pan Stanford Publishing*.

Mercurio, Arthur M, Isaac Rabinovitz, and Leslie M Shaw (2001). „The α6β4 integrin and epithelial cell migration." In: *Current opinion in cell biology* 13.5, pp. 541–545.

Miller, R Tyler (2017). „Mechanical properties of basement membrane in health and disease." In: *Matrix Biology* 57, pp. 366–373.

Miner, Jeffrey H (2005). „Building the glomerulus: a matricentric view." In: *Journal of the American Society of Nephrology* 16.4, pp. 857–861.

Morrissey, Meghan a and David R Sherwood (2015). „An active role for basement membrane assembly and modification in tissue sculpting." In: *Journal of cell science*, pp. 1661–1668. DOI: 10.1242/jcs.168021.

Muschler, John et al. (1999). „Division of labor among the α6β4 integrin, β1 integrins, and an E3 laminin receptor to signal morphogenesis and β-casein expression in mammary epithelial cells." In: *Molecular biology of the cell* 10.9, pp. 2817–2828.

Myllymäki, Satu Marja, Terhi Piritta Teräväinen, and Aki Manninen (2011). „Two distinct integrin-mediated mechanisms contribute to apical lumen formation in epithelial cells." In: *PLoS One* 6.5, e19453.

Nguyen, Nguyet M et al. (2005). „Epithelial laminin α5 is necessary for distal epithelial cell maturation, VEGF production, and alveolization in the developing murine lung." In: *Developmental biology* 282.1, pp. 111–125.

Nielsen, P K and Y Yamada (2001). „Identification of cell-binding sites on the Laminin alpha 5 N-terminal domain by site-directed mutagenesis." In:

The Journal of biological chemistry 276.14, pp. 10906–12. DOI: 10.1074/jbc.M008743200.

Nishiuchi, Ryoko et al. (2006). „Ligand-binding specificities of laminin-binding integrins: A comprehensive survey of laminin-integrin interactions using recombinant a3b1, a6b1, a7b1 and a6b4 integrins." In: *Matrix Biology* 25.3, pp. 189–197. DOI: 10.1016/j.matbio.2005.12.001.

Owen, Leanna M et al. (2017). „A cytoskeletal clutch mediates cellular force transmission in a soft, three-dimensional extracellular matrix." In: *Molecular biology of the cell* 28.14, pp. 1959–1974.

Page-McCaw, Andrea (2008). „Remodeling the model organism: matrix metalloproteinase functions in invertebrates." In: *Seminars in cell & developmental biology*. Vol. 19. 1. Elsevier, pp. 14–23.

Parsons, J Thomas, Alan Rick Horwitz, and Martin A Schwartz (2010). „Cell adhesion: integrating cytoskeletal dynamics and cellular tension." In: *Nature reviews Molecular cell biology* 11.9, p. 633.

Paszek, Matthew J and Valerie M Weaver (2004). „The tension mounts: mechanics meets morphogenesis and malignancy." In: *Journal of mammary gland biology and neoplasia* 9.4, pp. 325–342.

Paszek, Matthew J et al. (2005). „Tensional homeostasis and the malignant phenotype." In: *Cancer cell* 8.3, pp. 241–54. DOI: 10.1016/j.ccr.2005.08.010. arXiv: 24944547482.

Paul, Colin D, Panagiotis Mistriotis, and Konstantinos Konstantopoulos (2017). „Cancer cell motility: lessons from migration in confined spaces." In: *Nature Reviews Cancer* 17.2, p. 131.

Perez, Tomas D et al. (2008). „Immediate-early signaling induced by E-cadherin engagement and adhesion." In: *Journal of Biological Chemistry* 283.8, pp. 5014–5022.

Plodinec, Marija et al. (Nov. 2012). „The nanomechanical signature of breast cancer." In: *Nature nanotechnology* 7.11, pp. 757–65. DOI: 10.1038/nnano.2012.167.

Plopper, George E et al. (1998). „Migration of breast epithelial cells on Laminin-5: differential role of integrins in normal and transformed cell types." In: *Breast cancer research and treatment* 51.1, pp. 57–69.

Rodriguez-Boulan, Enrique and Ian G. Macara (2014). „Organization and execution of the epithelial polarity programme." In: *Nature Reviews Molecular Cell Biology* 15.4, pp. 225–242. DOI: 10.1038/nrm3775.

Rodriguez-Fraticelli, Alejo E and Fernando Martin-Belmonte (2014). „Picking up the threads: extracellular matrix signals in epithelial morphogenesis."

In: *Current Opinion in Cell Biology* 30, pp. 83–90. DOI: 10.1016/j.ceb.2014.06.008.

Sader, John E, James WM Chon, and Paul Mulvaney (1999). „Calibration of rectangular atomic force microscope cantilevers." In: *Review of Scientific Instruments* 70.10, pp. 3967–3969.

Shakouri-Motlagh, Aida et al. (2017). „Native and solubilized decellularized extracellular matrix: a critical assessment of their potential for improving the expansion of mesenchymal stem cells." In: *Acta biomaterialia* 55, pp. 1–12.

Sherwood, David R (2015). „A developmental biologist's "outside-the-cell" thinking." In: *J Cell Biol* 210.3, pp. 369–372.

Sim, Woogwang et al. (2017). „Rapid and quantitative measurement of cell adhesion and migration activity by time-series analysis on biomimetic topography." In: *Biotechnology and Bioprocess Engineering* 22.2, pp. 107–113.

Smyth, N. (Jan. 1999). „Absence of Basement Membranes after Targeting the LAMC1 Gene Results in Embryonic Lethality Due to Failure of Endoderm Differentiation." In: *The Journal of Cell Biology* 144.1, pp. 151–160. DOI: 10.1083/jcb.144.1.151.

Soofi, Shauheen S et al. (2009). „The elastic modulus of Matrigel™ as determined by atomic force microscopy." In: *Journal of structural biology* 167.3, pp. 216–219.

Spenle, Caroline et al. (2013). „Laminin a5 guides tissue patterning and organogenesis." In: *Cell Adhesion and Migration* 7.1, pp. 90–100. DOI: 10.4161/cam.22236.

Stevenson, B R et al. (1988). „Tight junction structure and ZO-1 content are identical in two strains of Madin-Darby canine kidney cells which differ in transepithelial resistance." In: *The Journal of cell biology* 107.6 Pt 1, pp. 2401–8. DOI: 10.1083/jcb.107.6.2401.

Streuli, Charles H (2009). „Integrins and cell-fate determination." In: *Journal of cell science* 122.2, pp. 171–177.

Taddei, Ilaria et al. (2008). „β1 Integrin deletion from the basal compartment of the mammary epithelium affects stem cells." In: *Nature Cell Biology* 10.6, pp. 716–722. DOI: 10.1038/ncb1734.

Timpl, Rupert et al. (Nov. 1981). „A Network Model for the Organization of Type IV Collagen Molecules in Basement Membranes." In: *Eur J Biochem* 120.2, pp. 203–211. DOI: 10.1111/j.1432-1033.1981.tb05690.x.

Trepat, Xavier et al. (May 2007). „Universal physical responses to stretch in the living cell." In: *Nature* 447.7144, pp. 592–5. DOI: 10.1038/nature05824.

Uechi, Guy et al. (July 2014). „Proteomic View of Basement Membranes from Human Retinal Blood Vessels, Inner Limiting Membranes, and Lens Capsules." In: *Journal of proteome research*. DOI: 10.1021/pr5002065.

Vidal, F et al. (June 1995). „Integrin beta 4 mutations associated with junctional epidermolysis bullosa with pyloric atresia." eng. In: *Nature genetics* 10.2, pp. 229–234. DOI: 10.1038/ng0695-229.

Wakatsuki, Tetsuro and Elliot L Elson (2002). „Reciprocal interactions between cells and extracellular matrix during remodeling of tissue constructs." In: *Biophysical chemistry* 100.1-3, pp. 593–605.

Walcott, Sam and Sean X Sun (2010). „A mechanical model of actin stress fiber formation and substrate elasticity sensing in adherent cells." In: *Proceedings of the National Academy of Sciences* 107.17, pp. 7757–7762.

Wang, Ning and Donald E Ingber (1994). „Control of cytoskeletal mechanics by extracellular matrix, cell shape, and mechanical tension." In: *Biophysical journal* 66.6, pp. 2181–2189.

Weaver, Valerie M et al. (1997). „Reversion of the malignant phenotype of human breast cells in three-dimensional culture and in vivo by integrin blocking antibodies." In: *The Journal of cell biology* 137.1, pp. 231–245.

Weaver, Valerie M et al. (2002). „β4 integrin-dependent formation of polarized three-dimensional architecture confers resistance to apoptosis in normal and malignant mammary epithelium." In: *Cancer cell* 2.3, pp. 205–216.

Weir, M Lynn et al. (2006). „Dystroglycan loss disrupts polarity and β-casein induction in mammary epithelial cells by perturbing laminin anchoring." In: *Journal of cell science* 119.19, pp. 4047–4058.

Wilhelmsen, Kevin, Sandy HM Litjens, and Arnoud Sonnenberg (2006). „Multiple functions of the integrin α6β4 in epidermal homeostasis and tumorigenesis." In: *Molecular and cellular biology* 26.8, pp. 2877–2886.

Xu, Jingsong et al. (2001). „Proteolytic exposure of a cryptic site within collagen type IV is required for angiogenesis and tumor growth in vivo." In: *The Journal of cell biology* 154.5, pp. 1069–1080.

Yamada, Soichiro and W. James Nelson (2007). „Localized zones of Rho and Rac activities drive initiation and expansion of epithelial cell-cell adhesion." In: *Journal of Cell Biology* 178.3, pp. 517–527. DOI: 10.1083/jcb.200701058.

Yurchenco, P. D. et al. (Jan. 1986). „Models for the self-assembly of basement membrane." In: *Journal of Histochemistry & Cytochemistry* 34.1, pp. 93–102. DOI: 10.1177/34.1.3510247.

Yurchenco, PD Peter D. (2011). „Basement membranes: cell scaffoldings and signaling platforms." In: *Cold Spring Harbor perspectives in ...* 3, pp. 1–28. DOI: 10.1101/cshperspect.a004911.

Zahir, N et al. (2002). „beta 1 integrin independent growth and survival in mammary tumors is linked to upregulation of laminin 5 and beta 4 integrin and enhanced activation of Rac and NF kappa B." In: *MOLECULAR BIOLOGY OF THE CELL.* Vol. 13. AMER SOC CELL BIOLOGY 8120 WOODMONT AVE, STE 750, BETHESDA, MD 20814-2755 USA, 65A–65A.

4

CONCLUSION & PERSPECTIVES

The work presented in this thesis provides essential insights into the role of microenvironment on cell and tissue mechanical responses in healthy and diseased state. In particular, I have addressed questions regarding organization and composition of the basement membrane specialized extracellular matrix, its interaction with epithelial cells in situ and its pivotal role in the cancer cell invasion The key findings are that 1) basement membranes (BMs) isolated from human tissues are bilayered with a laminin/perlecan side facing the epithelium and a collagen IV side facing the stroma and not as previously thought an interconnected meshwork of these proteins, 2) the mechanophenotype of the epithelial cells is regulated by the direct interactions between the β- but not α-integrins cellular receptors with the laminin α-subunits from the extra-cellular matrix (ECM) and 3) interaction between cancer cells and BM is facilitated in an matrix metalloproteinase (MMP)-independent manner, where carcinoma-associated fibroblasts (CAFs) physically disrupt the BM to promote cancer cell invasion. These findings have implications for numerous physiologically and clinically relevant functions of epithelial tissues as discussed in detail below.

4.1 BMS AS UNIVERSAL TISSUE FATE REGULATORS

Currently, general knowledge of BM structure and function is based mainly on transmission electron microscopy imaging, in vitro protein binding assays, and phenotype analysis of human patients, mutant mice and invertebrata. Data presented in this thesis are based on protein analysis, nanomechanical testing, high-resolution morphological analysis and cell adhesion assays with in vivo derived BMs that led to new and unexpected insights. Opposed to generally accepted knowledge on BMs (Pollard et al. 2008), we showed that basement membranes are not an intermixed meshwork of laminin, collagen IV, nidogen and perlecan. In contrast, perlecan and laminin form a thick layer that is interspersed with nidogen and opposing but connected to a thick layer of collagen IV (Halfter et al. 2013; Henrich et al. 2012; Oertle et al. 2018). The bilayer organization is a common feature of basement membranes of all germ layers. For example we demonstrated that the BM is forming bilayer in retina,

breast, colon and kidney epithelial tissues. Atomic force microscopy-based height measurements strongly suggest that BMs are more than two-fold thicker than previously estimated, providing greater freedom for modeling the large protein polymers within BMs. In addition, nanomechanical data showed that laminin has a crucial role in BM stability. Finally, we demonstrated that BMs are bi-functionally organized with side specific cell-ECM interactions, leading to the proposition that BM-sidedness contributes to the alternating epithelial and stromal tissue arrangements that are found in all metazoan species. More specifically, by using native basement membranes as substrates for culturing epithelial cells, we could demonstrate that BM composition, architecture and stiffness jointly shape specificity of functions of the adherent epithelial cells In the near future, and it will be an exciting opportunity to test if native basement membranes of different origin can reshape pluripotent cells into tissue-specific cells. Furthermore, we will investigate how perlecan and laminin support the supramolecular assembly of each other, since they are always associated together in human native BMs. This is especially interesting, since historically it is accepted that nidogen plays a key role in associating collagen and laminin together into an inter-connected layer which we show that is not the case. Hence this is opening new interesting questions into how other proteoglycans such as perlecan that were not closely investigate earlier contribute to BM assembly and function.

4.2 NEW PARADIGMS FOR MECHANO-SENSING AND -SIGNALING

The concept that local microenvironment plays an important role in regulating cell behavior is being increasingly accepted in cell biology (Bissell et al. 2001; Wiseman et al. 2002; Bissell et al. 2005). The ECM components exhibit remarkable and unique physical, biochemical, and biomechanical properties that are essential for regulating cell behavior. For example, the physical properties of the ECM, such as rigidity, porosity, insolubility, spatial arrangement and orientation (or topography), support tissue architecture and integrity. Additionally, by functioning as a barrier, anchorage site, or movement track, the ECM's physical properties play both negative and positive roles in cell migration. A burgeoning area in ECM biology is how its biomechanical properties, (that ranges from soft and compliant to stiff and rigid), contribute to normal development and diseases such as cancer (McBeath et al. 2004; Reilly et al. 2010). As it turns out, ECM mechanics helps determine how a cell senses and perceives external forces (Paszek et al. 2005; Lopez et al. 2008; Gehler et al. 2009) and thus provides a major environmental cue that determines

cell behavior (Kölsch et al. 2007; Montell 2008; Fernandez-Gonzalez et al. 2009; Pouille et al. 2009; Solon et al. 2009; DuFort et al. 2011). Indeed, the focal adhesion complex and hemidesmosomes, which consist of integrins and a multicomplex of adaptors and signaling proteins, can be viewed as a mechanosensor linking the actomyosin and intermediate filament cytoskeleton with the ECM. Together with the cytoskeleton and nuclear matrices, nuclear envelope, and chromatin, they constitute sophisticated mechanosensing machinery that determines how cells react to forces from the ECM (DuFort et al. 2011). Interestingly, changes in mechanical force can be converted into differences in signaling activities (Maeda et al. 2011), suggesting that conventional signaling pathways can be used to interpret the mechanical properties of the ECM and vice versa (Engler et al. 2006; Lutolf et al. 2009; Gilbert et al. 2010). However, the precise mechanisms as to how interactions between respective integrins and ECM components induce this mechanosignaling are under debate. For example, for the basement membrane, it has been suggested that the laminin α-chains might be responsible for interactions with integrins and the cellular mechanophenotype which we could corroborate in our experiments. However, it has also become evident from our data that blocking specific laminin α-chains differentially modulates cellular stiffness. The phenotypic response of either blocking integrins or laminins on native basement membrane substrates has revealed that mechanosignaling is induced only by βbut not αintegrins. This is very much in contrast to published data where the role of integrins, in particular in cancer is usually discussed in the light of the α-subunit (Stipp 2010). Interestingly, our data clearly demonstrated that blocking β1 and β4 both lead to a softening, indicating a common signaling triggered by the close co-operation of the focal adhesion (FA) and hemidesmosome (HD) and corresponding cytoskeleton networks. Moreover, the localization of the cytoskeleton is directly affected by the organization of FA (α7β1, α3β1 and α6β1) and HD (α6β4) at the basal side and is only stable on native laminin as compared to artificial substrates. This indicates a shift from the highly dynamic actin and microtubule networks towards more stable intermediate filament networks. Therefore, new light can be shed on the specific roles of FA and HD structures in healthy and diseased epithelia. The ratio of FA to HD and the composition of FA depend on the laminins present in the basement membrane and these vary slightly from tissue to tissue where the amount of also plays a role since it can activate canonical fibrillar collagen integrins (α2β1). These new insights into the supramolecular organization of the major BM proteins call for an in depth-analysis of BM molecules with respect to cell specific phenotypes.

In my work, I have focused on the laminin alpha chains, which are major regulators of the laminin-binding integrins. However, further in-vitro studies investigating integrins, laminin and perlecan in the setting of competitions assays should elucidate if the laminin-binding integrins are promiscuous for perlecan or if the these two BM molecules trigger independent pathways.

4.3   THE ROUTE OF METASTATIC CELLS REVISITED

In the carcinoma in situ, BM represents the first physical barrier that segregates tumor cells from the stroma and must be breached to allow dissemination of the tumor cells to adjacent tissues 5. Cancer cells can perforate BM using MMP-rich protrusions (Hotary et al. 2002; Schoumacher et al. 2010; Linder et al. 2011). Apart from being a physical barrier, native BM is also potent signaling reservoir that might influence cancer progression and it is currently disputed if laminins are pro- or anti-metastatic agents (Chia et al. 2007). Interestingly it has been shown that cell interaction with laminins confers cancer-drug resistance (Hodkinson et al. 2006; Tsurutani et al. 2005; Yang et al. 2010). The common scheme in cancer-drug resistance is that laminin binding to integrins or their associated tetraspanins can override phosphoinositide 3-kinase (PI3K) inhibition by directly activating Akt/MAPK pathways and inducing proliferation. In breast cancer, trastuzumab and lapatinib are used to inhibit activation of PI3K by ErbB2 and knockouts of $\alpha6\beta4$ integrins or CD151 (a tetraspanin cluster the integrins) can restore the cells response to the mentioned cancer drugs (Tsurutani et al. 2005) Moreover, accumulating evidence suggests that tumor cells do not act alone. Stromal cells also produce matrix proteases (Kalluri et al. 2006). As the tumor progresses, its surrounding microenvironment also evolves, becoming enriched in carcinoma-associated fibroblasts (CAFs), immune cells, blood vessels and ECM (Joyce et al. 2009; Hanahan et al. 2011). CAFs play a role in tumor formation, progression and metastasis 9,12-15 (Kalluri et al. 2006; Orimo et al. 2006; Calvo et al. 2013; Goetz et al. 2011; De Wever et al. 2004). In vitro, CAFs actively excavate stromal passageways that facilitate cancer cell invasion (Gaggioli et al. 2007). However, until now it remained unknown whether CAFs cooperate with cancer cells to breach the BM to trigger the transition of carcinoma in situ to an invasive stage. We showed that CAFs isolated from cancer patients promote cancer cell invasion through a native BM. In the presence of CAFs, cancer cells invade in an MMP-independent manner. Using live imaging and atomic force microscopy, we found that CAFs actively pull, stretch and soften the BM, forming gaps through which cancer cells can migrate.

By exerting contractile forces, CAFs alter the organization and the physical properties of the BM, making it permissive for cancer cell invasion. Based on experimental evidence we proposed a new paradigm that, in addition to proteolysis includes mechanical forces exerted by CAFs as a new mechanism of facilitating cancer cells to breach BM by physical remodeling. These results open a completely new field of translation research where blocking the ability of stromal cells to exert mechanical forces on the BM could represent a new therapeutic strategy against aggressive tumors.

4.4 BMS ARE A MAJOR OBSTACLE FOR CANCER BUT CAN BE OVERCOME
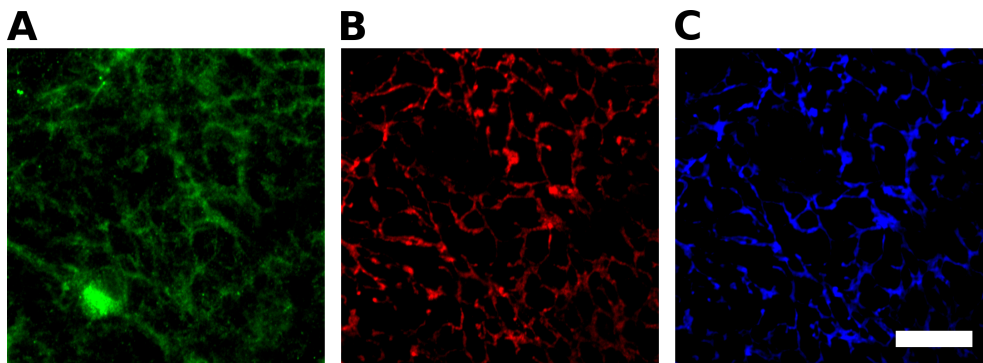
Figure 4.1 Immunostaining shows web-like structure of mesentery basement membrane (BM) proteins (A) collagen IV staining against 7S domain, (B) Perlecan staining (C) laminin α1β1γ1 (LN-111) staining. Scale bar is 10 μm.

In the context of cancer invasion, we examined mesenteries that were exposed to cancer cells. The mesentery is an excrescence of the peritoneum, which lines the abdominal cavity, and keeps the intestine in place by physically contacting it. While the peritoneum is a single membrane, the mesentery is a double membrane carrying blood vessels in its interior that maintain the intestine. The mouse mesentery used in this study consists of collagen IV, perlecan and LN-111 but lacks laminin α5-chains and contains a lot of fibrillar collagen I in between the two membrane layers. Unlike the ocular BMs or human BM of classical epithelial origin (chapter 3), the mesentery is a serous membrane and does not form thick layers of laminin, perlecan and collagen IV but the proteins seem to form a web-like structure with laminin and perlecan co-localizing and the collagen IV being loosely associated with laminin and perlecan (Figure 4.1). Serous membranes are membranes that bear epithelia which secrete serous fluids that are used as lubricants between

two tissues, in body cavities. It remains to be elucidate is this architecture is a common feature of serous membranes.

Figure 4.2 carcinoma-associated fibroblasts (CAFs) invasion setup
Invasion of cancer cells through CAF-modified mesenteries. (a) Mesenteries were modified with CAFs in a soft collagen matrix on the mesentery in the presence of distant cancer cells. (b) CAFs were subsequently killed to leave only the modified mesentery. (c) Cancer cells were cultured on CAF-modified mesentery for 5 days. For AFM analysis of modified mesenteries, cancer cells and collagen was removed before flat-mounting the mesentery for measurements. With permission from Alexandros Glentis.
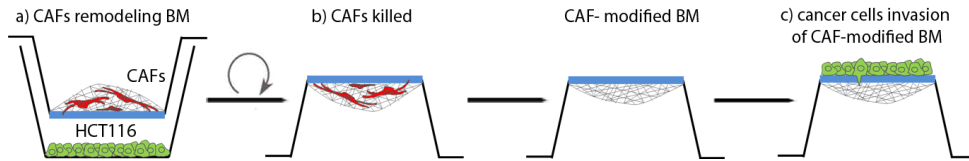
After being extracted from mice, the mesentery was strained onto a decapitated plastic tube (Schoumacher et al. 2010) to enable a co-culture of cancer cells on one side of the mesentery and primary human derived carcinoma-associated fibroblasts (CAFs) on the other side of the mesentery (Figure 4.2). In this work (Glentis et al., under revision) we showed that cancer cells alone cannot transmigrate the mesentery but when in co-clture with primary CAFs from cancer patients, invasion through mesentery was possible. Most importantly, we could show by using MS analysis of culture medium supernatant that this process occurs in the absence of an MMP increase. Moreover, by chemically blocking the MMP action we could not slow down or alter this behavior. However, when actomyosin contractility was inhibited by administering blebbistatin, no invasion was observed anymore, indicating that cells need to be able to exert a certain level of during migration (Figure 4.3).

The main question that we asked was if CAFs can make the BM more permissive for cancer cell invasion by physically changing the BM. With AFM we assessed mesenteries that (1) were not exposed to cancer cells nor CAFs, mesenteries that were (2) only exposed to cancer cells but not CAFs and finally mesenteries that (3) were exposed to CAF-remodeling, followed by cancer cell invasion (Figure 4.2). Data reproducibly showed that over the course of 5 days, transmigration of cancer cells was incread 4-fold upon mesentery remodeling by CAFs.

The reflection intensity signal from fibrillar structures reduced by 30 % (n = 7 mesenteries) in the presence of CAFs suggested that the organization of the mesentery was altered. This was further corroborated by AFM measurements that showed a marked decrease in mesentery stiffness in the case of both cancer cells alone on unadulterated mesentery and cancer cells on CAF
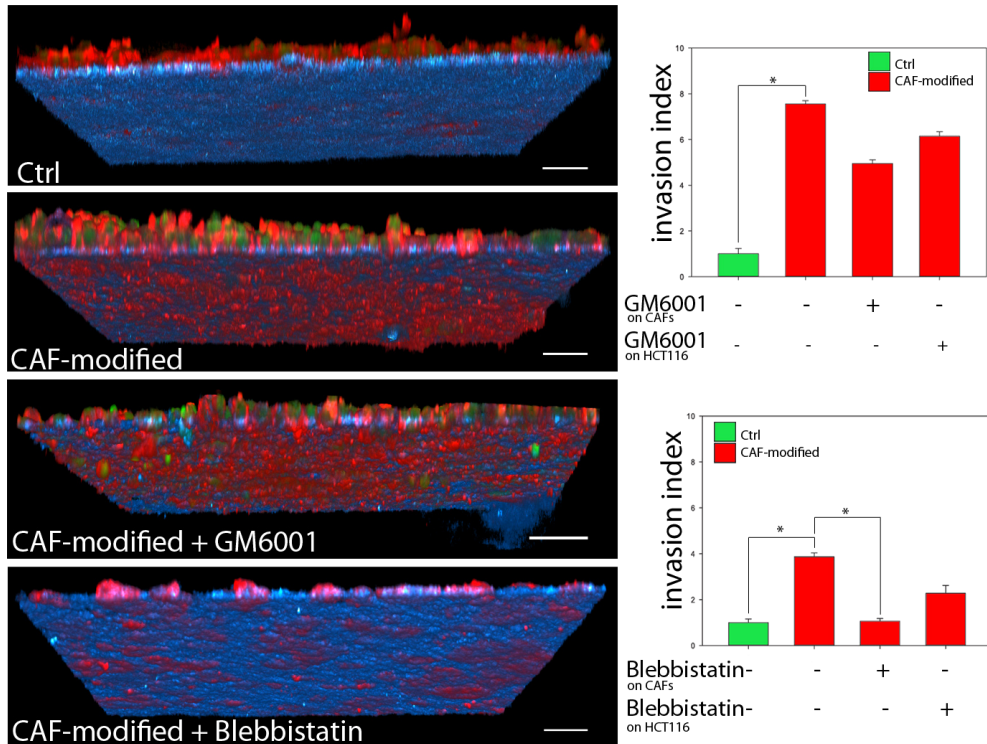
Figure 4.3 carcinoma-associated fibroblasts (CAFs) but not matrix metalloproteinases (MMPs) are required for mesentery transmigration

(Left) 3D reconstructions of confocal images show cancer cells (red) on a mesentery (blue). Cancer cells are seeded on the upper side of the mesentery and no cancer cells are visible on the lower side of mesentery in the Ctrl. After remodeling of the mesentery by carcinoma-associated fibroblasts (CAFs), transmigration to the lower side becomes apparent, even when blocking matrix metalloproteinases (MMPs) with GM6001. However, application of blebbistatin to block actomysion action prevents transmigration. (Right) quantification of the transmigration using an invasion index - the number of cancer cells visible per unit area at the lower side of the mesentery. With permission from Alexandros Glentis.
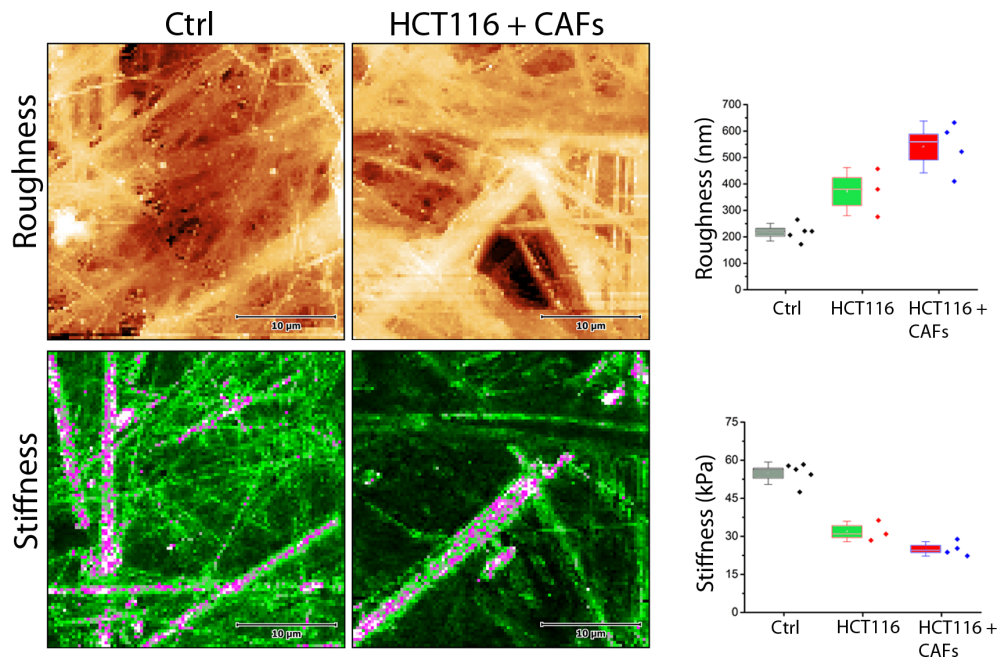
Figure 4.4 atomic force microscope (AFM) reveals mechanical and structural changes in mesentery upon cancer invasion

AFM quasi-height maps (upper panel) show roughness of non-treated mesentery (Ctrl) (colorscale = 1.2 um) and mesentery treated with cancer cells and carcinoma-associated fibroblasts (CAFs) (HCT116 + CAFs) (colorscale = 2.4 μm). AFM stiffness maps (lower panel) display sparse stiff fibers and many fibers with intermediate stiffness for the Ctrl condition, while in the HCT116 + CAF condition, only few thick fibers appear, interspersed through an inhomogeneous soft mass. Color scales = 20 - 250 kPa. Roughness and stiffness box plots show a 3-fold increase in roughness when adding cancer cells and CAFs and a 2 - 3 fold drop in stiffness. The roughness difference between only cancer cells and cancer cells + CAFs is significant, the stiffness difference is not. AFM maps are 30 μm x 15 μm, 100 x 100 force curves. The box indicates the standard deviation, the whiskers the standard error of mean, the horizontal rule is the median and the dot the mean.

remodelled mesentery. Interestingly, intermediately and very stiff or thick bundles of fibers seemed to be less affected by the cells whereas thin fibers seemed to disappear more or less completely, leaving behind an unstructured soft matter of collagen I, IV and glycoproteins. In addition, we have visualized holes in mesenteries that had been remodelled by CAFs. Intriguingly, even though cancer cells alone were also able to make the mesentery more rough, they were not able to create holes, and thereby missed to make it more permissive for invasion. Taken together, our dat showe that cancer cells and CAFs are individually able to make the mesentery softer and more rough, however only CAFs have the ability to physically remodel the mesentery such that large holes in the mesentery can enable cancer cells to invade through.

To summarize, both cancer cells and CAFs are able to modify mechanical and structural properties of mouse mesentery BMs. However, only CAFs had the ability to physically modify the membrane by introducing BM softening and roughening of the ECM molecules. It is important to note that invasion in the mesentery system takes more than a week to occur (Schoumacher et al. 2010). On the other hand, it takes only a day to invade through rBM models such as matrigel (Vignjevic et al. 2007). This furthermore strengthens our findings that an increased thickness and rigidity of native membranes plays a major role in the invasion process. Our findings suggest that the spotlight should be on the physical modification of the ECM rather than biochemical as extensively studied thus far. In the light of age-dependent changes found in BM it would be important to correlate BM associated changes during cancer progression with patient age.

4.5 EN ROUTE TO RAPID FORCE SPECTROSCOPY

Measurement speed is usually an important aspect of measuring living cells since many conditions that can be imposed on cells are time-dependent, as for example the disruption of stabilization of MFs or MTs when using specific drugs. AFM force mapping is an inherently slow technique because recording a meaningful force curve on a biological material takes about one second per force curve to penetrate the cell for several hundred nanometers to few micrometers. This corresponds to loading frequencies of a few Hertz. At higher indentation frequencies, the response is not meaningful anymore since this movements are not physiological and soft materials start to become very stiff when loaded too fast. There are imaging modes available, called quantitative imaging, in which the topography is scanned in an imaging mode, and at the same time the cantilever is slightly indenting the sample at

high frequency with very low amplitude, basically a sine or triangle wave is super-imposed onto the imaging. However, the loading frequencies are in the kHz regime and the indentation depths are few nanometers. In this case, the response of the cell membrane is recorded but not of the cytoskeleton or even deeper layers. Another way to speed up AFM measurements is to user multilever arrays (Figure 4.5). In this manner it could be possible to measure up to 8 spots in parallel. The biggest challenge in this setup is to align the sample perfectly parallel to the cantilever array, and to have a cantilever array where all the levers show the exact same bending properties. Since the force cannot be controlled on the single lever (the whole array is mounted on one piezo), a slightly different force is applied on each lever and in post-processing the forces curves need to be cut to the same loading force level.
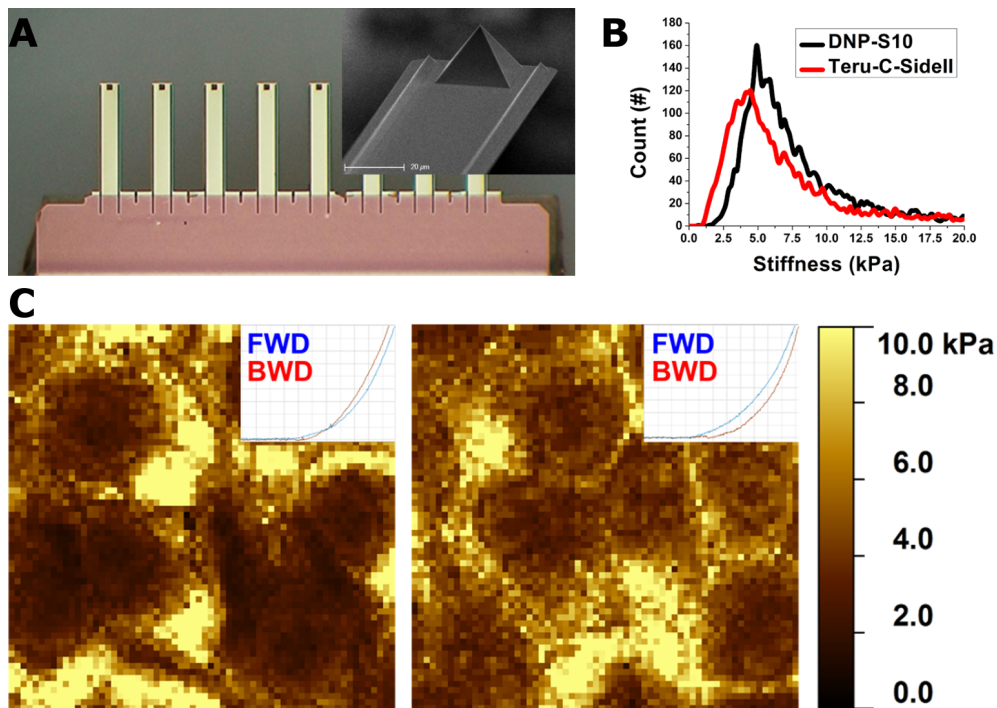
Figure 4.5 Multilever arrays can speed up stiffness measurements of biological samples.
(A) A multilever array with 8 SiN cantilevers in the frame of the Nanotera project PatLiSci II (Terunobu Akiyama, EPFL). The inset shows an scanning electron microscopy (SEM) image of a single tip. The tip height is 15 μm and is optimized for the roughness of biological samples. (B and C) A stiffness histogram recorded and force maps recorded with commercially available DNP-S10 (force map to the right) and custom made cantilever arrays (force map to the left) show almost identical results on MDCK cells. Insets in the force maps show an individual force curve. Force maps are 80 x 80 μm and 64 x 64 force curves.

4.6 TOWARDS MECHANO-OPTICAL MICROSCOPY

The mechanical properties of cells and adhesion forces between cells play an important role in a variety of biological processes including cell differentiation, proliferation, and tissue organization. atomic force microscope (AFM) has emerged as a powerful tool to quantify these mechanical properties at the cellular and molecular level. AFM uses a micron-scale cantilever and a micrometer bead or a sharp nanometer sized tip to probe a sample. For small deflections, the cantilever behaves like a Hookean spring, exerting a force proportional to its deflection. By detecting the position of the cantilever with an optical lever, forces exerted on a sample by the cantilever or imposed by the sample on the cantilever can be measured with high resolution (approximately 10^{-11} to 10^{-9} N) over a large force range (10^{-10} to 10^{-4} N). Because of these capabilities, AFM is an ideal tool to study mechanics at the cellular scale. For this purpose, AFM is often combined with brightfield and fluorescence microscopy to image cellular shape and labeled cellular proteins while making force measurements. Conventional AFMs typically allow straightforward combination with epi-fluorescence imaging systems that provide an image of the sample along a plane parallel to the surface, which we refer to as a "bottom-view". However, the most significant cellular deformations and cytoskeletal rearrangements are typically aligned with the applied force in a plane perpendicular to the surface. Imaging in this plane would allow one to relate specific cellular responses along the loading direction with the applied load. Nevertheless at this point is technically very challenging. Therefore by overcoming these challenges with hardware and software developments we are currently integrating an AFM with a spinning disk confocal for live cell experimentation. Such cutting edge setup will enable us to dissect and assign the mechanical contributions of the intra- and inter-cellular components to functional phenotypes of living cells.

REFERENCES

Bissell, M J and D Radisky (2001). „Putting tumours in context." In: *Nature reviews. Cancer* 1.1, pp. 46–54. DOI: 10.1038/35094059.
Bissell, Mina J and Mark A LaBarge (2005). „Context, tissue plasticity, and cancer: are tumor stem cells also regulated by the microenvironment?" In: *Cancer cell* 7.1, pp. 17–23.

Calvo, Fernando et al. (2013). „Mechanotransduction and YAP-dependent matrix remodelling is required for the generation and maintenance of cancer-associated fibroblasts." In: *Nature cell biology* 15.6, pp. 637–646.

Chia, Jenny et al. (2007). „Evidence for a role of tumor-derived laminin-511 in the metastatic progression of breast cancer." In: *The American journal of pathology* 170.6, pp. 2135–2148.

De Wever, Olivier et al. (2004). „Critical role of N-cadherin in myofibroblast invasion and migration in vitro stimulated by colon-cancer-cell-derived TGF-β or wounding." In: *Journal of cell science* 117.20, pp. 4691–4703.

DuFort, Christopher C, Matthew J Paszek, and Valerie M Weaver (2011). „Balancing forces: architectural control of mechanotransduction." In: *Nature reviews Molecular cell biology* 12.5, pp. 308–319.

Engler, Adam J et al. (2006). „Matrix elasticity directs stem cell lineage specification." In: *Cell* 126.4, pp. 677–689.

Fernandez-Gonzalez, Rodrigo et al. (2009). „Myosin II dynamics are regulated by tension in intercalating cells." In: *Developmental cell* 17.5, pp. 736–743.

Gaggioli, Cedric et al. (2007). „Fibroblast-led collective invasion of carcinoma cells with differing roles for RhoGTPases in leading and following cells." In: *Nature cell biology* 9.12, pp. 1392–1400.

Gehler, Scott et al. (2009). „Filamin A–β1 integrin complex tunes epithelial cell response to matrix tension." In: *Molecular biology of the cell* 20.14, pp. 3224–3238.

Gilbert, Penney M et al. (2010). „Substrate elasticity regulates skeletal muscle stem cell self-renewal in culture." In: *Science* 329.5995, pp. 1078–1081.

Goetz, Jacky G et al. (2011). „Biomechanical remodeling of the microenvironment by stromal caveolin-1 favors tumor invasion and metastasis." In: *Cell* 146.1, pp. 148–163.

Halfter, Willi et al. (Jan. 2013). „The bi-functional organization of human basement membranes." In: *PloS one* 8.7, e67660. DOI: 10.1371/journal.pone.0067660.

Hanahan, Douglas and Robert A Weinberg (2011). „Hallmarks of cancer: the next generation." In: *cell* 144.5, pp. 646–674.

Henrich, Paul B. et al. (June 2012). „Nanoscale Topographic and Biomechanical Studies of the Human Internal Limiting Membrane." In: *Investigative Opthalmology & Visual Science* 53.6, p. 2561. DOI: 10.1167/iovs.11-8502.

Hodkinson, PS et al. (2006). „ECM overrides DNA damage-induced cell cycle arrest and apoptosis in small-cell lung cancer cells through β1 integrin-dependent activation of PI3-kinase." In: *Cell Death & Differentiation* 13.10, pp. 1776–1788.

Hotary, Kevin B et al. (2002). „Matrix metalloproteinases (MMPs) regulate fibrin-invasive activity via MT1-MMP–dependent and–independent processes." In: *The Journal of experimental medicine* 195.3, pp. 295–308.

Joyce, Johanna A and Jeffrey W Pollard (2009). „Microenvironmental regulation of metastasis." In: *Nature Reviews Cancer* 9.4, pp. 239–252.

Kalluri, Raghu and Michael Zeisberg (2006). „Fibroblasts in cancer." In: *Nature Reviews Cancer* 6.5, pp. 392–401.

Kölsch, Verena et al. (2007). „Control of Drosophila gastrulation by apical localization of adherens junctions and RhoGEF2." In: *Science* 315.5810, pp. 384–386.

Linder, Stefan, Christiane Wiesner, and Mirko Himmel (2011). „Degrading devices: invadosomes in proteolytic cell invasion." In: *Annual review of cell and developmental biology* 27, pp. 185–211.

Lopez, JI, JK Mouw, and VM Weaver (2008). „Biomechanical regulation of cell orientation and fate." In: *Oncogene* 27.55, pp. 6981–6993.

Lutolf, Matthias P, Penney M Gilbert, and Helen M Blau (2009). „Designing materials to direct stem-cell fate." In: *Nature* 462.7272, pp. 433–441.

Maeda, Toru et al. (2011). „Conversion of mechanical force into TGF-β-mediated biochemical signals." In: *Current Biology* 21.11, pp. 933–941.

McBeath, Rowena et al. (2004). „Cell shape, cytoskeletal tension, and RhoA regulate stem cell lineage commitment." In: *Developmental cell* 6.4, pp. 483–495.

Montell, Denise J (2008). „Morphogenetic cell movements: diversity from modular mechanical properties." In: *Science* 322.5907, pp. 1502–1505.

Oertle, Philipp et al. (2018). „Native basement membranes enforce epithelial mechanophenotype." In preparation.

Orimo, Akira and Robert A Weinberg (2006). „Stromal fibroblasts in cancer: a novel tumor-promoting cell type." In: *Cell cycle* 5.15, pp. 1597–1601.

Paszek, Matthew J et al. (2005). „Tensional homeostasis and the malignant phenotype." In: *Cancer cell* 8.3, pp. 241–54. DOI: 10.1016/j.ccr.2005.08.010. arXiv: 24944547482.

Pollard, Thomas D. and William C. Earnshaw (2008). *Cell Biology*. 2nd. Philadelphia, p. 545.

Pouille, Philippe-Alexandre et al. (2009). „Mechanical signals trigger Myosin II redistribution and mesoderm invagination in Drosophila embryos." In: *Sci Signal* 2.66, ra16.

Reilly, Gwendolen C and Adam J Engler (2010). „Intrinsic extracellular matrix properties regulate stem cell differentiation." In: *Journal of biomechanics* 43.1, pp. 55–62.

Schoumacher, Marie et al. (2010). „Actin, microtubules, and vimentin intermediate filaments cooperate for elongation of invadopodia." In: *The Journal of cell biology* 189.3, pp. 541–556.

Solon, Jerome et al. (2009). „Pulsed forces timed by a ratchet-like mechanism drive directed tissue movement during dorsal closure." In: *Cell* 137.7, pp. 1331–1342.

Stipp, Christopher S (2010). „Laminin-binding integrins and their tetraspanin partners as potential antimetastatic targets." In: *Expert reviews in molecular medicine* 12, e3.

Tsurutani, Junji et al. (2005). „Inhibition of the phosphatidylinositol 3-kinase/ Akt/ mammalian target of rapamycin pathway but not the MEK/ERK pathway attenuates laminin-mediated small cell lung cancer cellular survival and resistance to imatinib mesylate or chemotherapy." In: *Cancer research* 65.18, pp. 8423–8432.

Vignjevic, Danijela et al. (2007). „Fascin, a novel target of β-catenin-TCF signaling, is expressed at the invasive front of human colon cancer." In: *Cancer Research* 67.14, pp. 6844–6853. DOI: 10.1158/0008-5472.CAN-07-0929.

Wiseman, Bryony S and Zena Werb (2002). „Stromal effects on mammary gland development and breast cancer." In: *Science* 296.5570, pp. 1046–1049.

Yang, Xiuwei H et al. (2010). „Disruption of laminin-integrin-CD151-focal adhesion kinase axis sensitizes breast cancer cells to ErbB2 antagonists." In: *Cancer research* 70.6, pp. 2256–2263.

NOTATION

MECHANICAL PROPERTIES

SYMBOL	UNITS	MEANING
A_c	m²	Contact area
c_d	m	Cantilever deflection
c_p	m	Contact point
d	V	Photodiode deflection
DS	m/V	Deflection Sensitivity
E	Pa	E-modulus or contact stiffness
F	N	Force
f_c	Hz	Center frequency
Q	-	Quality factor
k	N/m	Spring constant
ν	-	Poisson ratio
p_d	m	Piezo distance
tsd	m	Tip-sample distance
S	N/m	(Bending) stiffness
Θ	°	Cantilever half-opening angle

ACRONYMS

3D   three-dimensional

AFM   atomic force microscope

AGE   advanced glycation endproducts

AJ   adherens junction

BM   basement membrane

BMP1   bone-morphogenetic protein-1

BPAG1   bullous pemphigoid antigen 1

BrM   Bruch's membrane

BSA   bovine serum albumin

CAF   carcinoma-associated fibroblast

CIP   contact inhibition of proliferation

CK   cytokeratin

ColIV   collagen IV

ColIV-ILM   collagen IV side of inner limiting membrane

DDR1   discoidin domain receptor 1

DDR2   discoidin domain receptor 2

DM   Descemet's membrane

DS   deflection sensitivity

ECM   extra-cellular matrix

EC1   extracellular cadherin domain 1

EGF   epidermal growth factor

EHS	Engelbreth-Holm-Swarm
EM	electron microscopy
EMT	epithelial-mesenchymal transition
Ep	epithelial
EPP	epithelial polarity program
ER	endoplasmatic reticulum
ERM	ezrin, radixin and moesin
FA	focal adhesion
FAK	focal adhesion kinase
GBM	glomerular basement membrane
GJ	gap junction
HD	hemidesmosome
HS	heparansulfate
HSPG	heparansulfate-proteoglycan
ICM	inner cell mass
IF	intermediate filament
Ig	immunoglobulin
ILM	inner limiting membrane
INM	inner nuclear membrane
LC	lens capsule
LDL	low density lipoprotein
LE	laminin-type epidermal growth factor-like repeats
LF	unique globule of β-subunits
LG	carboxy-terminal laminin globular domains

Ln   laminin

LN   amino-terminal laminin globule

LN-111   laminin $\alpha 1\beta 1\gamma 1$

LN-211   laminin $\alpha 2\beta 1\gamma 1$

LN-221   laminin $\alpha 2\beta 2\gamma 1$

LN-332   laminin $\alpha 3\beta 3\gamma 2$

LN-411   laminin $\alpha 4\beta 1\gamma 1$

LN-511   laminin $\alpha 5\beta 1\gamma 1$

LN-521   laminin $\alpha 5\beta 2\gamma 1$

LN-ILM   laminin-side of inner limiting membrane

LN521-PA laminin-521 coated poly-acrylamide

LTM   laser tracking microscopy

ME   microenvironment

MMP   matrix metalloproteinase

MHB   modified Hank's buffer

MF   microfilament

MS   mass spectrometry

MSD   mean square displacement

MT   microtubule

MTC   magnetic twisting cytometry

MTOC   microtubule organizing center

MT-MMP membrane-type matrix metalloproteinase

NC   non-collagenous

OMTC   optical magnetic twisting cytometry

ONM	outer nuclear membrane
PA	poly-acrylamide
PCP	planar cell polarity
PDMS	polydimethylsiloxane
PG	proteoglycan
PI3K	phosphoinositide 3-kinase
PKC	protein kinase C
PLL	poly-L-lysine
PLL-PA	poly-L-lysine coated poly-acrylamide
PM	plasma membrane
rBM	reconstituted basement membrane
rBM-PA	reconstituted basement membrane coated poly-acrylamide
RGD	tripeptide Arg-Gly-Asp
ROI	region of interest
RT	room temperature
SEA	sea urchin enterokinase and agrin domain
SEM	scanning electron microscopy
SGL	sulfated glycolipids
SGM	soft glass material
SGR	soft glass rheology
St	stromal
TEM	transmission electron microscopy
TER	trans-epithelial resistance
TFM	traction force microscopy

TJ   tight junction

Ty   thyroglobulin type I repeats

UAR   uniaxial rheometry

PUBLICATIONS

The following publications are included in parts or in an extended version in this thesis:

- Daphne Asgeirsson et al. (2015). „Nanotechnology for Human Health." In: ed. by Bert Mueller et al. 1st edition. Chap. The Nanomechanical Signature of Tissues in Health and Disease

- Willi Halfter et al. (Jan. 2013). „The bi-functional organization of human basement membranes." In: *PloS one* 8.7, e67660. DOI: 10.1371/journal.pone.0067660

- Willi Halfter et al. (2015). „New concepts in basement membrane biology." In: *FEBS Journal* 282.23, pp. 4466–4479

The following work is published or in preparation and included in an extended version in this thesis:

- Philipp Oertle et al. (2018). „Native basement membranes enforce epithelial mechanophenotype." In preparation

- Alexandros Glentis et al. (2017). „Cancer-associated fibroblasts induce metalloprotease-independent cancer cell invasion of the basement membrane." In: *Nature communications* 8.1, p. 924

ACKNOWLEDGMENTS

First and foremost I want to thank my advisors Marija Plodinec and Roderick YH Lim. I want to thank both of you for giving me a lot of freedom in performing great science and engineering work in the lab and for great and intense times. I also would like to thank Ernst Meyer for taking his time to be my co-examiner and Fiona Doetsch for chairing my defense.

Many thanks go the my old and current lab mates, Janne, Kai, Bref, and Schoch; to Christian, Lajko, Suncica, Yusuke, Daphne, Larissa, RK, Chantal, Binlu, Tina and Tobi for having a fun time together and the good discussions about science and everything else.

Special thanks go the army of civil servants, Urs, Leon, Adrian, Florian, Pascal and Noe, and their boss Marko with whom I spent a lot of time building things and improving AFMs.

For very fruitful scientific discussions and a lot of inspiration I want to thank Willi and Bernhard who also taught me a lot about the human and especially how to get these basement membranes out.

I also want to warmly thank the team at Pathology Basel, Ellen and Serenella, without whom I would be stuck to measuring non-human samples only.

And of course Beat, and the electrical an mechanical workshops of the Biozentrum for an endless flow of tools and screws and cables.

And finally my deepest grattitude and love go to my girlfriend Irina who supported me and beared with me all the time during my PhD years.

CURRICULUM VITAE

PERSONAL INFOR-
MATION

Philipp Oertle

Kannenfeldstrasse 34, 4056 Basel (Switzerland)
(+41) 79 305 16 67
philipp.oertle@gmail.com
Skype jelipeo

WORK EXPERIENCE

1 Nov 2017 - present	Head of Technology Development, ARTIDIS AG, Basel (Switzerland)
1 Jul 2016 - Oct 2017	Post-Doc, Biozentrum, University of Basel, Basel (Switzerland)
Jul 2010 - Aug 2010	Intern, Clarendon Laboratory, University of Oxford, Oxford (United Kingdom)
Jul 2009 - Sep 2009	Software Developer, CSEM Landquart, Landquart (Switzerland)

EDUCATION AND
TRAINING

1 Jul 2012 - 30 Jun 2016	PhD in Nanoscience University of Basel, Basel (Switzerland) Thesis title: • "Mechanobiology of the Basement Membrane" (grade "summa cum laude")
2010 - 2012	Master of Science in Nanoscience, Major in Physics University of Basel, Basel (Switzerland) Project works and Master Project: • Improvement of the duty cycle of miniaturized atomic clocks and development of a pulsed Rubidium source, Paris Observatory

- Development of an enhanced drift compensation algorithm for atomic force microscopy, Biozentrum Basel

Master thesis

- Development of a new atomic force microscopy based methodology for the early detection of osteoarthritis, Biozentrum Basel

2007 - 2010	Bachelor of Science in Nanoscience University of Basel, Basel (Switzerland)

- Biology
- Chemistry
- Computer Science
- Mathematics
- Physics

2000 - 2007	Eidgenössische Matura
	Gymnasium Vaduz, Vaduz (Liechtenstein)

PERSONAL SKILLS

Mother tongue(s)	German
Other language(s)	
English	C2
French	A2
Spanish	A1
Communication skills	Good communication skills gained through my experience as president of a students associations local committee (IAESTE Switzerland, Local Committee Basel)
	Presented at various scientific conferences (posters and talks)
Organisational / managerial skills	Former president of IAESTE Local Committee Basel
	Supervision of undergrad and graduate students at Biozentrum
	Lead of development team of 3 engineers at Professor Lims group

Digital competence	Good command of office suite (word, outlook, excel, power point)
	Good command of various software used for scientific analysis and publishing (OriginPro, Inkscape, GIMP, AdobeAcrobat, Fiji/ImageJ, Imaris, CellProfiler)
	Experienced user of National Instruments products (LabVIEW, FPGA and RealTime-Modules, Vision Acquisition, Data Acquisition)
	Experienced Python user (Python 3.x, Sci-kit Learn, numpy, pandas, matplotlib)
	Basic knowledge in Java programming
	Basic knowledge in software modeling (UML 2.x)

ADDITIONAL INFOR-
MATION

Scientific Papers

Plodinec et al., "The nanomechanical signature of breast cancer", Nature nanotechnology, 7, 11, 757-765, 2012

Halfter et al., "The Bi-Functional Organization of Human Basement Membranes", PLOS ONE, 8, 7, e67660, 2013

To et al., "Diabetes-induced morphological, biomechanical, and compositional changes in ocular basement membranes", Experimental eye research, 116, 298-307, 2013

Halfter et al., "New concepts in basement membrane biology", FEBS Journal, 282, 23, 4466-4479, 2015

Reyes and Oertle et al., "Superior Rim Stability of the Lens Capsule Following Manual Over Femtosecond Laser Capsulotomy", Investigative ophthalmology & visual science, 57, 6, 2839-2849, 2016

Emilsson et al., "Surface Plasmon Resonance Methodology for Monitoring Polymerization Kinetics and Morphology Changes of Brushes - Evaluated with Poly (N-isopropylacrylamide)", Applied Surface Science, 2016

Glentis et al. "Cancer-associated fibroblasts induce metalloprotease-independent cancer cell invasion of the basement membrane." Nature communications 8, 1, 924, 2017

Halfter et al. "Diabetes-related changes in the protein composition and the biomechanical properties of human retinal vascular basement membranes." PloS one 12, 12, e0189857, 2017

Melo et al. "HtrA1 Mediated Intracellular Effects on Tubulin Using a Polarized RPE Disease Model." EBioMedicine, 2017

Occhetta et al. "A three-dimensional in vitro dynamic micro-tissue model of cardiac scar formation." Integrative Biology 10,3, 174-183, 2018

Ganier et al. "Structural centrosome aberrations promote non-cell-autonomous invasiveness." The EMBO journal, e98576, 2018

Book Chapters   Asgeirsson et al., "The Nanomechanical Signature of Tissues" in Health and Disease,Nanoscience and Nanotechnology for Human Health, 209-240, 2016, Wiley-VCH Verlag GmbH & Co. KGaA

Patents   Plodinec et al., "Nanomechanical profiling of breast cancer molecular subtypes", EP3159690 A1, 2017